

Dissertation
submitted to the
Combined Faculties for the Natural Sciences and for Mathematics
of the Ruperto-Carola University of Heidelberg, Germany
for the degree of
Doctor of Natural Sciences

presented by

Kai Richter, M.Sc.

born in: Bremen, Germany

Oral examination: 26th October 2017

**Identification and characterization of
novel regulators of the tumor suppressor and
ubiquitin ligase SCF-FBXW7**

Referees: Prof. Dr. Ingrid Hoffmann
Prof. Dr. Frauke Melchior

Hiermit erkläre ich an Eides statt, dass ich die vorliegende Dissertation selbstständig und ohne unerlaubte Hilfsmittel durchgeführt habe.

Heidelberg, den 27. Juli 2017

.....

(Kai Richter)

Table of contents

I. Summary	1
II. Zusammenfassung	3
1. Introduction	5
1.1. The ubiquitin system	5
1.1.1. The ubiquitylation reaction	5
1.1.2. Types of ubiquitin ligases	7
1.1.3. The ubiquitin code	8
1.1.4. Effects of substrate ubiquitylation	8
1.1.5. Ubiquitin-like modifiers	9
1.2. The SCF complex is a Cullin-RING ubiquitin ligase	9
1.2.1. Cullin-RING ubiquitin ligases (CRLs)	9
1.2.2. Regulation of CRL activity	11
1.2.3. The SCF complex uses F-box proteins to target its substrates	11
1.3. FBXW7 is a tumor suppressor protein	13
1.3.1. FBXW7 is conserved from yeast to human	13
1.3.2. Domain organization of human FBXW7	14
1.3.3. Human FBXW7 isoforms	14
1.3.4. The CDC4 phosphodegron	15
1.3.5. FBXW7 substrates	16
1.3.5.1. FBXW7 mediates the degradation of important oncoproteins	16
1.3.5.2. Regulation of transcription by FBXW7	17
1.3.5.3. FBXW7 is a regulator of cell survival	18
1.3.5.4. Other substrates of FBXW7	18
1.3.6. FBXW7 is frequently mutated in human cancers	18
1.3.7. Regulation of FBXW7	19
1.3.7.1. Regulation of FBXW7 expression by transcription factors	19
1.3.7.2. Regulation of FBXW7 expression by microRNAs	19
1.3.7.3. Regulation of FBXW7 protein stability	19
1.3.7.4. Regulation of FBXW7 protein localization	20
1.3.7.5. Regulation of SCF-FBXW7 ubiquitin ligase activity	21
1.4. MYCBP2 and FBXO45 form a ubiquitin ligase complex	21
1.5. RAE1 is a mitotic regulator that interacts with MYCBP2	22

1.6. XIAP is an anti-apoptotic ubiquitin ligase	23
1.7. Objectives.....	23
2. Materials and methods.....	25
2.1. Materials.....	25
2.1.1. Chemicals and reagents	25
2.1.2. Laboratory equipment.....	27
2.1.3. Buffers and media	29
2.1.4. Antibodies	31
2.1.4.1. Primary antibodies	31
2.1.4.2. Secondary antibodies	32
2.1.5. Small interfering RNAs (siRNAs)	32
2.1.6. Primers.....	33
2.1.7. Plasmids	36
2.1.8. Bacterial strains	38
2.1.9. Cell lines	39
2.1.10. Kits.....	39
2.1.11. Antibiotics.....	39
2.2. Methods.....	40
2.2.1. Methods in molecular biology	40
2.2.1.1. Polymerase chain reaction (PCR)	40
2.2.1.2. Agarose gel electrophoresis	41
2.2.1.3. Restriction digest of DNA.....	41
2.2.1.4. Extraction of DNA fragments from agarose gels	41
2.2.1.5. Ligation of DNA fragments.....	42
2.2.1.6. Transformation of chemically competent <i>E. coli</i>	42
2.2.1.7. Isolation of plasmid DNA from <i>E. coli</i>	42
2.2.1.8. Determination of DNA concentration	43
2.2.2. Methods in cell biology.....	43
2.2.2.1. Cell culture.....	43
2.2.2.2. Harvesting and freezing of cells.....	43
2.2.2.3. Transient transfection of mammalian cells	44
2.2.2.3.1. Transfection of cells with plasmid DNA using polyethylenimine (PEI).....	44
2.2.2.3.2. Transfection of cells with siRNA using Lipofectamine 2000	44

2.2.2.4. Cell cycle synchronization	45
2.2.2.5. MG132 and cycloheximide treatment	45
2.2.2.6. Live-cell imaging	45
2.2.3. Methods in protein biochemistry	46
2.2.3.1. Preparation of protein extracts from mammalian cells.....	46
2.2.3.2. Determination of protein concentration	46
2.2.3.3. SDS polyacrylamide gel electrophoresis (SDS-PAGE)	47
2.2.3.4. Electrotransfer and Western blot	47
2.2.3.5. Immunoprecipitation assays	48
2.2.3.5.1. Immunoprecipitation of Flag-tagged proteins using Flag M2 affinity beads	48
2.2.3.5.2. Immunoprecipitation of endogenous proteins using NHS- activated sepharose	48
2.2.3.5.3. Sequential immunoprecipitation for the analysis of protein complexes	49
2.2.3.6. Colloidal Coomassie staining.....	49
2.2.3.7. Mass spectrometry analysis	50
2.2.3.8. <i>In vivo</i> ubiquitylation assays	50
2.2.3.9. Expression and purification of recombinant proteins	51
2.2.3.9.1. Expression and purification of MBP-tagged proteins.....	51
2.2.3.9.2. Expression and purification of His-tagged proteins	52
2.2.3.10. <i>In vitro</i> transcription and translation and <i>in vitro</i> binding assays ...	52
2.2.3.11. Pull-down assay with recombinant proteins.....	53
3. Results.....	54
3.1. Identification of novel FBXW7 α interaction partners	54
3.1.1. Identification of FBXW7 α interaction partners by Flag-FBXW7 α immunoprecipitation and mass spectrometry analysis	54
3.1.2. WDR5 is a putative substrate of FBXW7	56
3.1.3. Analysis of putative FBXW7 regulators.....	58
3.2. Characterization of XIAP as a novel interaction partner of FBXW7 α	60
3.2.1. XIAP interacts with FBXW7 α <i>in vivo</i>	60
3.2.2. XIAP specifically interacts with FBXW7 α	61
3.2.3. The interaction between FBXW7 α and XIAP does not require the F-box or WD40 domains of FBXW7 α	62

3.2.4. XIAP interacts with the N-terminal domain of FBXW7 α	64
3.2.5. XIAP does not interact with the N-terminus of FBXW7 α <i>in vitro</i>	68
3.3. RAE1, FBXO45 and MYCBP2 form a complex with FBXW7 α and XIAP	69
3.3.1. Identification of XIAP interaction partners	69
3.3.2. XIAP and RAE1 bind to a similar domain within the N-terminus of FBXW7 α	70
3.3.3. Amino acid residues 106-126 of FBXW7 α contain a negatively charged sequence motif that is highly conserved among vertebrates	74
3.3.4. FBXW7 α , XIAP and RAE1 form a complex	75
3.3.5. Identification of additional FBXW7 α -XIAP complex components.....	76
3.3.6. Screen for RAE1 interaction partners	78
3.3.7. Both FBXO45 and MYCBP2 interact with the N-terminal domain of FBXW7 α	78
3.3.8. FBXW7 α and FBXO45 bind to the central domain of MYCBP2.....	79
3.3.9. FBXW7 α forms a complex with MYCBP2 and FBXO45	82
3.3.10. FBXO45 interacts with FBXW7 α <i>in vitro</i>	83
3.3.11. FBXO45 specifically interacts with FBXW7 α	84
3.4. Characterization of FBXO45 and MYCBP2 as novel regulators of FBXW7 α .	84
3.4.1. FBXW7 α protein levels decrease during mitotic arrest.....	84
3.4.2. The FBXO45/MYCBP2 ubiquitin ligase regulates FBXW7 α protein levels.....	85
3.4.3. FBXO45 and MYCBP2 promote the ubiquitylation of FBXW7 α	88
3.4.4. FBXO45 mediates FBXW7 α destabilization during mitotic arrest.....	90
3.4.5. FBXW7 α interacts with the C-terminus of FBXO45	91
3.4.6. FBXO45 and MYCBP2 promote mitotic slippage	92
4. Discussion	94
4.1. Identification of novel FBXW7 α interaction partners	94
4.2. WDR5 is a putative FBXW7 substrate	94
4.3. Analysis of putative FBXW7 α regulators.....	96
4.4. XIAP, RAE1, FBXO45, MYCBP2 and SPRYD3 form a complex with FBXW7 α	96
4.5. FBXO45 and MYCBP2 promote the degradation of FBXW7 α during mitotic arrest.....	98
4.6. Degradation of FBXW7 α by FBXO45/MYCBP2 might promote	

resistance to spindle poisons	99
4.7. Different FBXW7 substrates could mediate the effect of FBXO45/MYCBP2 on mitotic cell fate.....	100
4.8. A negatively charged motif within the N-terminal domain of FBXW7 α is recognized by FBXO45/MYCBP2	102
4.9. Putative roles of RAE1, XIAP and SPRYD3 in the complex with FBXW7 α , FBXO45 and MYCBP2.....	103
4.10. Outlook and perspectives.....	104
4.10.1. WDR5 as a putative FBXW7 substrate.....	104
4.10.2. Verification of the FBXW7 α regulation by FBXO45/MYCBP2.....	105
4.10.3. Unraveling the roles of RAE1, XIAP and SPRYD3 in the complex.....	107
4.10.4. Identification of mitotic FBXW7 substrate(s)	108
5. References	110
6. Annex	126
6.1. Abbreviations.....	126
6.2. List of figures	127
6.3. List of tables	129
7. Acknowledgements	130

I. Summary

The evolutionarily conserved protein ubiquitin serves as a posttranslational modification in eukaryotic cells. Ubiquitylation links specific proteins with different effector reactions and pathways, including proteasomal degradation. The canonical ubiquitylation machinery transfers ubiquitin to substrate proteins in a cascade reaction comprising three different enzymes (E1, E2, E3). In human cells, there exist more than 600 E3s, denoted ubiquitin ligases. Ubiquitin ligases provide the ubiquitin system with substrate specificity as they directly interact with the target proteins and mediate the final step of the ubiquitylation reaction.

Cullin-RING ubiquitin ligases are the largest subfamily of ubiquitin ligases. The SCF complex is a Cullin-RING ubiquitin ligase that contains a central CUL1 subunit, the RING domain containing protein RBX1, the adaptor protein SKP1 and an F-box protein. The F-box protein is the SCF subunit that recruits the substrate. In humans, there are about 70 F-box proteins. They are interchangeable within the SCF complex and have different substrate specificities.

One of the best-characterized F-box proteins is FBXW7. FBXW7 promotes the proteasomal degradation of important oncoproteins, including Cyclin E, MYC, JUN and NOTCH. Accordingly, FBXW7 functions as a tumor suppressor protein. Indeed, FBXW7 is frequently mutated in human cancers. While the downstream effects of FBXW7 are already well-characterized, the upstream regulation of FBXW7 is only poorly understood so far. In order to unravel novel regulation mechanisms for FBXW7, a biochemical screen for FBXW7 interaction partners was performed in the presented study.

Immunoprecipitation combined with mass spectrometry identified FBXO45, MYCBP2, XIAP and RAE1 as putative interaction partners of FBXW7. *In vivo* verification of the putative interactions revealed that FBXO45, MYCBP2, XIAP and RAE1 specifically interact with a negatively charged motif within the N-terminal domain of the FBXW7 α -isoform. Additional interaction studies indicated that FBXW7 α , FBXO45, MYCBP2, XIAP and RAE1 are found in a complex. *In vitro*, only FBXO45 interacted with the N-terminus of FBXW7 α , suggesting that FBXO45 is the direct interaction partner of FBXW7 α within the complex.

FBXO45 and MYCBP2 have been described to form a ubiquitin ligase complex. siRNA-mediated downregulation of FBXO45 and MYCBP2 caused an increase in

FBXW7 α protein levels, which was specifically observed during mitotic arrest. Furthermore, FBXO45 and MYCBP2 promoted ubiquitylation of FBXW7 α . FBXO45 depletion led to a stabilization of FBXW7 α in a cycloheximide chase experiment. These findings suggest that FBXO45 and MYCBP2 promote the proteasomal degradation of FBXW7 α upon mitotic arrest.

FBXW7 is a known regulator of mitotic cell fate. Upon mitotic arrest, FBXW7 promotes mitotic cell death and prevents mitotic slippage. In contrast to FBXW7, this thesis identified FBXO45 and MYCBP2 to promote mitotic slippage and to prevent mitotic cell death. Hence, FBXW7 and FBXO45/MYCBP2 have opposing effects on mitotic cell fate.

In conclusion, this thesis describes FBXO45 and MYCBP2 as novel regulators of FBXW7 α protein levels during mitotic arrest. Thus, the presented thesis contributes to a better understanding of the regulatory mechanisms underlying the function of the important tumor suppressor protein FBXW7. As FBXW7 contributes to mitotic cell death, the FBXO45/MYCBP2-FBXW7 α axis could be a novel target for the improvement of chemotherapy approaches.

II. Zusammenfassung

Das evolutionär konservierte Protein Ubiquitin dient in eukaryontischen Zellen als posttranslationale Proteinmodifikation. Die Ubiquitylierung verknüpft spezifische Proteine mit unterschiedlichen Effektor-Reaktionen und -Signalwegen, wie z. B. der proteasomalen Degradation. In einer kaskadenartigen Reaktion, die drei unterschiedliche Enzyme (E1, E2, E3) benötigt, wird Ubiquitin auf Substrat-Proteine übertragen. In menschlichen Zellen existieren mehr als 600 E3-Enzyme, die auch als Ubiquitin-Ligasen bezeichnet werden. Ubiquitin-Ligasen verleihen dem Ubiquitin-System die Substrat-Spezifität, da sie direkt mit den Ziel-Proteinen interagieren und den finalen Schritt der Ubiquitylierungsreaktion vermitteln.

Cullin-RING Ubiquitin-Ligasen bilden die größte Unterfamilie der Ubiquitin-Ligasen. Als SCF-Komplex wird eine Cullin-RING Ubiquitin-Ligase bezeichnet, die die zentrale Untereinheit CUL1, das RING-Domäne enthaltende Protein RBX1, das Adapter-Protein SKP1 sowie ein F-Box-Protein enthält. Die Bindung des Substrats an den SCF-Komplex erfolgt über das F-Box-Protein. Humane Zellen verfügen über ungefähr 70 F-Box-Proteine. Diese sind innerhalb des SCF-Komplexes austauschbar und besitzen unterschiedliche Substrat-Spezifitäten.

Eines der am besten charakterisierten F-Box-Proteine ist FBXW7. FBXW7 vermittelt die proteasomale Degradation von wichtigen Onkoproteinen, wie z.B. Cyclin E, MYC, JUN und NOTCH. Dementsprechend wirkt FBXW7 als Tumorsuppressor-Protein und liegt bei verschiedenen Krebsarten häufig mutiert vor. Während bereits eine Reihe von Substraten des FBXW7-Proteins beschrieben wurden, sind die Regulationsmechanismen von FBXW7 selbst bisher nur in Ansätzen verstanden. Um neue Regulationsmechanismen von FBXW7 zu finden, wurde in der vorliegenden Arbeit ein biochemischer Screen für FBXW7-Interaktionspartner durchgeführt.

Immunpräzipitation kombiniert mit Massenspektrometrie identifizierten FBXO45, MYCBP2, XIAP und RAE1 als mögliche Interaktionspartner von FBXW7. Die *in vivo* Verifikation dieser Interaktionen zeigte, dass FBXO45, MYCBP2, XIAP und RAE1 spezifisch mit einem negativ geladenen Motiv in der N-terminalen Domäne der α -Isoform von FBXW7 interagierten. Weitere Interaktionsstudien deuteten darauf hin, dass FBXW7 α , FBXO45, MYCBP2, XIAP und RAE1 einen Komplex bilden. *In vitro* interagierte nur FBXO45 mit dem N-Terminus von FBXW7 α . Dieses Ergebnis deutet

darauf hin, dass FBXO45 in dem Komplex der direkte Interaktionspartner von FBXW7 α ist.

Es wurde bereits in der Literatur beschrieben, dass FBXO45 und MYCBP2 einen Ubiquitin-Ligase-Komplex bilden. Eine durch siRNA vermittelte Runterregulation von FBXO45 und MYCBP2 verursachte einen Anstieg der FBXW7 α -Proteinmengen. Dieser Anstieg wurde spezifisch während eines mitotischen Arrests beobachtet. Außerdem bewirkten FBXO45 und MYCBP2 die Ubiquitylierung von FBXW7 α . Eine Verringerung von FBXO45 führte in einem Cycloheximid-Experiment zu einer erhöhten Stabilität von FBXW7 α . Diese Erkenntnisse lassen darauf schließen, dass FBXO45 und MYCBP2 während eines mitotischen Arrests den proteasomalen Abbau von FBXW7 α stimulieren.

Es ist bekannt, dass FBXW7 den mitotischen Zelltod reguliert. Während eines mitotischen Arrests fördert FBXW7 den Zelltod und verhindert so das Entkommen von Zellen aus dem mitotischen Arrest. In dieser Arbeit wurde gezeigt, dass FBXO45 und MYCBP2 – im Gegensatz zu FBXW7 – den mitotischen Arrest auflösen und auf diese Weise den mitotischen Zelltod verhindern.

Zusammenfassend kann gesagt werden, dass in der vorliegenden Arbeit ein Komplex aus FBXO45 und MYCBP2 als neuer Regulator von FBXW7 α während eines mitotischen Arrests gefunden wurde. Daher tragen die vorliegenden Ergebnisse zu einem besseren Verständnis der Regulationsmechanismen des Tumorsuppressor-Proteins FBXW7 bei. Da FBXW7 den mitotischen Zelltod reguliert, könnte die Regulation von FBXW7 α durch FBXO45/MYCBP2 neue Ansätze für eine effizientere Chemotherapie liefern.

1. Introduction

Specific and efficient degradation of target proteins is required for many important cellular processes. For example, cell-cycle progression could not be maintained in an ordered and unidirectional manner without the highly regulated and fast degradation of cell-cycle key players, such as cyclins (Evans et al., 1983; Glotzer et al., 1991).

The ubiquitin-proteasome system, which mediates the specific degradation of target proteins, uses a small, ~9 kDa protein called ubiquitin as a posttranslational modification to induce the recognition and degradation of the target protein by the proteasome. In addition to protein degradation, the ubiquitin system has been found to cause other effects, depending on the type of ubiquitin modification. The ubiquitin system and the types of ubiquitylation turned out to be highly complex and they are now thought to be involved in most, if not all, processes within the cell. Accordingly, misfunction of ubiquitin system components can cause a plethora of diseases, including cancer (reviewed by Hoeller et al., 2006). Because of the immense importance of the ubiquitin system for the cell, Aaron Ciechanover, Avram Hershko and Irwin Rose were awarded the Nobel Prize in Chemistry 2004 for the original discovery of ubiquitin-mediated protein degradation (Ciechanover et al., 1978, 1980, 1981, Hershko et al., 1979, 1980, 1983).

1.1. The ubiquitin system

1.1.1. The ubiquitylation reaction

For the modification of a substrate protein with ubiquitin (Fig. 1), a three-step cascade reaction is performed by three sequentially acting enzymes (E1, E2, E3). In a first, ATP-dependent reaction, the C-terminal carboxyl group of ubiquitin gets covalently bound to a cysteine residue of the E1 enzyme (ubiquitin activating enzyme), forming a thioester bond. The ubiquitin molecule is then transferred from the E1 enzyme to a cysteine residue of the E2 enzyme (ubiquitin conjugating enzyme). Finally, the E3 enzyme (ubiquitin ligase) mediates the direct or indirect transfer of ubiquitin from the E2 to the substrate protein. In most cases, the C-terminal carboxyl group of ubiquitin gets covalently bound to the ϵ -amino group of a lysine residue in the substrate protein, forming an isopeptide bond (reviewed by Buetow and Huang, 2016).

In an antagonizing reaction, the ubiquitin modification can specifically be cleaved from the substrate protein by members of the de-ubiquitylating enzyme (DUB) family. In human cells, there are about 100 different DUBs (reviewed by Komander et al., 2009).

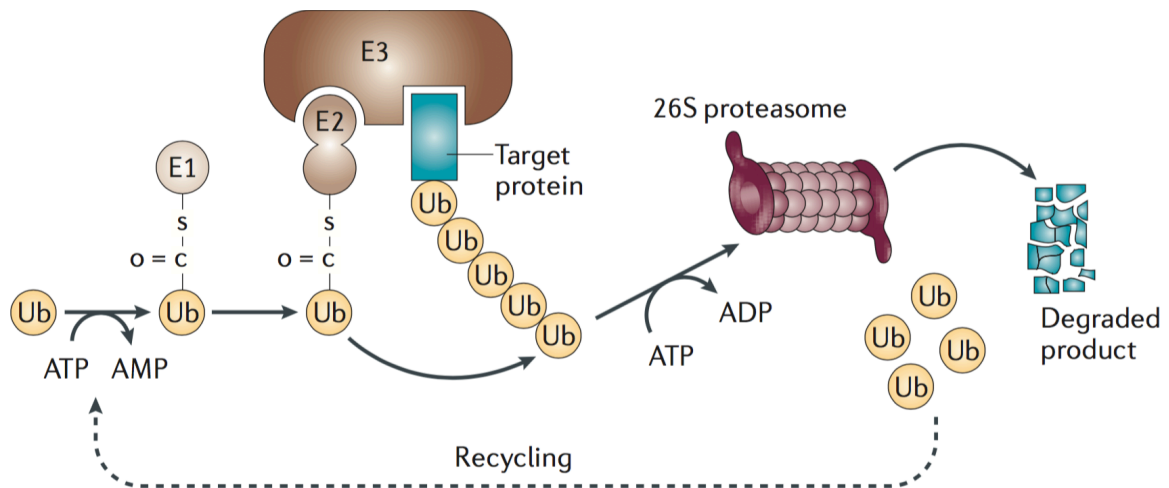


Fig. 1: The ubiquitin-proteasome pathway.

Ubiquitin is attached to a substrate in a three-step cascade reaction mediated by E1, E2 and E3 enzymes. First, ubiquitin is activated in an ATP-dependent reaction and covalently attached to a catalytic cysteine of the ubiquitin activating enzyme (E1). The activated ubiquitin is then transferred from the E1 to a catalytic cysteine of the ubiquitin conjugating enzyme (E2). Finally, the ubiquitin ligase (E3) catalyzes the transfer of the activated ubiquitin to the substrate. While ubiquitin forms thioester bonds with the enzymes of the ubiquitylation pathway, it is bound to the substrate via an isopeptide bond. Depending on the type of ubiquitin ligase, ubiquitin is either directly transferred from the E2 to the substrate (RING E3s) or ubiquitin is first attached to a catalytic cysteine of the E3 and then transferred to the substrate (HECT and RBR E3s). Ubiquitylation can have different consequences depending on the type of modification. For example, K48-linked polyubiquitylation is one of the most important modifications that targets the substrate protein for proteasomal degradation (modified from Nakayama and Nakayama, 2006).

E1, E2 and E3 enzymes are hierarchically organized, with only two E1 enzymes, about 40 E2 enzymes and more than 600 E3 enzymes encoded by the human genome. As implicated by this organization, E3 enzymes are the components of the system that provide substrate specificity, whereas they share a limited number of E1 and E2 enzymes with less specificity (Buetow and Huang, 2016).

The above described ubiquitylation reaction represents the canonical and major pathway for labeling of substrate proteins with ubiquitin molecules. However, it has recently been discovered that this is not the only type of ubiquitylation reaction.

SdeA, a *Legionella* effector protein secreted into the host cytosol, is able to catalyze substrate ubiquitylation without the need for host E1, E2, E3 or ATP. Instead, it mediates the ADP-ribosylation of an arginine residue (R42) of ubiquitin in an NAD⁺-dependent reaction. The ADP-ribosylated ubiquitin is then transferred to a serine residue of the substrate, releasing AMP and thereby forming a phospho-diester bond between the substrate and the phospho-ribosylated ubiquitin (Bhogaraju et al., 2016; Kotewicz et al., 2017; Qiu et al., 2016). In the future, it will be interesting to see whether this type of ubiquitylation reaction is also used by other pathogenic enzymes or even mammalian enzymatic systems and whether there are additional, yet undiscovered pathways that differ from the canonical ubiquitylation machinery.

1.1.2. Types of ubiquitin ligases

As already mentioned above, the family of E3 ubiquitin ligases represents the most diverse part of the ubiquitylation machinery. Based on their functional domains, ubiquitin ligases can be subdivided into three families, RING (Really Interesting New Gene), HECT (Homologous to E6-AP carboxyl terminus) and RBR (RING-betweenRING-RING) ubiquitin ligases.

There are about 600 RING ubiquitin ligases in humans. They either contain a RING domain, which binds zinc, or a U-box domain, which has a similar structure as the RING domain but lacks zinc. The RING or U-box domain is responsible for the recruitment of the E2, whereas other domains bind to the substrates. With respect to the ubiquitylation reaction, RING ubiquitin ligases serve as adaptors for the direct transfer of ubiquitin from the E2 to the substrate without covalently binding the transferred ubiquitin themselves (reviewed by Lipkowitz and Weissman, 2011).

In contrast to RING E3s, the subfamily of HECT ubiquitin ligases is much smaller, comprising about 30 enzymes in humans. The HECT domain recruits the E2 enzyme. From the E2, the activated ubiquitin is first transferred to a catalytic cysteine in the HECT domain and is then transferred to the substrate. Therefore, in contrast to RING E3s, HECT ubiquitin ligases do not catalyze the direct transfer of ubiquitin to the substrate, but they form a ubiquitin-bound intermediate (reviewed by Rotin and Kumar, 2009).

Finally, there are about 10 RBR ubiquitin ligases in humans. RBR E3s contain two predicted RING domains (RING1 and RING2), which are separated by an in-between-RING (IBR) domain. RING1 recruits the E2, whereas RING2 contains a

catalytic cysteine. Similar to HECT E3s, the catalytic cysteine of RING2 covalently binds the activated ubiquitin before it is transferred to the substrate protein (reviewed by Smit and Sixma, 2014).

1.1.3. The ubiquitin code

The modification of a substrate protein with a single ubiquitin (monoubiquitylation) is only one possible outcome of the ubiquitylation reaction. Several additional types of ubiquitylation are possible, thus adding complexity to the ubiquitin code (reviewed by Komander and Rape, 2012; Yau and Rape, 2016). Instead of a single substrate lysine being modified by a single ubiquitin, multiple lysines can be modified by single ubiquitin molecules (multi-monoubiquitylation). In addition, ubiquitin chains can be formed on a substrate by adding further ubiquitin molecules to an already existing ubiquitin modification (polyubiquitylation). For this polyubiquitylation, the C-terminal carboxyl group of the newly attached ubiquitin gets covalently attached to the already existing ubiquitin modification via one of its lysine residues (K6, K11, K27, K29, K33, K48, K63) or via its N-terminal amino group (M1). The resulting polyubiquitin chain is either homotypic, with only one linkage type occurring in the whole chain, or heterotypic, with different ubiquitin linkage types within the chain. Heterotypic chains can be mixed chains, where every ubiquitin is linked to only one additional ubiquitin via one of its lysines or its N-terminus, or branched chains, where at least one ubiquitin in the chain is linked to more than one ubiquitin via its lysines or its N-terminus. Moreover, the ubiquitin molecules can be modified themselves, for example by acetylation or by phosphorylation. In summary, these complexities enable the ubiquitin system to encode highly diverse information by modifying a specific substrate protein.

1.1.4. Effects of substrate ubiquitylation

The diverse topologies of different ubiquitin modifications are specifically recognized by ubiquitin receptors that use ubiquitin-binding domains (UBDs) to interact with ubiquitylated proteins. By specifically binding to ubiquitylated proteins, ubiquitin receptors are able to interpret the ubiquitin code and to link ubiquitylated proteins to corresponding effector pathways. For example, K48-linked polyubiquitin chains are recognized by the proteasome, which then degrades the ubiquitylated substrate protein and releases free ubiquitin monomers (Fig. 1). But also other effects apart

from degradation can be caused by ubiquitylation. Ubiquitylation plays a central role for important cellular processes such as NF- κ B signaling, DNA repair, as well as xenophagy and mitophagy (reviewed by Dikic et al., 2009).

1.1.5. Ubiquitin-like modifiers

Similar to ubiquitin, ubiquitin-like modifiers have been discovered to become covalently attached to substrate proteins by a comparable machinery of E1s, E2s and E3s. Examples for ubiquitin-like modifiers are SUMO, NEDD8, ATG8, ATG15, ISG15 and FAT10. SUMO modifications have various effects, for example on the regulation of protein localization, signaling, DNA replication, transcription as well as DNA repair (reviewed by Flotho and Melchior, 2013). NEDD8 has mainly been characterized as an activator of Cullin-RING ubiquitin ligases, but also has other functions (reviewed by Enchev et al., 2015). ATG8 and ATG15 are regulators of autophagy (reviewed by Ohsumi, 2001). ISG15 and FAT10 are involved in the regulation of the immune system (reviewed by Liu et al., 2005).

1.2. The SCF complex is a Cullin-RING ubiquitin ligase

1.2.1. Cullin-RING ubiquitin ligases (CRLs)

Among the large subfamily of RING E3s, there is a group of multi-subunit ubiquitin ligase complexes called Cullin-RING ubiquitin ligases (CRLs). CRLs have a modular organization (Fig. 2) and dramatically increase their potential of substrate binding by incorporating numerous interchangeable substrate recognition subunits (reviewed by Petroski and Deshaies, 2005; Skaar et al., 2013).

CRLs all contain a central Cullin subunit. In humans, there are 6 closely related Cullin family members (CUL1, CUL2, CUL3, CUL4A, CUL4B and CUL5). In addition, there are two more distantly related Cullin proteins (CUL7 and CUL9), which form atypical Cullin-based ligase complexes. Also APC2, a central subunit of the APC/C, is related to the Cullin protein family.

Within CRL complexes, the Cullin subunit serves as a central scaffold. On the one hand, it interacts with a RING domain containing protein (either RBX1 or RBX2), which is responsible for the recruitment of the E2 enzyme to the complex. On the other hand, the Cullin protein interacts with a substrate recognition module that recruits the substrate to the complex. In most cases, the substrate recognition

module consists of several subunits, a substrate binding subunit and one or two adaptor proteins that link the substrate binding subunit to the Cullin scaffold.

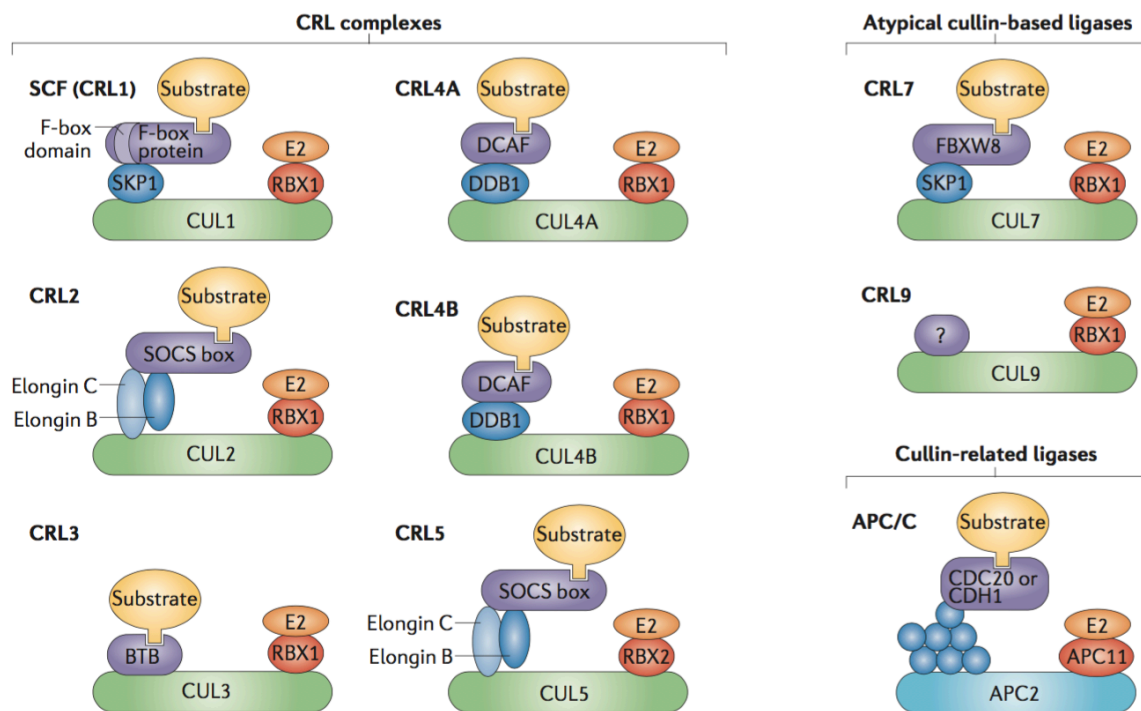


Fig. 2: Overview of Cullin-RING ubiquitin ligases (CRLs).

Six Cullin proteins (CUL1, CUL2, CUL3, CUL4A, CUL4B and CUL5) form canonical CRL complexes in humans. The Cullin protein serves as the central scaffold and recruits other subunits that mediate interactions with E2s and substrates. The RING domain containing proteins RBX1 and RBX2 recruit E2 enzymes to CRLs, whereas different substrate recognition modules have evolved for the different CRL complexes. SKP1 and F-box proteins form the substrate recognition module in CRL1 (SCF complex). SKP1 acts as an adaptor protein that interacts with the F-box domain of the F-box protein and thereby links the F-box protein to the rest of the complex. The F-box protein directly interacts with the substrate. Adaptor and substrate binding proteins are also found in CRL2/CRL5 (Elongin B and Elongin C as well as SOCS box proteins) and CRL4A/B (DDB1 and DCAF proteins). In CRL3, a BTB protein unites the functions of adaptor and substrate binding proteins. Atypical CRL complexes are formed by CUL7 and CUL9. Also the APC2 subunit of the APC/C is related to the Cullin protein family (adopted from Skaar et al., 2013).

CUL1 binds to the adaptor protein SKP1 (S phase kinase-associated protein 1), which interacts with a substrate binding F-box protein. CUL2 as well as CUL5 use the two adaptor proteins Elongin B and Elongin C to recruit a SOCS (suppressor of cytokine signaling) box protein for substrate binding. CUL4A and CUL4B bind to the adaptor protein DDB1 (DNA damage-binding protein 1), whereas a DCAF (DDB1- and CUL4-associated factor) protein serves as the substrate binding subunit. CUL3,

however, interacts with a single BTB (bric-a-brac-tramtrack-broad complex) protein, which unites the functions of the adaptor and substrate binding proteins (reviewed by Petroski and Deshaies, 2005; Skaar et al., 2013).

1.2.2. Regulation of CRL activity

There are several mechanisms for the fine-tuning of CRL activity. Whereas many of them target specific CRL subunits and thereby have a limited effect on CRL complexes, other regulators have a more general effect on CRL activity. NEDD8 is a ubiquitin-like modifier that can be attached to a Cullin protein in a cascade reaction requiring E1, E2 and E3 enzymes. Modification of the Cullin subunit by neddylation causes a conformational change that increases the efficiency of ubiquitin transfer from the E2 to the substrate, thus enhancing CRL activity (Osaka et al., 1998; Read et al., 2000). On the other hand, the NEDD8 modification can be removed from the Cullin by the COP9 signalosome (Cope et al., 2002; Lyapina et al., 2001; Yang et al., 2002). Furthermore, CAND1 (Cullin-associated and neddylation-dissociated 1) is a protein that binds to Cullins in their deneddylated state and promotes the interchange of substrate recognition modules within CRLs (Goldenberg et al., 2004; Liu et al., 2002; Pierce et al., 2013; Zheng et al., 2002a).

1.2.3. The SCF complex uses F-box proteins to target its substrates

As described above, CRL1 complexes consist of a central CUL1 subunit, the RING domain containing protein RBX1, the adaptor protein SKP1 and an F-box protein. According to this composition, a CRL1 complex is also referred to as the SCF (SKP1-CUL1-F-box protein) complex (Feldman et al., 1997). The SCF complex is the best-characterized complex among the CRLs as many important substrates of the SCF have been identified and characterized.

In humans, there are about 70 F-box proteins. They all share a conserved F-box domain, which was originally identified in Cyclin F (FBXO1) and which mediates the interaction with SKP1 (Bai et al., 1996; Skowyra et al., 1997). The F-box domain is necessary but not sufficient for the incorporation of an F-box protein into the SCF complex. In addition to the SKP1-F-box protein interaction, there is a direct interaction between the F-box protein and CUL1 (Zheng et al., 2002b). Therefore, F-box proteins that interact with SKP1 are not necessarily incorporated into the SCF complex (Galan et al., 2001; Kaplan et al., 1997; Seol et al., 2001).

In addition to the F-box domain, there are further domains in F-box proteins that mediate interactions with substrates. According to these substrate binding domains, F-box proteins can be classified into three major subfamilies, FBXW proteins (with a WD40 domain), FBXL proteins (with a leucine-rich domain) and FBXO proteins (with other domains). 12 FBXW, 21 FBXL and 36 FBXO proteins are encoded by the human genome. As they are interchangeable within the SCF complex and many F-box proteins have been shown to target numerous substrates for ubiquitylation, the SCF complex regulates a broad range of substrates and processes in the cell (reviewed by Skaar et al., 2013).

Several F-box proteins recognize their substrate proteins upon posttranslational modification of degron motifs within the substrates. In many cases, F-box proteins bind to their substrates in a phospho-dependent manner, but also other modifications, such as glycosylation, induce substrate binding by F-box proteins (reviewed by Skaar et al., 2013).

The SCF complex has a predominant role in the regulation of the cell cycle. Numerous F-box proteins were identified as regulators of important cell-cycle processes. For example, β -TRCP (FBXW1/FBXW11) regulates EMI1, an inhibitor of the APC/C, and PLK4, the master regulator of the centrosome-cycle (Cunha-Ferreira et al., 2009; Margottin-Goguet et al., 2003). FBXW5 mediates the degradation of SAS6 and EPS8, thus regulating centrosome duplication and mitotic progression (Puklowski et al., 2011; Werner et al., 2013). FBXW7 regulates Cyclin E (Koepp et al., 2001; Moberg et al., 2001; Strohmaier et al., 2001) and SKP2 (FBXL1) promotes the degradation of CDK inhibitors (Carrano et al., 1999; Tsvetkov et al., 1999; Yu et al., 1998), whereas FBXO28 promotes mitotic progression (Kratz et al., 2016). There are further examples of cell-cycle regulation by F-box proteins. But F-box proteins also control other essential cellular processes, such as NF- κ B signaling, DNA damage repair and apoptosis.

There are some well-characterized F-box proteins with pronounced roles in cancer. On the one hand, F-box proteins can have oncogenic functions by inducing the degradation of proteins with tumor suppressor functions. An example for such an oncogenic F-box protein is SKP2, which promotes the degradation of the CDK inhibitors p21 and p27. A well-characterized F-box protein with a tumor suppressor function is FBXW7 (reviewed by Wang et al., 2014).

1.3. FBXW7 is a tumor suppressor protein

1.3.1. FBXW7 is conserved from yeast to human

The F-box protein FBXW7 (also called FBW7, Fig. 3) was originally identified in *Saccharomyces cerevisiae* as CDC4 in a genetic screen for cell division cycle mutants (Hartwell et al., 1973). Additional orthologues were identified in *Caenorhabditis elegans* (SEL-10), *Drosophila melanogaster* (Archipelago, AGO) and mouse (Fbxw7). Identification of substrates in *Caenorhabditis elegans* and *Drosophila melanogaster* led to the characterization of the first FBXW7 substrates in humans, NOTCH1 and Cyclin E (Hubbard et al., 1997; Koepp et al., 2001; Moberg et al., 2001; Strohmaier et al., 2001).

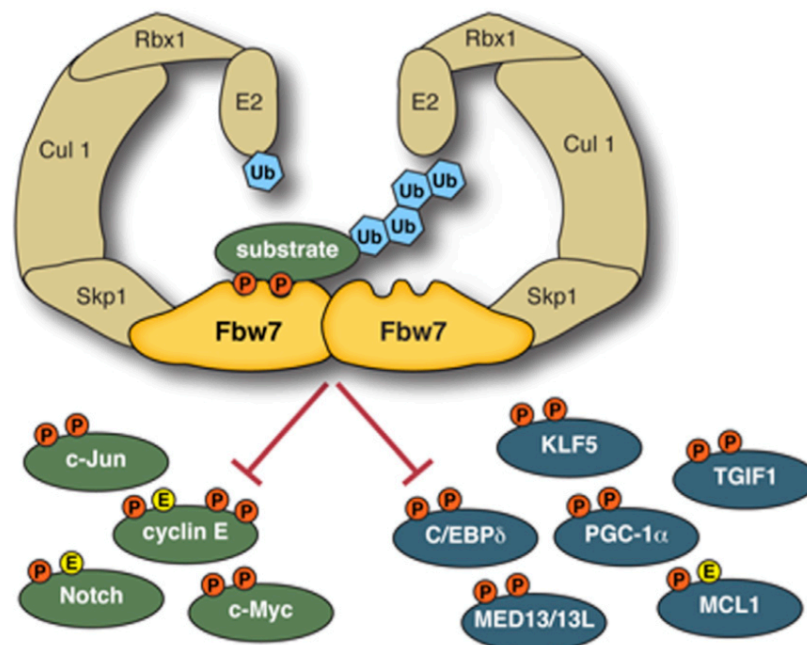


Fig. 3: FBXW7 mediates the SCF-dependent ubiquitylation of important oncoproteins.

FBXW7 (or FBW7) is an F-box protein that serves as the substrate binding subunit of the SCF complex. In addition to the F-box protein, the SCF complex contains the subunits CUL1, SKP1 and RBX1. The E2 binds to RBX1 and transfers an activated ubiquitin to the substrate. FBXW7 is able to dimerize, which is thought to increase substrate ubiquitylation efficiency. FBXW7 interacts with its substrates in a phospho-dependent manner. The CDC4 phosphodegron (CPD) is the motif that is recognized by FBXW7. CPDs usually contain two conserved phosphorylation sites, but one of the phosphorylation sites is also replaced by a negatively charged amino acid residue in some CPDs. Among the substrates of FBXW7 are important oncoproteins, like Cyclin E, NOTCH, MYC and JUN (shown in green). Also other cancer-related substrates are targeted by FBXW7, such as KLF5, TGIF1, MCL1, C/EBP δ , PGC-1 α and MED13/MED13L (shown in blue). By promoting the proteasomal degradation of these substrates, FBXW7 has a pronounced tumor suppressor function (adopted from Davis et al., 2014).

1.3.2. Domain organization of human FBXW7

FBXW7 contains several conserved domains with important functions. Like all F-box proteins, FBXW7 contains an F-box domain that mediates the interaction with SKP1 and thereby enables the incorporation of FBXW7 into the SCF complex (Fig. 4). Moreover, FBXW7 contains a WD40 domain for substrate binding and a dimerization domain (reviewed by Davis et al., 2014; Welcker and Clurman, 2008). FBXW7 dimerization has been shown to improve the efficiency of substrate ubiquitylation as the number of lysines within the substrate that can be attacked by E2s from two different positions is increased (Hao et al., 2007; Kominami et al., 1998; Tang et al., 2007; Welcker and Clurman, 2007; Welcker et al., 2013; Zhang and Koepp, 2006).

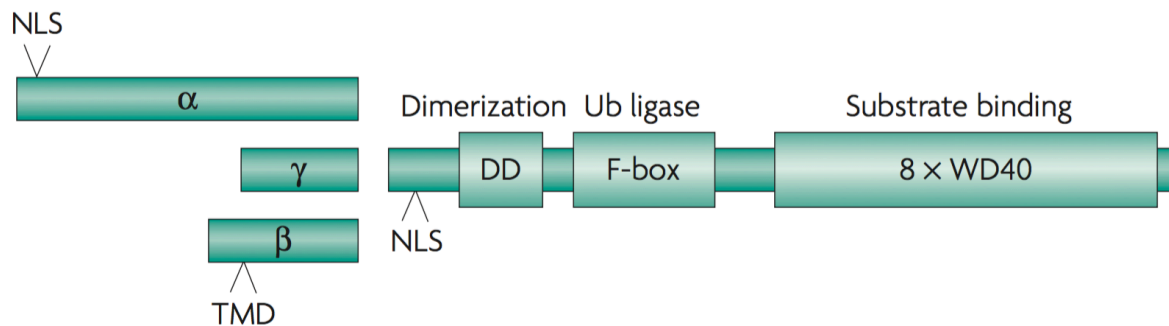


Fig. 4: FBXW7 domain organization.

In humans, there are three FBXW7 isoforms, called FBXW7 α , FBXW7 β and FBXW7 γ . The isoforms only differ in their N-terminal domains, whereas the rest of the protein is conserved among the isoforms. Due to an NLS in its N-terminal domain, FBXW7 α is localized in the nucleoplasm. FBXW7 β contains a transmembrane domain (TMD) in its N-terminal domain, which targets it to cytoplasmic membranes of the ER. FBXW7 γ is localized in nucleoli. The conserved part of FBXW7 contains the F-box domain, which interacts with SKP1, a WD40 domain, which binds FBXW7 substrates, and a dimerization (DD) domain (modified from Welcker and Clurman, 2008).

1.3.3. Human FBXW7 isoforms

In humans, there are three FBXW7 isoforms, FBXW7 α , FBXW7 β and FBXW7 γ . The different isoforms are produced by alternative splicing and the isoform transcripts only differ in their first exon (Fig. 4). Consistently, the protein isoforms contain different N-terminal domains, whereas the rest of the protein, including the dimerization, F-box and WD40 domains, is shared by all FBXW7 isoforms (Spruck et al., 2002).

The differences in the N-terminal FBXW7 domains lead to different FBXW7 isoform localizations. FBXW7 α localizes to the nucleoplasm, whereas FBXW7 β resides in the

cytoplasm and FBXW7 γ is found in nucleoli (Kimura et al., 2003; Welcker et al., 2004).

FBXW7 isoforms also show tissue-specific expression. While FBXW7 α is ubiquitously expressed, FBXW7 β is mainly found in the brain and FBXW7 γ is highly expressed in muscles. In general, FBXW7 α shows higher expression levels than FBXW7 β and FBXW7 γ in many cell lines (Matsumoto et al., 2006; Spruck et al., 2002).

1.3.4. The CDC4 phosphodegron

FBXW7 recognizes its substrates via a short, phosphorylated degron motif that was first identified in yeast and is therefore called CDC4 phosphodegron or CPD (Nash et al., 2001). The CPD usually contains two conserved phosphorylation sites, which are embedded in a proline-rich environment (Table 1). Instead of the phosphorylation sites, some CPDs contain negatively charged amino acid residues (glutamate or aspartate). CPDs with negatively charged residues instead of one or both phosphorylation sites are considered as weak degrons. Substrates with weak CPDs usually require the dimerization of FBXW7 for their efficient ubiquitylation, whereas dimerization-deficient mutants of FBXW7 are not able to mediate the ubiquitylation of these substrates (Welcker et al., 2013).

Table 1: Overview of representative CDC4 phosphodegron (CPD) motifs in Cyclin E, NOTCH1, MYC and JUN.

For each protein, the known degron sequences are specified. A CPD usually contains a central phosphorylation site (marked in red), which is embedded in a proline-rich environment. Counting from the central phosphorylation site, there is an additional phosphorylation site or a negatively charged amino acid residue in the +4 position (marked in bold). The position of the central phosphorylation site in the protein sequence is indicated. The conserved CPD motif has also been discovered in other FBXW7 substrates.

protein name	degron sequence	position	reference
Cyclin E	LIP T PDKE D DD	T62	(Strohmaier et al., 2001)
	GLL T PPQ S GKK	T380	
NOTCH1	PFL T PSP E SPD	T2512	(Thompson et al., 2007)
MYC	LLP T PPL S PSR	T58	(Yada et al., 2004)
JUN	PGE T PPL S PID	T239	(Wei et al., 2005)

The phospho-dependent recognition of substrates by FBXW7 enables different kinases to mediate the regulation of substrates by FBXW7. FBXW7 thereby integrates signals from different pathways in order to ensure ubiquitylation of its substrates in the correct context and under the right conditions. A kinase that is involved in the phosphorylation of many FBXW7 substrates is GSK3 (reviewed by Davis et al., 2014; Welcker and Clurman, 2008).

1.3.5. FBXW7 substrates

1.3.5.1. FBXW7 mediates the degradation of important oncoproteins

One of the first identified FBXW7 substrates was Cyclin E (Koepp et al., 2001; Moberg et al., 2001; Strohmaier et al., 2001). Cyclin E is an important oncoprotein that regulates cell-cycle entry and proliferation in cooperation with CDK2 (Dulić et al., 1992; Koff et al., 1992). Cyclin E contains two CPDs (Table 1), a strong degron around threonine 380 (T380) and a weak degron around threonine 62 (T62). Interestingly, Cyclin E is involved in its own degradation because CDK2 phosphorylates T380 together with GSK3 and a second phosphorylation site in the strong degron motif, S384. By this feedback mechanism, Cyclin E degradation is coupled to CDK2 activity (Clurman et al., 1996; Welcker et al., 2003; Won and Reed, 1996; Ye et al., 2004). A mechanism that opposes the autocatalytically induced degradation of Cyclin E is the dephosphorylation of S384 by the PP2A-B56 phosphatase (Davis et al., 2017).

NOTCH is an additional important oncoprotein that is regulated by FBXW7 (Hubbard et al., 1997). NOTCH is a transmembrane protein, whose intracellular domain gets cleaved by the γ -secretase proteolytic complex and translocates to the nucleus. In the nucleus, the NOTCH intracellular domain acts as a transcription factor that regulates differentiation (reviewed by Artavanis-Tsakonas et al., 1999; Radtke et al., 2005). Interestingly, the NOTCH pathway is not only regulated by FBXW7 via the degradation of its key player NOTCH. In addition, FBXW7 mediates the degradation of Presenilin, which has a NOTCH-activating function because it is part of the γ -secretase proteolytic complex (Li et al., 2002; Wu et al., 1998).

MYC and JUN are transcription factors that are frequently found overexpressed in cancer. By regulating the expression levels of their downstream target genes, MYC and JUN positively regulate cell growth and proliferation (reviewed by Grandori et al.,

2000; Shaulian and Karin, 2002). FBXW7 has a negative effect on this regulation by mediating the degradation of MYC and JUN (Nateri et al., 2004; Yada et al., 2004). Because of the immense importance of the oncoproteins Cyclin E, NOTCH, MYC and JUN for the cell, their protein levels are tightly regulated. Therefore, not all of these proteins are solely regulated by the SCF-FBXW7 complex. For example, Cyclin E is additionally regulated by SCF-SKP2 and a CRL3 complex (Nakayama et al., 2000; Singer et al., 1999). However, as FBXW7 is involved in the regulation of these important oncoproteins, FBXW7 has a prominent tumor suppressor function within the cell.

1.3.5.2. Regulation of transcription by FBXW7

As already described above, FBXW7 regulates the protein levels of transcription factors with important oncogenic functions. In addition, FBXW7 mediates the degradation of further proteins involved in the regulation of transcription, whose roles in FBXW7-linked cancers are not well-characterized so far. However, it is interesting that FBXW7 is able to indirectly regulate the levels of a plethora of proteins involved in many different processes by mediating the degradation of their upstream transcription factors.

For example, FBXW7 has been shown to regulate the lipid and energy metabolism via SREBP and PGC-1 α (Olson et al., 2008; Sundqvist et al., 2005), angiogenesis via HIF-1 α (Cassavaugh et al., 2011; Flügel et al., 2012), pancreatic cell differentiation via NGN3 (Sancho et al., 2014), heat-shock response via HSF1 (Kourtis et al., 2015) and the amplitude of the circadian clock via REV-ERB α (Zhao et al., 2016). Moreover, the cancer-related transcription factors SRC3, KLF5 and MYB were identified as FBXW7 substrates (Kanei-Ishii et al., 2008; Liu et al., 2010; Wu et al., 2007b; Zhao et al., 2010). FBXW7 indirectly regulates TGF β signaling by mediating the degradation of TGIF1, a negative regulator of TGF β -dependent transcription (Bengoechea-Alonso and Ericsson, 2010).

In addition to transcription factors, FBXW7 has also been identified as a regulator of the Mediator complex. The Mediator subunits MED13 and MED13L serve as the direct substrates of FBXW7 within the Mediator complex (Davis et al., 2013). The Mediator complex is involved in a broad range of transcriptional processes, thus highlighting the pronounced role of FBXW7 in the regulation of transcription.

1.3.5.3. FBXW7 is a regulator of cell survival

FBXW7 regulates apoptosis by mediating the degradation of MCL1. MCL1 is an oncogenic protein with an anti-apoptotic function. In the absence of FBXW7, cell survival is increased, thus promoting chemoresistance (Inuzuka et al., 2011; Wertz et al., 2011).

FBXW7 additionally regulates cell survival by targeting the NF- κ B pathway. The NF- κ B pathway component p100 is a substrate of FBXW7. Depending on the tissue context, the regulation of p100 by FBXW7 has different effects on cell survival. Whereas some publications have shown a negative regulation of cell survival by FBXW7-mediated p100 degradation, FBXW7 was shown to act as a pro-survival factor in multiple myeloma (Arabi et al., 2012; Busino et al., 2012; Fukushima et al., 2012).

1.3.5.4. Other substrates of FBXW7

There are additional FBXW7 substrates in the literature that cannot be classified according to the above categories. The Aurora kinases Aurora-A and Aurora-B are important cell-cycle regulators. They have both been suggested as substrates of FBXW7 (Mao et al., 2004; Teng et al., 2012). Also the mTOR kinase, which regulates cell growth and proliferation, is regulated by FBXW7 (Mao et al., 2008). Finally, FBXW7 supports antiviral responses by mediating the degradation of SHP2, which leads to the stabilization of RIG-I, a receptor that recognizes RNA viruses (Song et al., 2017).

1.3.6. FBXW7 is frequently mutated in human cancers

Consistent with its role as a tumor suppressor protein, FBXW7 is frequently found mutated in cancer. While FBXW7 is mutated in about 10% of all human tumors, there are clear differences in FBXW7 mutation rates depending on the cancer type. While FBXW7 is often found mutated in T-ALL, cholangiocarcinoma, colorectal cancer and endometrial cancer, it hardly shows mutations in breast cancer or leukemia apart from T-ALL (reviewed by Davis et al., 2014; Welcker and Clurman, 2008).

Interestingly, there is a strong selection for certain heterozygous FBXW7 hot-spot mutations in cancer. Most mutations are found in the WD40 domain of FBXW7, and especially three arginine residues (R465, R479, R505) that mediate interactions with substrate CPDs are frequently mutated. These point mutations occur much more

often than truncations or heterozygous deletions of *FBXW7*. This surprising finding is explained by the fact that arginine point mutants of *FBXW7* are still able to form dimers with wild-type *FBXW7* via their dimerization domain. It is thought that this dimerization of wild-type and mutated versions of *FBXW7* could have dominant-negative effects (reviewed by Davis et al., 2014; Welcker and Clurman, 2008).

1.3.7. Regulation of *FBXW7*

As described above, the downstream effects of *FBXW7* are already well-characterized. On the other hand, the upstream regulation mechanisms of *FBXW7* are still being identified and are only poorly understood so far. In the following, known mechanisms for the regulation of *FBXW7* expression, protein stability, localization and activity will be described.

1.3.7.1. Regulation of *FBXW7* expression by transcription factors

p53 has been described to positively regulate *FBXW7* transcription. However, p53 does not have a general effect on overall *FBXW7* transcript levels, but specifically induces the expression of *FBXW7* β (Kimura et al., 2003; Mao et al., 2004). On the other hand, C/EBP- δ and HES5 were shown to repress *FBXW7* expression. HES5 was described to specifically target *FBXW7* β expression (Balamurugan et al., 2010; Sancho et al., 2013).

1.3.7.2. Regulation of *FBXW7* expression by microRNAs

Protein expression is negatively regulated by microRNAs as they cause degradation of the corresponding mRNA or inhibition of translation (reviewed by Jonas and Izaurralde, 2015). *FBXW7* expression is targeted by several microRNAs, including miR-25, miR-27a, miR-92a and miR-223 (Lerner et al., 2011; Lu et al., 2012; Xu et al., 2010; Zhou et al., 2015).

1.3.7.3. Regulation of *FBXW7* protein stability

Like many other ubiquitin ligases, *FBXW7* performs auto-ubiquitylation within the SCF complex (Galan and Peter, 1999). The level of *FBXW7* auto-ubiquitylation is regulated by other proteins. For example, GLMN binds to the RBX1 subunit of the SCF complex and inhibits its activity. The inhibition of SCF-*FBXW7* activity caused by

GLMN binding causes an increased FBXW7 auto-ubiquitylation, thus leading to decreased FBXW7 protein levels (Tron et al., 2012).

Another regulator of FBXW7 auto-ubiquitylation is PIN1. PIN1 was suggested to directly bind FBXW7 and inhibit its dimerization. The resulting FBXW7 monomers showed an increase in auto-ubiquitylation (Min et al., 2012). However, these findings are still under debate because another study showed that only ectopic FBXW7 monomers are unstable, whereas there is no difference between endogenous FBXW7 monomer and dimer stabilities. Moreover, the inhibitory effect of PIN1 on FBXW7 dimerization could not be confirmed (Welcker et al., 2013).

PLK2 was shown to phosphorylate FBXW7, thereby promoting its destabilization (Cizmecioglu et al., 2012). An additional study showed that FBXW7 is stabilized upon phosphorylation by PI3K (Schülein et al., 2011).

The only ubiquitin ligase that has been identified as a regulator of FBXW7 protein levels so far is Parkin. However, Parkin is not a general regulator of all human FBXW7 isoforms. Instead, it specifically regulates the protein levels of FBXW7 β (Ekholm-Reed et al., 2013).

It was suggested that FAM83D regulates the protein levels of FBXW7 (Wang et al., 2013). However, the mechanism of this putative regulation is only poorly characterized so far and further investigation is required to confirm this observation.

As observed for many other proteins that are degraded after ubiquitylation, FBXW7 is stabilized by the de-ubiquitylating activity of DUBs. USP28 is involved in the regulation of FBXW7 protein levels (Schülein-Völk et al., 2014).

1.3.7.4. Regulation of FBXW7 protein localization

As the three human FBXW7 isoforms reside in different compartments of the cell, a change in FBXW7 isoform localization affects FBXW7 function. In the literature, there are examples for factors that are able to regulate FBXW7 localization. The FBXW7 pseudosubstrate EBP2 was shown to mediate the nucleolar localization of FBXW7 γ (Welcker et al., 2011). Moreover, protein kinase C (PKC) phosphorylates FBXW7 α in close proximity of one of its NLS motifs and thereby modulates the nuclear localization of FBXW7 α (Durgan and Parker, 2010).

1.3.7.5. Regulation of SCF-FBXW7 ubiquitin ligase activity

The ubiquitin ligase activity of the SCF-FBXW7 complex can be regulated without affecting the protein levels of FBXW7 or other SCF subunits. As described above, there are general mechanisms for the regulation of overall SCF activity, including neddylation or CAND1 activity. However, there are proteins that have been described as specific regulators of SCF-FBXW7 activity.

The pseudophosphatase STYX has been suggested to inhibit SCF-FBXW7 activity by the direct interaction with the F-box domain of FBXW7, thereby preventing the incorporation into the SCF complex. As the F-box domain is conserved among F-box proteins, further analysis of the specificity of this mechanism is required (Reiterer et al., 2017). On the other hand, NUMB4 has been suggested to promote the formation of the SCF-FBXW7 complex (Jiang et al., 2012).

1.4. MYCBP2 and FBXO45 form a ubiquitin ligase complex

MYCBP2 (MYC binding protein 2) or PAM (protein associated with MYC) is a large, ~500 kDa protein that was originally identified as a MYC interaction partner in human cells (Guo et al., 1998). MYCBP2 is a member of the conserved PHR protein family. Its orthologues are called RPM-1 in *Caenorhabditis elegans*, Highwire in *Drosophila melanogaster* and Phr1 in mouse. Apart from an RCC1-like domain and two PHR domains, whose functions are only poorly characterized so far, MYCBP2 contains a RING domain, providing MYCBP2 with ubiquitin ligase activity (reviewed by Grill et al., 2016; Po et al., 2010).

FBXO45 is an F-box protein that has been shown to interact with MYCBP2. The interaction between FBXO45 and MYCBP2 is conserved, as the FBXO45 orthologues (FSN-1 in *Caenorhabditis elegans* and DFsn in *Drosophila melanogaster*) interact with the corresponding orthologues of MYCBP2 (Liao et al., 2004; Saiga et al., 2009; Wu et al., 2007a). Together with MYCBP2, FBXO45 forms a RING ubiquitin ligase complex, where the RING domain is provided by MYCBP2. This complex also contains SKP1, whereas it is not clear whether CUL1 is involved in the complex formation. FBXO45 contains a conserved F-box domain and a SPRY domain, which recruits substrates to the ubiquitin ligase complex (Chen et al., 2014; Kugler et al., 2010).

MYCBP2 and FBXO45 show high expression levels in the nervous system. In invertebrates, they are specifically expressed in the nervous system, while they are

also found in other tissues in vertebrates. They have conserved functions in the nervous system, including the regulation of synapse and axon formation (reviewed by Grill et al., 2016; Po et al., 2010). MYCBP2 and FBXO45 orthologues partly fulfill their functions in the nervous system by mediating the ubiquitin-dependent degradation of the MAP kinase pathway regulator DLK-1/Wallenda in *C. elegans* and *Drosophila* (Nakata et al., 2005; Wu et al., 2007a).

In human cells, MYCBP2 was described as a negative regulator of adenylyl cyclase activity (Pierre et al., 2004). In addition, it was shown to promote the degradation of Tuberin and the GDP/GTP exchange of Rheb, leading to a positive regulation of mTOR signaling (Han et al., 2008; Maeurer et al., 2009; Murthy et al., 2004). Furthermore, a guanosine exchange factor function of MYCBP2 with respect to Ran was proposed in the nervous system (Dörr et al., 2015).

Human FBXO45 inhibits apoptosis by promoting the degradation of p73 and PAR4 (Chen et al., 2014; Peschiaroli et al., 2009). The degradation of p73 has been suggested to depend on the canonical SCF complex. Therefore, the question remains whether FBXO45 can act as an E3 ligase only in complex with MYCBP2 or also in complex with the canonical SCF.

1.5. RAE1 is a mitotic regulator that interacts with MYCBP2

RAE1 is a WD40 domain containing protein that was originally identified as an mRNA export factor in yeast (Brown et al., 1995). In vertebrates, RAE1 has been described to regulate the mitotic checkpoint as loss of RAE1 leads to mitotic checkpoint defects and chromosome missegregation (Babu et al., 2003). Furthermore, RAE1 mediates mitotic spindle assembly in a ribonucleoprotein complex as well as in cooperation with NUMA (Blower et al., 2005; Wong et al., 2006). In addition, RAE1 inhibits APC/C-CDH1 during mitosis (Jeganathan et al., 2005). These findings indicate that RAE1 has important functions with respect to mitotic progression.

Two studies in *Drosophila melanogaster* and *Caenorhabditis elegans* have identified RAE1 as an interaction partner of the corresponding MYCBP2 orthologues (Grill et al., 2012; Tian et al., 2011). The interaction between RAE1 and MYCBP2 is conserved. However, the functional mechanism of this interaction remains elusive. While *Drosophila* RAE1 stabilizes Highwire by preventing its autophagy-dependent degradation, *C. elegans* RAE1 is proposed to act downstream of RPM-1.

1.6. XIAP is an anti-apoptotic ubiquitin ligase

XIAP (X chromosome-linked IAP, also called BIRC4) is a RING ubiquitin ligase that belongs to the IAP (inhibitor of apoptosis protein) family. Additional IAP family members that are encoded by the human genome are cellular IAPs (cIAP1 and cIAP2) as well as neuronal IAP (NIAP), melanoma IAP (MLIAP), IAP-like protein 2 (ILP2), Survivin and Apollon (reviewed by Fulda and Vucic, 2012).

Similar to other IAP family members, XIAP has an anti-apoptotic function. On the one hand, XIAP prevents apoptosis by inhibiting caspases. XIAP is both able to promote the ubiquitin-dependent degradation of caspases and to inhibit caspases in a ubiquitin-independent manner (Deveraux et al., 1997; Eckelman et al., 2006; Suzuki et al., 2001a). Moreover, XIAP negatively regulates apoptosis by stimulating the NF- κ B pathway (Hofer-Warbinek et al., 2000).

XIAP binds to its substrates via BIR (baculoviral IAP repeat) domains, which are conserved among the IAP family (reviewed by Fulda and Vucic, 2012). Interestingly, XIAP inhibitors have evolved which act as pseudosubstrates and bind to the BIR domains of XIAP and other IAP family members, thereby preventing the interaction of IAPs with their substrates. Two proteins that have been identified as IAP inhibitors are SMAC and HTRA2/OMI (Du et al., 2000; Suzuki et al., 2001b).

XIAP and other IAPs are frequently found overexpressed in human cancers and are thought to promote cancer by inhibiting cancer cell apoptosis. Therapeutic approaches aim at mimicking the SMAC motif that is responsible for the interactions with IAPs. The corresponding drugs are called SMAC mimetics. They are tested in clinical trials as they have the potential to sensitize cancer cells to apoptotic stimuli (reviewed by Fulda and Vucic, 2012).

1.7. Objectives

FBXW7 is an important tumor suppressor protein that is frequently found mutated in human cancers (reviewed by Davis et al., 2014; Welcker and Clurman, 2008). The downstream network of FBXW7 substrates is already well-characterized. As described above, FBXW7 promotes the degradation of proteins that are involved in the regulation of processes like transcription, cell-cycle progression and cell survival. However, the regulation of FBXW7 itself by upstream effectors is only poorly understood so far. Apart from factors that influence FBXW7 expression, there are only few known regulators of FBXW7 protein stability. It has been described that

FBXW7 protein levels are regulated by auto-ubiquitylation (Galan and Peter, 1999). In addition, auto-ubiquitylation can be modulated by additional factors, such as PIN1 and GLMN (Min et al., 2012; Tron et al., 2012). Moreover, kinases like PLK2 and PI3K were shown to phosphorylate FBXW7 and thereby regulate FBXW7 protein stability (Cizmecioglu et al., 2012; Schülein et al., 2011). However, it is not clear whether phospho-dependent changes in FBXW7 stability are solely mediated by its auto-ubiquitylation or whether there are additional E3 ligase(s) regulating FBXW7 degradation. The only E3 ligase that has been shown to regulate FBXW7 protein levels so far is Parkin (Ekholm-Reed et al., 2013). But this regulation has only been observed for the FBXW7 β isoform, whereas E3 ligases regulating the other FBXW7 isoforms remain to be identified. In the literature, there are several well-studied examples of key ubiquitin ligases, which are regulated by other E3s. For example, the degradation of the oncogenic F-box protein SKP2 is promoted by APC/C-CDH1 (Bashir et al., 2004; Wei et al., 2004). It is conceivable that ubiquitin ligases with pronounced tumor suppressor or oncogenic functions need to be tightly controlled by several upstream pathways in order to prevent cancer formation. The identification of novel FBXW7 regulators has the potential to link an important tumor suppressor with novel upstream oncogenic pathways.

This study therefore aims to identify and characterize novel regulators of FBXW7. In order to identify such regulators, I will perform a screen for FBXW7 interaction partners. The screen will be based on an immunoprecipitation and mass spectrometry approach. FBXW7 interaction partners with E3 ubiquitin ligase activity are regarded as putative FBXW7 regulators. In order to confirm the regulation of FBXW7 by the identified proteins, the interactions between FBXW7 and its regulators will be verified. Moreover, I will analyze the effects of the putative regulators on FBXW7 protein levels. Finally, the functional mechanism underlying FBXW7 regulation needs to be identified and characterized.

2. Materials and methods

2.1. Materials

2.1.1. Chemicals and reagents

Acetic acid	Sigma-Aldrich
Agar	Sigma-Aldrich
Agarose	Sigma-Aldrich
Ammonium peroxodisulfate (APS)	Roth
Ampicillin	AppliChem
Amylose resin	New England Biolabs
Aprotinin	Roche
Bio-Rad Protein Assay	Bio-Rad
Bovine Serum Albumin (BSA)	Sigma-Aldrich
Bromophenol blue	Sigma-Aldrich
CL4B sepharose	Pharmacia
Coomassie Brilliant Blue G250	Roth
CnBr-activated sepharose 4B	GE Healthcare
Dimethyl sulfoxide (DMSO)	Sigma-Aldrich
Dithiothreitol (DTT)	Roth
1 kb DNA ladder	Invitrogen
100 bp DNA ladder	Invitrogen
DNA polymerase (DeepVent)	New England Biolabs
dNTPs	GE Healthcare
ECL Western blotting substrate	Millipore
Ethanol	Sigma-Aldrich
Ethanolamine	Sigma-Aldrich
Ethidiumbromide	AppliChem
Ethylenediaminetetraacetic acid (EDTA)	Roth
Fetal bovine serum (FBS)	Sigma-Aldrich, Thermo Scientific
Flag M2 affinity gel, 3xFlag peptide	Sigma-Aldrich
Glucose	Merck
Glycerol	VWR

Materials and methods

Glycine	AppliChem
α -HA agarose	Sigma-Aldrich
Hydrochloric acid	VWR
Kanamycin	AppliChem
IPTG	Biomol
Isopropanol	Sigma-Aldrich
Leupeptin	Roche
Lipofectamine 2000	Invitrogen
Maltose	Sigma-Aldrich
β -mercaptoethanol	Sigma-Aldrich
Methanol	Sigma-Aldrich
Milk powder	Roth
MG132 (Z-Leu-Leu-Leu-al)	Sigma-Aldrich
N-ethylmaleimide (NEM)	Sigma-Aldrich
Nocodazole	Applichem
Nonidet NP40 (Igepal)	MP Biochemicals
Oligonucleotides/primers	Sigma-Aldrich
PBS	Thermo Scientific
Ortho-Phosphoric acid 85%	Roth
PIN	Roche
Ponceau S solution	Serva
Polyethylenimine linear MW ~25000	Polysciences
Prolong Gold	Molecular Probes
Protein A Sepharose	GE Healthcare
Protein marker PageRuler	Thermo Scientific
Protogel (acrylamide/bisacrylamide)	National Diagnostic
Restriction enzymes	New England Biolabs
RiboLock RNase inhibitor	Thermo Scientific
[³⁵ S]-methionine	Perkin Elmer
Sodium azide	Merck
Sodium chloride	Sigma-Aldrich
Sodium dodecyl sulfate (SDS)	Gerbu
Sodium fluoride	Merck
Sodium hydroxide	J.T. Baker

Sodium vanadate		Sigma-Aldrich
T4 DNA ligase		Thermo Scientific
N,N,N',N'-Tetramethylethylenediamine (TEMED)		Roth
Thymidine		Sigma-Aldrich
TLCK (1-Chloro-3-tosylamido-7-amino-2-butanon)		Roche
TPCK (1-Chloro-3-tosylamido-7-amino-2-heptanon)		Roche
Triton X-100		Sigma-Aldrich
Trizma base		Sigma-Aldrich
0.05% Trypsin-EDTA		Thermo Scientific
Trypton		Roth
Tween 20		Sigma-Aldrich
Yeast extract		Gerbu

2.1.2. Laboratory equipment

Autoradiography cassettes	Dr. Goos Suprema	Neolab
Autoradiography films	Fuji X-Ray Film RX1824	Fuji
Cell counting chamber	Neubauer Improved	Brand
Cell culture dishes	Cellstar	Greiner Bio-One
Centrifuges	5415 R	Eppendorf
	5810 R	Eppendorf
	Fresco 17	Thermo Scientific
	Megafuge 1.0R	Heraeus
	RC5C	Sorvall
	Varifuge RF	Heraeus
	WX Ultra 80	Thermo Scientific
Developing machine	CURIX 60	AGFA
DNA gel electrophoresis	Wide Mini-Sub Cell	Bio-Rad
Electrotransfer unit	Transblot SD	Bio-Rad
Filter paper		Whatman
Fluorescence microscope	Cell Observer Z1	Zeiss
Fridge (4°C)	ProfiLine	Liebherr
Freezer (-20°C)	Premium	Liebherr
Freezer (-80°C)	-80°C/HeraFreeze	Heraeus/Sanyo
Gel documentation	Gelstick	Intas

Materials and methods

Glassware	Glass pipettes, measuring cylinders, flasks, bottles	Brand, Schott
Heat block	Thermomixer Compact	Eppendorf
Incubation shaker	Minitron	Infors HT
Laboratory balance	Extend	Sartorius
Light microscope	Axio Vert. A1	Zeiss
Live-cell imaging dish	μ -Slide 8 Well	Ibidi
Luminescent image analyzer	ImageQuant LAS 4000	GE Healthcare
Magnetic stirrers	Ikamag RTC	IKA Labortechnik
Microplate absorbance reader	SPECTROstar Nano	BMG Labtech
Microwave		Sharp
Nitrocellulose membrane	Amersham Protran 0.45 μ m	GE Healthcare
PAGE system	Mini Protean III	Bio-Rad
Parafilm	Parafilm M	New England Biolabs
PCR thermocycler	Mastercycler epgradient S	Eppendorf
pH-meter	Seven Easy	Mettler Toledo
Photometer	BioPhotometer	Eppendorf
Pipettes	Pipetman	Gilson
Pipettor	Pipetboy	Integra
Plasticware	Reaction tubes, falcons, pipette tips, PCR tubes, petri dishes	Eppendorf, Nerbe Plus, Falcon, Biozym, Greiner Bio-One
Power supply	PowerPac Basic/HC	Bio-Rad
Rocking platform shaker	Duomax 2030	Heidolph
Rotating wheel	Test tube rotator	Snijders
Sonifier	Sonifier 250	Branson
Sterile workbench	Sterile GARD Hood A/B3	Baker Company
(Ultra)centrifuge tubes		Beckmann
Vacuum dryer	Geldryer 583	Bio-Rad
Vortex shaker	VF2	IKA Labortechnik
Water bath	12B WNB7	Julabo EM Memmert

2.1.3. Buffers and media

Column buffer:	20 mM Tris-HCl pH 7.4 200 mM NaCl 1 mM EDTA 10 mM β -mercaptoethanol
6x DNA sample buffer:	0.25% bromophenol blue 50 mM Tris-HCl pH 7.6 60% glycerol in ddH ₂ O
4x Laemmli buffer:	0.1 M Tris-HCl pH 6.8 4% SDS 20% glycerol 0.1 M DTT 0.02% bromophenol blue
LB agar plates:	3% agar in LB medium
LB medium:	10 g/l Trypton 5 g/l yeast extract 10 g/l NaCl pH 7.0
NP40 lysis buffer:	40 mM Tris-HCl pH 7.5 150 mM NaCl 5 mM EDTA 10 mM β -glycerophosphate 5 mM NaF 0.5% NP40 freshly added before use: 1 mM DTT 10 μ g/ml TPCK 5 μ g/ml TLCK 0.1 mM Na ₃ VO ₄

Materials and methods

	1 µg/ml Aprotinin
	1 µg/ml Leupeptin
	10 µg/ml Trypsin inhibitor from soybean
PBS:	140 mM NaCl
	2.7 mM KCl
	1.5 mM KH ₂ PO ₄
	8.1 mM Na ₂ HPO ₄
	pH 7.4
PBST:	0.05% Tween-20 in PBS
RIPA lysis buffer:	50 mM Tris-HCl pH 7.4
	1% NP40
	0.5% Na-deoxycholate
	0.1% SDS
	150 mM NaCl
	2 mM EDTA
	50 mM NaF
	freshly added before use:
	1 mM DTT
	10 µg/ml TPCK
	5 µg/ml TLCK
	0.1 mM Na ₃ VO ₄
	1 µg/ml Aprotinin
	1 µg/ml Leupeptin
	10 µg/ml Trypsin inhibitor from soybean
SDS running buffer:	190 mM glycine
	25 mM Tris-HCl, pH 8.3
	0.1% SDS
Semi-dry transfer buffer:	39 mM glycine
	48 mM Tris

3.7% SDS
20% methanol

TAE buffer: 40 mM Tris-HCl pH 7.6
20 mM acetic acid
1 mM EDTA

TBS: 50 mM Tris-HCl pH 7.4
150 mM NaCl

Western blot blocking buffer: 5% milk powder in PBST

Wet transfer buffer: 25 mM Tris
192 mM glycine
20% methanol

2.1.4. Antibodies

2.1.4.1. Primary antibodies

Primary antibodies that were used in the presented thesis are summarized in Table 2.

Table 2: List of primary antibodies.

antibody	origin	WB dilution	clone	source
Caspase-3	rabbit	1:500	H-277	Santa Cruz
Cyclin B1	rabbit	1:1000	---	I.Hoffmann, DKFZ
Cyclin E	mouse	1:1000	HE12	Santa Cruz
FBXO45	rabbit	1:500	NBP1-91891	Novus
FBXW7 α	rabbit	1:1000	A301-720A	Bethyl
Flag (tag)	mouse	1:5000	M2 (F3165)	Sigma-Aldrich
HA (tag)	mouse	1:1000	16B12	Babco
MCL1	rabbit	1:1000	4572	Cell Signaling
MYC	rabbit	1:1000	9402	Cell Signaling

Myc (tag)	mouse	1:500	9E10	Santa Cruz
MYCBP2	rabbit	1:750	---	(Dörr et al., 2015)
RAE1	rabbit	1:1000	---	(Blower et al., 2005)
SKP1	rabbit	1:1000	H-163	Santa Cruz
α -Tubulin	mouse	1:10000	B-5-1-2	Sigma-Aldrich
Ubiquitin	mouse	1:1000	P4D1 (sc-8017)	Santa Cruz
Vinculin	mouse	1:5000	hVIN-1	Sigma-Aldrich
WDR5	rabbit	1:1000	---	(Wysocka et al., 2003)
XIAP	mouse	1:5000	610763	BD Biosciences

2.1.4.2. Secondary antibodies

Secondary antibodies that were used in the presented thesis are summarized in Table 3.

Table 3: List of secondary antibodies.

antibody	origin	WB dilution	source
α -mouse IgG HRP	goat	1:5000	Novus
α -rabbit IgG HRP	donkey	1:5000	Jackson Laboratories

2.1.5. Small interfering RNAs (siRNAs)

Small interfering RNAs (siRNAs) that were used in the presented thesis are summarized in Table 4.

Table 3: List of siRNAs.

siRNA name	siRNA sequence (5'-3')	target gene	source
clAP1	GGCUUGAGGUGUUGGGAAUtt	clAP1	Ambion
CUL4A	GACAAUCCGAAUCAGUACctt	CUL4A	Ambion
DCAF7	GCUGAUCGCCCAUGACAAAtt	DCAF7	Ambion
DDB1	ACACUUUGGUGCUCUCUUUtt	DDB1	Ambion
FBXO45 #1	GGAGAAAGAAUUCGAGUCAtt	FBXO45	Eurofins
FBXO45 #2	ACACAUGGUUAUUGCGUAUtt	FBXO45	Eurofins
FBXO45 #3	GGAGAAAGAAUUCGAGUCA	FBXO45	Dharmacon
	ACACAUGGUUAUUGCGUAU		(SMARTpool)

	AAACACAUGAAGUCGUAAA		
	GUAUGAAACUGGUUGGGUU		
FBXW2 #1	CGGUGAAGUUUGAUGAACAtt	FBXW2	Ambion
FBXW2 #2	CAUGCUGCCUCGUCUCUAAtt	FBXW2	Ambion
FBXW7	ACAGGACAGUGUUUACAAAtt	FBXW7	Ambion
GL2	CGUACGCGGAAUACUUCGAtt	firefly luciferase	Ambion/Eurofins
MYCBP2 #1	CCCGAGAUCUUGGGAAUAAtt	MYCBP2	Eurofins
MYCBP2 #2	GGAAGUAGUUCUGUUUUUU	MYCBP2	Dharmacon
	GCAGAAAUGCCCACACUUU		(SMARTpool)
	GAAUAGUUGUGGUUGGUUU		
	GCAAGGAUUUGGUGUGUGU		
SHPRH #1	GAUACGAUGUUCAACGGAAtt	SHPRH	Ambion
SHPRH #2	GGUCUGAAACUCUACUAUAtt	SHPRH	Ambion
TRAF2 #1	CGAGGGCAUAUAUGAAGAAtt	TRAF2	Ambion
TRAF2 #2	GGACCACGUCAAGACUUGUtt	TRAF2	Ambion
UBR5	AGACAAAUCUCGGACUUGAtt	UBR5	Ambion
VPRBP	GAUGGCGGAUGCUUUGAUAtt	VPRBP	Ambion
XIAP	AAGTGCTTTCCTGTGGAGGA	XIAP	Eurofins

2.1.6. Primers

Primers that were used in the presented thesis for the generation of plasmids are summarized in Table 4.

Table 4: List of primers for the generation of plasmids.

primer name	primer sequence (5'-3')	no.
Flag_Fbxo45_1-110_BamHI_Fw	GCATGGATCCATGGCGGCGC CG	1
Flag_Fbxo45_1-110_XhoI_Rv	GCATCTCGAGTCAAGCACGTA TCTTGGCCTTG	2
Flag_Fbxo45_111-287_BamHI_Fw	GCATGGATCCTTTCAACATGC CTTCAGC	3
Flag_Fbxo45_111-287_XhoI_Rv	GCATCTCGAGCGGCCGCTCAT C	4
Flag_MycBP2_1-1500_XhoI_Fw	GCATCTCGAGATGCCGGTTCC	5

	CGACGGC	
Flag_MycBP2_1-1050_XhoI_Rv	GCATCTCGAGCTAGCCTATTA TGTGTTTACTGGC	6
Flag_MycBP2_1051-1950_XhoI_Fw	GCATCTCGAGTTGGTACCTGC TTCTATATCAGAACC	7
Flag_MycBP2_1051-1950_XhoI_Rv	GCATCTCGAGCTAATACTTCT GATTCAAAATGGCAACTG	8
Flag_MycBP2_1951-2950_XhoI_Fw	GCATCTCGAGGCACCGCCTGC CTTCAACC	9
Flag_MycBP2_1951-2950_XhoI_Rv	GCATCTCGAGCTATATTTTGG GAGATGCTCTCATTTCC	10
Flag_MycBP2_2951-3600_XhoI_Fw	GCATCTCGAGAGTCGAAAATG TGCTAATAGACAC	11
Flag_MycBP2_2951-3600_XhoI_Rv	GCATCTCGAGCTAGTCTGAGA GTGGATGTTTCC	12
Flag_MycBP2_3601-4640_XhoI_Fw	GCATCTCGAGATAGTGATTGC CGGGGAAGC	13
Flag_MycBP2_2951-4640_XhoI_Rv	GCATCTCGAGCTAAAAAGTGT GGGCATTTCTGC	14
Myc-Flag-Rae1_EcoRI_Fw	GCATGAATTCATGAGTCTGTTT GGATCAACC	15
Myc-Flag-Rae1_HindIII_Rv	GCATAAGCTTCTATTTCTTATT CCTTGGCTTTAGC	16
Flag-Fbxw7_C322_deltaF4_HindIII_Rv	GCATAAGCTTTCACCTTCATGTC CACATC	17
Flag_Fbxw7_C9_EcoRI_Fw	GCATGAATTCGGGCAGCAAAA GACGACGAACTGG	18
Flag_Fbxw7_C19_EcoRI_Fw	GCATGAATTCGCTGAGAGGTA ACCCTTCCTCAAGCC	19
Flag_Fbxw7_C40_EcoRI_Fw	GCATGAATTCGGAACAGCAAC AGCAACTCAG	20
Flag_Fbxw7_C85_EcoRI_Fw	GCATGAATTCGATTTCCGGTAG ATGAGGACTCC	21
Flag_Fbxw7_C127_EcoRI_Fw	GCATGAATTCGCAGTCTGATG	22

	ATAGTAGCAGAG	
Flag_Fbxw7_C148_EcoRI_Fw	GCATGAATTCGAGTATTGTGG ACCTGCCCGTTC	23
Flag_Fbxw7_C168_EcoRI_Fw	GCATGAATTCGATGAAAAGAA AGTTGGACCATG	24
Flag_Fbxw7_C322_EcoRI_Fw	GCATGAATTCGAGAGAGAAAT GCAAAGAAGAGG	25
Flag_Fbxw7_N283_N515_deltaF1_EcoRI_Fw	GCATGAATTCGATGAATCAGG AACTGCTC	26
Flag_Fbxw7_delta40-167_Fw	CGTGTGGTAGAGGAGATGAAA AGAAAGTTGG	27
Flag_Fbxw7_delta40-167_Rv	CCAAC TTTCTTTTCATCTCCTC TACCACACG	28
Flag_Fbxw7_delta40-84_Fw	CGTGTGGTAGAGGAGATTTTCG GTAGATGAG	29
Flag_Fbxw7_delta40-84_Rv	CTCATCTACCGAAATCTCCTCT ACCACACG	30
Flag_Fbxw7_delta85-167_Fw	GAAAACAATAATAGATTTATGA AAAGAAAGTTGG	31
Flag_Fbxw7_delta85-167_Rv	CCAAC TTTCTTTTCATAAATCT ATTATTGTTTTTC	32
Flag_Fbxw7_delta106-126_Fw	GATGAAGAACATGCTCAGTCT GATGATAGTAG	33
Flag_Fbxw7_delta106-126_Rv	CTACTATCATCAGACTGAGCAT GTTCTTCATC	34
Flag_Fbxw7_deltaF2_Rv	TTTGCATTTCTCTCTCAATGAA ATGAAGTC	35
Flag_Fbxw7_deltaF3_Fw	GACTTCATTTTCATTGAGAGAGA AATGCAAA	36
Flag_Fbxw7_N105_HindIII_Rv	GCATAAGCTTTCAAGCATGTTC TTCATCTTCCTC	37
Flag_Fbxw7_N117_HindIII_Rv	GCATAAGCTTTCACTCCTCCTC CTCCTCATCC	38
Flag_Fbxw7_N126_HindIII_Rv	GCATAAGCTTTCAATCAAATC	39

	GCTACTCTCC	
Flag_Fbxw7_N137_HindIII_Rv	GCATAAGCTTTCAATGTTTCATC TTCTCTGCTAC	40
Flag_Fbxw7_N147_HindIII_Rv	GCATAAGCTTTCAACTGGAGT TCGTGACACTG	41
Flag_Fbxw7_N157_HindIII_Rv	GCATAAGCTTTTCAGAGTTGGT GAACGGGCAGG	42
Flag_Fbxw7_N167_new_HindIII_Rv	GCATAAGCTTTTCATTTTGTGT TTTTGTATAGAATGG	43
Flag_Fbxw7_N283_HindIII_Rv	GCATAAGCTTTTCACAATGAAAT GAAGTCTCGTTG	44
Flag_Fbxw7_N515_HindIII_Rv	GCATAAGCTTTCAAACAACCCT CCTGCCATCATATTG	45
His_XIAP_NdeI_Fw	GATCCATATGACTTTTAAACAGT TTTG	46
His_XIAP_Sall_Rv	GATCGTCGACCGTAATACGAC TCACTATAG	47
MBP_Fbxw7_FL_N167_EcoRI_Fw	GATCGAATTCATGAATCAGGA ACTGCTCTCTG	48
MBP_Fbxw7_N283_HindIII_Rv	GATCAAGCTTTTCACAATGAAAT GAAGTCTCGTTG	49

2.1.7. Plasmids

Provided and generated plasmids that were used in the presented thesis are summarized in Table 5 and in Table 6.

Table 5: List of provided plasmids.

plasmid (antibiotic resistance, used as DNA template no.)	source
HA-mRAE1 (ampicillin, 1)	D. Lyles, Wake Forest Bapt. Health
HA-Ubiquitin (ampicillin)	T. Hofmann, DKFZ
pCDNA3-Flag-FBXW7 α Δ WD40 (ampicillin)	M. Pagano, New York, USA
pCDNA3.1-Flag-FBXO45 (ampicillin, 2)	A. Peschiaroli, Rome

pCDNA3.1-Flag-FBXW5 (ampicillin)	F. Melchior, ZMBH Heidelberg
pCDNA-Flag-SKP2 (ampicillin)	I. Hoffmann, DKFZ
pCMV-3Tag1A/C, pCMV-3Tag2A (kanamycin)	Agilent
pCMV-3Tag1A-Flag-DCAF5 (kanamycin)	A.-S. Kratz, DKFZ
pCMV-3Tag1A-Flag-FBXO28 (kanamycin)	M. Schmitt, DKFZ
pCMV-3Tag1A-Flag-PLK4 (kanamycin)	M. Arnold, DKFZ
pCMV-3Tag1C-Flag-FBXW7 α (kanamycin, 3)	O. Cizmecioglu, DKFZ
pCMV-Flag-FBXW7 β (ampicillin)	B. Clurman, Seattle, USA
pCMV-Flag-FBXW7 γ (ampicillin)	B. Clurman, Seattle, USA
pCMV-Flag-MISP (kanamycin)	F. Settele, DKFZ
pCMV-Myc-CUL4A (kanamycin)	Y. Xiong, Chapel Hill, USA
pCMV-Myc-DDB1 (kanamycin)	M. Arnold, DKFZ
pCMV-Myc-MYCBP2 (kanamycin, 4)	Addgene #42570
pCS2-HA-XIAP (ampicillin, 5)	E. Lee, Vanderbilt university
pCS2-Myc-XIAP (ampicillin)	E. Lee, Vanderbilt university
pMAL-C2 (ampicillin)	NEB

Table 6: List of plasmids generated by PCR or by PCR-free subcloning.

plasmid	DNA template no.	primer no.	enzymes
pCDNA3.1-HA-FBXO45	2	---	BamHI/XhoI
pCMV-3Tag1A-Flag-FBXO45	2	---	BamHI/XhoI
pCMV-3Tag1A-Flag-FBXO45-N110	2	1,2	BamHI/XhoI
pCMV-3Tag1A-Flag-FBXO45-C111	2	3,4	BamHI/XhoI
pCMV-3Tag2A-Myc-FBXO45	2	---	BamHI/XhoI
pCMV-3Tag1A-Flag-MYCBP2(1-1050)	4	5,6	XhoI
pCMV-3Tag1A-Flag-MYCBP2(1051-1950)	4	7,8	XhoI
pCMV-3Tag1A-Flag-MYCBP2(1951-2950)	4	9,10	XhoI
pCMV-3Tag1A-Flag-MYCBP2(2951-3600)	4	11,12	XhoI
pCMV-3Tag1A-Flag-MYCBP2(3601-4640)	4	13,14	XhoI
pCMV-3Tag1A-Flag-RAE1	1	15,16	EcoRI/HindIII
pCMV-3Tag1A-Flag-XIAP	5	---	EcoRI/Sall

pCMV-3Tag1C-Flag-FBXW7 α -C9	3	17,18	EcoRI/HindIII
pCMV-3Tag1C-Flag-FBXW7 α -C19	3	17,19	EcoRI/HindIII
pCMV-3Tag1C-Flag-FBXW7 α -C40	3	17,20	EcoRI/HindIII
pCMV-3Tag1C-Flag-FBXW7 α -C85	3	17,21	EcoRI/HindIII
pCMV-3Tag1C-Flag-FBXW7 α -C127	3	17,22	EcoRI/HindIII
pCMV-3Tag1C-Flag-FBXW7 α -C148	3	17,23	EcoRI/HindIII
pCMV-3Tag1C-Flag-FBXW7 α -C168	3	17,24	EcoRI/HindIII
pCMV-3Tag1C-Flag-FBXW7 α -C322	3	17,25	EcoRI/HindIII
pCMV-3Tag1C-Flag-FBXW7 α Δ 40-167	3	17,26,27,28	EcoRI/HindIII
pCMV-3Tag1C-Flag-FBXW7 α Δ 40-84	3	17,26,29,30	EcoRI/HindIII
pCMV-3Tag1C-Flag-FBXW7 α Δ 85-167	3	17,26,31,32	EcoRI/HindIII
pCMV-3Tag1C-Flag-FBXW7 α Δ 106-126	3	17,26,33,34	EcoRI/HindIII
pCMV-3Tag1C-Flag-FBXW7 α Δ F-box	3	17,26,35,36	EcoRI/HindIII
pCMV-3Tag1C-Flag-FBXW7 α -N105	3	26,37	EcoRI/HindIII
pCMV-3Tag1C-Flag-FBXW7 α -N117	3	26,38	EcoRI/HindIII
pCMV-3Tag1C-Flag-FBXW7 α -N126	3	26,39	EcoRI/HindIII
pCMV-3Tag1C-Flag-FBXW7 α -N137	3	26,40	EcoRI/HindIII
pCMV-3Tag1C-Flag-FBXW7 α -N147	3	26,41	EcoRI/HindIII
pCMV-3Tag1C-Flag-FBXW7 α -N157	3	26,42	EcoRI/HindIII
pCMV-3Tag1C-Flag-FBXW7 α -N167	3	26,43	EcoRI/HindIII
pCMV-3Tag1C-Flag-FBXW7 α -N283	3	26,44	EcoRI/HindIII
pCMV-3Tag1C-Flag-FBXW7 α -N515	3	26,45	EcoRI/HindIII
pET22b-His-XIAP	5	46,47	NdeI/Sall
pMAL-MBP-FBXW7 α -N167	3	48,49	EcoRI/HindIII

2.1.8. Bacterial strains

The following bacterial strains were used in the presented thesis:

E. coli XL1-Blue: *recA1 endA1 gyrA96 thi-1 hsdR17 supE44 relA1 lac*
 [F' *proAB lac^fZAM15 Tn10 (Tet^r)*]; Agilent Technologies

E. coli Rosetta (DE3): F' *ompT hsdS_B(r_B⁻ m_B⁻) gal dcm* (DE3) pRARE2 (Cam^R);
 Merck

2.1.9. Cell lines

Cell lines that were used in the presented thesis are summarized in Table 7.

Table 7: List of cell lines.

cell line	cell type	source
HCT116 <i>FBXW7</i> ^{+/+} , HCT116 <i>FBXW7</i> ^{-/-}	Human colorectal carcinoma cells; the <i>FBXW7</i> alleles are either wild-type (^{+/+}) or have been inactivated by homologous recombination (^{-/-})	(Rajagopalan et al., 2004)
HEK-293T	Human embryonic kidney cells; the cells constitutively express the SV40 large T antigen	ATCC
HeLa	Human epithelial cervix adenocarcinoma cells; the cells contain HPV-18 sequences	ATCC
U2OS	Human osteosarcoma cells	ATCC

2.1.10. Kits

The following kits were used in the presented thesis:

PureLink Quick Gel Extraction Kit	Invitrogen
QIAGEN Plasmid Maxi Kit	QIAGEN
QIAGEN Plasmid Midi Kit	QIAGEN
QIAprep Spin Miniprep Kit	QIAGEN
QIAquick Gel Extraction Kit	QIAGEN
TNT Coupled Reticulocyte Lysate System	Promega

2.1.11. Antibiotics

Antibiotics that were used in the presented thesis are summarized in Table 8.

Table 8: List of antibiotics.

antibiotic	stock concentration	working concentration
ampicillin	100 mg/ml in ddH ₂ O	100 µg/ml
kanamycin	50 mg/ml in ddH ₂ O	50 µg/ml

2.2. Methods

2.2.1. Methods in molecular biology

2.2.1.1. Polymerase chain reaction (PCR)

Polymerase chain reaction (PCR) was performed in order to amplify DNA fragments for molecular cloning. Forward and reverse primers were designed so that they contained restriction sites. By using these primers for the PCR, the amplified DNA fragments contained the corresponding restriction sites at their 5' and 3' ends. Thus, the DNA fragments could be inserted into DNA vectors with the same restriction sites.

PCR reactions were composed as follows:

ThermoPol Reaction Buffer (NEB):	1x
DNA template:	50 ng
Forward primer:	1 μ M
Reverse primer:	1 μ M
dNTP mix:	0.5 mM
Deep Vent DNA polymerase (NEB):	1 U
ddH ₂ O:	add to 50 μ l

The PCR was performed in a PCR thermocycler with the following settings:

Initial denaturation:	95°C, 2 min	
Denaturation:	95°C, 30 s	} 30 cycles
Annealing:	50-60°C, 30s	
Elongation:	72°C, 1 min/kb	
Final elongation:	72°C, 5 min	
Cooling:	4°C	

The annealing temperature was chosen depending on the melting temperatures (T_m) of the primers. The time for the elongation step depended on the length of the amplified DNA fragment. After the PCR, the amplified DNA fragment was analyzed by agarose gel electrophoresis or purified using the PureLink Quick or the QIAquick gel extraction kits.

2.2.1.2. Agarose gel electrophoresis

Agarose gel electrophoresis was performed in order to separate DNA fragments according to their size. Agarose gels were prepared by boiling 1% agarose in TAE buffer. After the agarose was completely dissolved, the solution was poured into a gel chamber. A comb was inserted into the solution in order to allow well formation. Ethidium bromide was added to a final concentration of 0.5 µg/ml to the solution. After the gel had solidified, it was placed into an electrophoresis chamber. The electrophoresis chamber was filled with TAE buffer until the gel was covered. The DNA samples were mixed with 6x DNA sample buffer and loaded into the wells of the gel. A molecular weight DNA ladder (100 bp or 1 kb) was loaded into an additional well of the gel in order to allow estimation of DNA fragment sizes. The gel was run at 100 V until the dye line was approximately 50% of the way down the gel. DNA fragments in the gel were visualized by UV light. UV light at a wavelength of either 312 nm (for analytical gels) or 366 nm (for preparative gels) was used.

2.2.1.3. Restriction digest of DNA

DNA fragments or DNA vectors were digested by different combinations of restriction enzymes (NEB). In the case of DNA fragments obtained after PCR, the entire PCR product was used for the restriction digest. In the case of DNA vectors, 1-5 µg of DNA were used for the restriction digest. Reactions were performed with 0.5-1 µl of each restriction enzyme and the corresponding NEB reaction buffer in a total volume of 50 µl. The restriction digest reaction was incubated at 37°C for 1-2 h or over night. Reaction buffers, enzyme combinations, and the length of incubation was chosen according to the manufacturer's recommendations. Digested DNA was separated by analytical or preparative agarose gel electrophoresis. Digested DNA was extracted from preparative gels as described in 2.2.1.4.

2.2.1.4. Extraction of DNA fragments from agarose gels

In order to extract DNA fragments from preparative agarose gels, DNA fragments in the gel were visualized by UV light at a wavelength of 366 nm. The desired DNA band was cut out from the gel and transferred to a reaction tube. The DNA was extracted from the agarose gel using the PureLink Quick or the QIAquick gel extraction kit. The extraction was performed according to the manufacturer's

instructions. The DNA was finally eluted with 30-50 μ l ddH₂O. DNA concentration was determined as described in 2.2.1.8.

2.2.1.5. Ligation of DNA fragments

After restriction digest, preparative agarose gel electrophoresis and gel extraction, purified PCR products and DNA vector backbones were ligated. 50 ng of linearized vector DNA was mixed with a fourfold molar concentration of the insert. The DNA mixture was incubated with 2 U of T4 DNA ligase and 1x T4 DNA ligase buffer (Thermo) in a total volume of 10 μ l. The ligation reaction was carried out at RT for 1 h. The whole ligation reaction was used for the transformation of chemically competent *E. coli* XL1-Blue as described in 2.2.1.6.

2.2.1.6. Transformation of chemically competent *E. coli*

Chemically competent *E. coli* XL1-Blue were transformed for plasmid amplification and cloning purposes, whereas chemically competent *E. coli* Rosetta (DE3) were transformed for protein expression. 1 μ g of plasmid DNA or 10 μ l of a ligation reaction were mixed with 100 μ l of chemically competent *E. coli* and incubated on ice for 15 min. The bacteria were then heat-shocked at 42°C for 90 s. After the heat-shock, the transformation reactions were incubated on ice for 2 min. 1 ml of LB medium was added to the bacteria and the cell suspension was incubated at 37°C for 1 h with gentle shaking at 180 rpm. Finally, the bacteria were centrifuged at maximal speed in an Eppendorf 5415 R centrifuge for 1 min. The cell pellet was resuspended in 100 μ l of LB medium and the cell suspension was evenly spread on an LB agar plate containing the appropriate antibiotic (for antibiotic concentrations, see 2.1.11.). The LB agar plate was incubated over night at 37°C. Single *E. coli* colonies were used for the inoculation of overnight cultures containing the appropriate antibiotic.

2.2.1.7. Isolation of plasmid DNA from *E. coli*

E. coli XL1-Blue cells transformed with plasmid DNA were incubated over night in 5 ml (for Miniprep) or 200-250 ml (for Midi- and Maxiprep) LB medium containing the appropriate antibiotic at 37°C with constant shaking at 180 rpm. The plasmid DNA was isolated from the bacteria with the QIAprep Spin Miniprep Kit or the QIAGEN Plasmid Midi/Maxi Kits according to the manufacturer's instructions. Finally, the DNA was dissolved in ddH₂O. DNA concentration was measured as described in 2.2.1.8.

0.5-1 µg of isolated plasmid DNA was analyzed by restriction digest. Plasmid DNA was sequenced with the sequencing services of GATC Biotech or LGC Genomics.

2.2.1.8. Determination of DNA concentration

DNA concentration was determined with a microplate absorbance reader (SPECTROstar Nano, BMG Labtech). 2 µl of the DNA solution were applied onto an LVis plate (BMG Labtech). 2 µl of ddH₂O were used as a blank. The optical density of the samples was measured at 260 nm and 280 nm. The DNA concentration was calculated based on the fact that for a pathlength of 1 cm, an OD₂₆₀ of 1 corresponds to a concentration of double-stranded DNA of 50 µg/ml. The ratio of OD₂₆₀ and OD₂₈₀ was calculated in order to evaluate the quality of the isolated DNA. An OD₂₆₀/OD₂₈₀ ratio of about 1.8 indicates that the DNA solution is pure.

2.2.2. Methods in cell biology

2.2.2.1. Cell culture

Human cell lines were grown in a humidified atmosphere with 5% CO₂ at 37°C. HeLa and U2OS cells were cultured in Dulbecco's Modified Eagle's Medium (DMEM, Sigma-Aldrich) with 1 g/l glucose. HEK-293T cells were grown in DMEM with 4.5 g/l glucose. HCT116 cells were cultured in McCoy's 5A Modified Medium. The media were supplemented with 10% fetal bovine serum (FBS, Sigma-Aldrich or Thermo Scientific).

When the cells reached a confluency of 80-90%, they were subcultured. They were washed once with PBS (Thermo Scientific) and were then incubated for 3-5 min with 0.05% Trypsin-EDTA (Thermo Scientific) at 37°C. After the cells had detached from the cell culture dish, they were resuspended in fresh growth medium. 10-40% of the cell suspension were transferred into a fresh cell culture dish for further culturing.

Cell culture work was performed under sterile conditions. Cell line authentication was regularly performed by Multiplexion in Heidelberg.

2.2.2.2. Harvesting and freezing of cells

HeLa, U2OS and HCT116 cells were harvested by washing with PBS and incubation with 0.05% Trypsin-EDTA for 5 min at 37°C. After the cells had detached from the cell culture dish, they were resuspended in fresh growth medium. Alternatively, HEK-

293T cells were detached from the cell culture dish by rinsing them with growth medium. Cell suspensions were transferred to centrifuge tubes and they were centrifuged at 1300 rpm for 3 min (Eppendorf 5810 R or Heraeus Megafuge 1.0R). Cell pellets were washed once with PBS. Finally, the cell pellets were directly used for the preparation of cell extracts or they were stored at -80°C.

For cell freezing, the cells were washed with PBS and detached from the cell culture dish by incubation with 0.05% Trypsin-EDTA for 5 min at 37°C. The cells were resuspended in growth medium and centrifuged at 1300 rpm for 3 min. The cell pellet was washed with PBS once. Finally, the cell pellet was resuspended in 1 ml of freezing medium (growth medium supplemented with 10% DMSO and 20% FBS instead of 10% FBS) and the cell suspension was transferred to a 1.5 ml cryo vial (Thermo Scientific). The cell suspension was frozen using a freezing container (Nalgene, Thermo Scientific) with a rate of cooling of -1°C/min. When the cryo vial had reached a temperature of -80°C, it was transferred to liquid nitrogen for long-term storage.

2.2.2.3. Transient transfection of mammalian cells

2.2.2.3.1. Transfection of cells with plasmid DNA using polyethylenimine (PEI)

HEK-293T cells were transiently transfected with plasmid DNA using polyethylenimine (PEI, Polysciences). Cells were seeded into cell culture dishes so that they reached a confluency of 70-80% on the day of transfection. For transfections in 10 cm/15 cm dishes, 5-10 µg/10-15 µg of plasmid DNA were mixed with 1.7 ml/4.6 ml of DMEM (4.5 g/l glucose, without FBS) and 34.2 µl/92.5 µl PEI (1 mg/ml in ddH₂O, pH 7.4, sterile filtered). The transfection mixture was vortexed and incubated at RT for 10 min. 5 ml/14 ml of DMEM (4.5 g/l glucose, 5% FBS) were added to the transfection mixture. The transfection mixture was vortexed and added to the cells. The cells were incubated at 37°C and harvested 24-48 h after transfection. If the cells were harvested 48 h after transfection, the transfection mixture was removed 24 h after transfection and replaced by fresh growth medium.

2.2.2.3.2. Transfection of cells with siRNA using Lipofectamine 2000

For the transfection of HeLa or U2OS cells with siRNA, the transfection reagent Lipofectamine 2000 was used according to the manufacturer's instructions. Cells

were seeded into 6-well plates (1×10^5 cells/well) one day before transfection. For each well, 5 μ l of Lipofectamine 2000 were diluted in 150 μ l of DMEM (1 g/l glucose, without FBS). In addition, 30 pmol of siRNA (for a final concentration of 30 nM) were diluted in 150 μ l of DMEM (1 g/l glucose, without FBS). After an incubation for 5 min at RT, both mixtures were combined and incubated for 15 min at RT. The transfection mixture was added to the cells in a dropwise manner in a final volume of 1 ml. The cells were harvested 72 h after transfection.

2.2.2.4. Cell cycle synchronization

In order to arrest HeLa cells in G1/S phase, a double-thymidine block was performed. The cells were treated with 2 mM thymidine for 16 h. After the first thymidine block, the cells were released into the cell cycle by washing three times with PBS and incubation in fresh growth medium for 8 h. The release was followed by a second thymidine block with 2 mM thymidine for 16 h. The cells were finally released from the double-thymidine block by washing three times with PBS and incubation in fresh growth medium. 10-12 h after the release, the cells were enriched in mitosis.

In order to arrest HeLa cells in prometaphase, cells were first synchronized in G1/S phase by treatment with 2 mM thymidine for 17 h. The cells were released into the cell cycle by washing three times with PBS and incubation with fresh growth medium for 5 h. Finally, the cells were treated with 100-250 ng/ml nocodazole for 16-17 h. Mitotic cells were collected by a mitotic shake-off.

2.2.2.5. MG132 and cycloheximide treatment

In order to inhibit proteasomal degradation in HEK-293T cells, the cells were treated with 10 μ M MG132 (Sigma-Aldrich) for 4-5 h before harvesting. In order to inhibit protein synthesis in HeLa cells, they were treated with 100 μ g/ml cycloheximide (Sigma-Aldrich). For a cycloheximide chase assay, the cells were harvested at different time points after cycloheximide treatment.

2.2.2.6. Live-cell imaging

For the analysis of mitotic cell fate, live-cell imaging was performed. U2OS cells were transfected with 30 nM siRNA targeting GL2, FBXW7, FBXO45 or MYCBP2. 48 h after transfection, 2.5×10^4 cells were seeded into Ibidi dish chambers. 72 h after transfection, the cells were treated with 250 ng/ml nocodazole. 4 h after the

nocodazole treatment, the cells were monitored by a 10x/0.3 EC PlnN Ph1 DIC objective on a Zeiss Cell Observer Z1 inverted microscope (AxioCam MRm camera system) with incubation at 5% CO₂ and 37°C. Multi-tile phase-contrast images were taken every 10 min for 48 h using the Zeiss ZEN blue software. Data analysis was performed with ImageJ Fiji software. Cell death was defined by cell morphology and cessation of movement. Mitotic slippage was defined by mitotic exit without cell division.

2.2.3. Methods in protein biochemistry

2.2.3.1. Preparation of protein extracts from mammalian cells

For the preparation of HeLa, HEK-293T or HCT116 cell extracts, the cells were harvested as described in 2.2.2.2. Cell pellets were resuspended in 3-5 volumes of RIPA or NP40 lysis buffer. RIPA lysis buffer was used for the preparation of HCT116 cell extracts. HEK-293T and HeLa cell extracts were either prepared with NP40 lysis buffer (for immunoprecipitations) or with RIPA lysis buffer (for the analysis of protein levels in whole cell extracts and for *in vivo* ubiquitylation assays). The cell lysates were incubated on ice for 30 min with short vortexing every 5-10 min. The lysates were cleared by centrifugation at maximal speed and 4°C in an Eppendorf 5415 R centrifuge for 15 min. The supernatants were transferred to fresh reaction tubes. The protein concentration of the extracts was determined as described in 2.2.3.2. For long-term storage, the cell extracts were frozen in liquid nitrogen and kept at -80°C. For SDS-PAGE, the cell extracts were mixed with equal volumes of 2x Laemmli buffer and incubated at 95°C for 5 min.

2.2.3.2. Determination of protein concentration

The protein concentration of a cell extract was determined according to the Bradford method in a Bio-Rad Protein assay. 1 µl of a cell extract was diluted in 800 µl of ddH₂O. For the calibration curve, different amounts of BSA (0 µg, 3 µg, 5 µg, 7 µg, 10 µg) were diluted in 800 µl of ddH₂O. 200 µl of Bio-Rad Protein Assay solution were added to each reaction tube and the solutions were mixed by inverting the tubes three times. 200 µl of each mixture were transferred to a 96-well plate and the OD₅₉₅ was measured with a microplate reader. Protein concentration of the cell extract was calculated by comparing the OD₅₉₅ with the calibration curve.

2.2.3.3. SDS polyacrylamide gel electrophoresis (SDS-PAGE)

SDS polyacrylamide gel electrophoresis (SDS-PAGE) was performed in order to separate proteins according to their molecular weight. For the preparation and running of polyacrylamide gels, the Mini-Protean vertical electrophoresis system (Bio-Rad) was used. Each polyacrylamide gel consisted of a stacking gel and a separating gel. The stacking gel contained 5% acrylamide (5% acrylamide/bisacrylamide, 125 mM Tris-HCl pH 6.8, 0.1% SDS, 0.1% APS, 0.1% TEMED), whereas the separating gel contained 7-15% acrylamide depending of the size of the proteins to be resolved (7-15% acrylamide/bisacrylamide, 375 mM Tris-HCl pH 8.8, 0.1% SDS, 0.1% APS, 0.1% TEMED). After the polyacrylamide gel had polymerized, 10-30 µg of protein of each sample were incubated in Laemmli buffer at 95°C for 5 min and loaded onto the gel. 3 µl of a prestained protein marker (PageRuler) were also loaded onto the gel in order to allow estimation of protein size. The gel was run at 20 mA/gel in an electrophoresis chamber filled with SDS running buffer.

2.2.3.4. Electrotransfer and Western blot

After SDS-PAGE, the proteins were transferred from the polyacrylamide gel onto a nitrocellulose membrane. Electrotransfer of the proteins was performed using a semi-dry blotting apparatus (Semi-dry blotter MAXI, Roth) or using a wet blotting chamber (Mini Trans-Blot Cell, Bio-Rad). Semi-dry electrotransfer was carried out with semi-dry transfer buffer at 60 mA/gel for 70 min. Wet electrotransfer was performed with wet transfer buffer at 100 V for 60 min or at 30 V over night with constant cooling at 4°C.

In order to assess the quality of the electrotransfer, the nitrocellulose membrane was stained with Ponceau S solution. For the reduction of unspecific antibody binding, the membrane was then incubated with Western blot blocking buffer (5% milk powder, 0.05% Tween-20 in PBS) for 30 min at RT with gentle shaking. In order to detect the protein of interest, the membrane was first incubated with the primary antibody diluted in Western blot blocking buffer for 2 h at RT or over night at 4°C (primary antibodies were diluted as indicated in 2.1.4.1.). After the incubation with the primary antibody, the membrane was washed three times for 10 min each with the washing buffer PBST (0.05% Tween-20 in PBS). The membrane was then incubated with the appropriate HRP-conjugated secondary antibody diluted in Western blot blocking

buffer for 1-2 h at RT (secondary antibodies were diluted as indicated in 2.1.4.2.). The membrane was washed with PBST three times for 10 min each. Chemiluminescence signals were detected using the luminescent image analyzer ImageQuant LAS4000 after incubation of the membrane with ECL Western blotting substrate (Millipore) according to the manufacturer's instructions. Data were processed using the ImageJ Fiji software.

2.2.3.5. Immunoprecipitation assays

2.2.3.5.1. Immunoprecipitation of Flag-tagged proteins using Flag M2 affinity beads

Immunoprecipitations of Flag-tagged proteins were performed using α -Flag M2 affinity beads (Sigma-Aldrich). For each immunoprecipitation reaction, 10-40 μ l of the α -Flag M2 affinity bead suspension were used. The beads were washed twice with TBS, once with glycine buffer (0.1 M glycine-HCl pH 3.5) and three times with TBS. Buffers and beads were kept on ice and centrifugations were performed at 5000 rpm and 4°C for 2 min in an Eppendorf 5415 R centrifuge. HEK-293T cell extracts were prepared with NP40 lysis buffer (as described in 2.2.3.1.) and 6-15 mg of each extract were transferred to the prepared beads. Each reaction was filled up to a final volume of 1 ml using NP40 lysis buffer. The reactions were incubated over night on a rotating wheel at 4°C. After the incubation, the beads were washed 3-5 times with NP40 lysis buffer. Immunoprecipitated proteins were eluted from the beads by competition with 100 μ l of a 3x Flag peptide solution (100-500 ng/ μ l in NP40 lysis buffer). The elution was carried out on ice for 30 min with short vortexing every 5-10 min. After the elution, the beads were centrifuged at 5000 rpm and 4°C for 2 min. 90 μ l of the supernatant were transferred to a fresh reaction tube and 30 μ l of 4x Laemmli buffer were added. After incubation at 95°C for 2 min, 20-40% of the immunoprecipitation sample were analyzed by SDS-PAGE and Western blotting.

2.2.3.5.2. Immunoprecipitation of endogenous proteins using NHS-activated sepharose

Endogenous XIAP was immunoprecipitated using XIAP antibodies covalently bound to NHS sepharose beads (GE). For the coupling of the antibodies to the beads, 20 μ l of the NHS sepharose bead suspension were activated with 1 mM HCl and washed

three times with PBS. 3 μg of the XIAP antibody were added to the beads with PBS in a total volume of 50 μl . For the control reaction, 3 μg of mouse IgG were added to the beads. The reaction was incubated on a rotating wheel at 4°C over night. The beads were centrifuged at 5000 rpm and 4°C for 2 min and the supernatant was removed. 1 ml of a glycine solution (200 mM glycine pH 8.0) was added to the beads and the suspension was incubated on a rotating wheel at RT for 2 h. The beads were washed with PBS twice. HeLa cell extract was prepared using NP40 lysis buffer (as described in 2.2.3.1.). 5-6 mg of the HeLa cell extract were added to the prepared beads in a final volume of 1 ml. The reactions were incubated on a rotating wheel at 4°C over night. After the incubation, the beads were washed three times with NP40 lysis buffer. Finally, the beads were incubated with 30 μl of 2x Laemmli buffer at 95°C for 5 min. After a final centrifugation at 5000 rpm for 5 min, the supernatant was transferred to a fresh tube. 20-25 μl of each sample were analyzed by SDS-PAGE and Western blotting.

2.2.3.5.3. Sequential immunoprecipitation for the analysis of protein complexes

In order to analyze whether proteins exist in ternary complexes, sequential immunoprecipitations were performed. In the first step of the experiment, 15-20 mg of HEK-293T cell extracts were used for an immunoprecipitation directed against a Flag-tagged protein (Flag-FBXW7 α or Flag-MYCBP2). The immunoprecipitation was performed as described above (see 2.2.3.5.1.). Instead of mixing the eluate with Laemmli buffer, it was used for a second immunoprecipitation directed against endogenous XIAP or HA-FBXO45. For the XIAP immunoprecipitation, the procedure was as described above (see 2.2.3.5.2.). HA-FBXO45 was immunoprecipitated with 20 μl of α -HA agarose beads (Sigma-Aldrich) according to the manufacturer's instructions. Finally, the beads were incubated with 30 μl of 2x Laemmli buffer at 95°C for 5 min. The supernatant was analyzed by SDS-PAGE and Western blotting.

2.2.3.6. Colloidal Coomassie staining

As an alternative to electrotransfer and Western blotting after SDS-PAGE, proteins in a polyacrylamide gel were visualized by Colloidal Coomassie staining. Gels were fixed and stained by an incubation with Colloidal Coomassie solution (2% ortho-phosphoric acid, 10% ammonium sulfate, 0.1% Brilliant Blue G250, 20% methanol) with gentle shaking at RT over night. The gel was destained with ddH₂O until the

desired staining intensity was achieved. Stained gels were either analyzed by mass spectrometry or dried on filter paper at 80°C for 1 h in a vacuum dryer.

2.2.3.7. Mass spectrometry analysis

In order to identify interaction partners of Flag-FBXW7 α , Flag-XIAP, Flag-RAE1 or of the Flag-FBXW7 α /XIAP complex, immunoprecipitation assays were performed (as described in 2.2.3.5.). Immunoprecipitation samples were analyzed by SDS-PAGE and stained by Colloidal Coomassie. Analysis was performed by M. Schnölzer (DKFZ Protein Analysis Facility, Heidelberg). Briefly, whole gel lanes were cut into slices. Proteins were reduced and alkylated by incubation with 10 mM DTT in 40 mM NH₄HCO₃ for 1 h at 56°C in the dark and incubation with 55 mM iodoacetamide in 40 mM NH₄HCO₃ for 30 min at 25°C. After washing of the slices with H₂O and 50% acetonitrile, they were dried with 100% acetonitrile. Proteins were digested in-gel with trypsin (0.17 μ g in 10 μ l 40 mM NH₄HCO₃, Promega) at 37°C over night. Tryptic peptides were extracted with 50% acetonitrile/0.1% TFA and 100% acetonitrile. Supernatants were lyophilized and redissolved in 0.1% TFA/5% hexafluoroisopropanol. Solutions were analyzed by nanoLC-ESI-MS/MS. Peptides were separated with a nanoAcquity UPLC system (Waters GmbH). Peptides were loaded on a C18 trap column with a particle size of 5 μ m (Waters GmbH). Liquid chromatography was carried out on a BEH130 C18 column with a particle size of 1.7 μ m (Waters GmbH). A 1 h gradient was applied for protein identification. The nanoUPLC system was connected to an LTQ Orbitrap XL mass spectrometer (Thermo Scientific). Data were acquired with the Xcalibur software 2.1 (Thermo Scientific). The SwissProt database (taxonomy human) was used for database searches with the MASCOT search engine (Matrix Science). Data from individual gel slices were merged. Peptide mass tolerance was 5 ppm, fragment mass tolerance was 0.4 Da and significance threshold was $p < 0.01$.

2.2.3.8. *In vivo* ubiquitylation assays

HEK-293T cells transiently transfected with the indicated plasmids were treated with 10 μ M MG132 4-5 h before harvesting. Cells were harvested (as described in 2.2.2.2.) and cell extracts were prepared with RIPA lysis buffer containing 10 mM of the DUB inhibitor N-ethylmaleimide (NEM, cell extract preparation as described in 2.2.3.1.). 2-3 mg of protein extract were used for each sample. Flag-FBXW7 α was

immunoprecipitated with α -Flag affinity beads (as described in 2.2.3.5.1.). Immunoprecipitation and washing steps were performed with RIPA lysis buffer containing 10 mM NEM. Alternatively, endogenous FBXW7 α was immunoprecipitated by incubation of each protein extract with 1 μ g of FBXW7 α antibody on a rotating wheel at 4°C over night. After the incubation with the antibody, the extracts were incubated with 15 μ l of protein A sepharose beads (GE Healthcare) on a rotating wheel at 4°C for 1 h. The beads were washed four times with RIPA lysis buffer containing 10 mM NEM. Finally, the beads were incubated in 30 μ l of 2x Laemmli buffer at 95°C for 5 min. 25 μ l of the supernatant were analyzed by SDS-PAGE and Western blotting.

2.2.3.9. Expression and purification of recombinant proteins

2.2.3.9.1. Expression and purification of MBP-tagged proteins

Chemically competent *E. coli* Rosetta (DE3) were transformed with pMAL-MBP-FBXW7 α -N167 (as described in 2.2.1.6.). A single colony was used to inoculate 10 ml of LB medium containing 100 μ g/ml ampicillin and 0.2% glucose. The culture was incubated over night at 30°C with constant shaking at 180 rpm. The overnight culture was used to inoculate 1 l of LB medium containing 100 μ g/ml ampicillin and 0.2% glucose. The culture was incubated at 37°C with constant shaking at 180 rpm. When an OD₆₀₀ of 0.5 was reached, the culture was cooled down on ice at 4°C and protein expression was induced by the addition of 0.4 mM isopropyl- β -D-thiogalactopyranoside (IPTG). The culture was further incubated over night at 18°C with constant shaking at 180 rpm. Bacteria were harvested by centrifugation at 5000 rpm and 4°C for 15 min (F10-6x500Y rotor, Piramoon). The pellet was resuspended in 25 ml of cold column buffer. Cell lysis was performed with a high pressure homogenizer (15000-17000 psi/1030-1170 bar for one pass, EmulsiFlex C5, Avestin). The lysate was centrifuged at 20000 g and 4°C for 20 min (WX Ultra 80, Thermo Scientific). The supernatant was applied onto a column with 1 ml of equilibrated amylose resin (NEB). The column with the beads and the extract was incubated on a rotating wheel at 4°C for 1 h. Afterwards, the beads were washed three times with 15 ml of column buffer. Finally, the proteins bound to the beads were eluted with 5 ml of column buffer containing 10 mM maltose. 10 fractions of 500 μ l each were collected. Protein containing fractions were identified by spotting the

fractions on nitrocellulose and staining with Ponceau S solution. Protein containing fractions were pooled and MBP-FBXW7 α -N167 was further purified with a preparative Superdex 200 column in 50 mM Tris-HCl pH 8.0, 100 mM NaCl, 5 mM β -mercaptoethanol, 5% glycerol. Purified MBP-FBXW7 α -N167 fractions were analyzed by SDS-PAGE and Colloidal Coomassie staining. Protein containing fractions were aliquoted, frozen in liquid nitrogen and stored at -80°C.

2.2.3.9.2. Expression and purification of His-tagged proteins

Chemically competent *E. coli* Rosetta (DE3) were transformed with pET22b-His-XIAP (as described in 2.2.1.6.). Protein expression and purification was performed as described in 2.2.3.9.1. with the following modifications: The LB medium was not supplemented with glucose. Instead of column buffer, an *E. coli* lysis buffer (50 mM Tris-HCl pH 8.0, 300 mM NaCl, 5 mM β -mercaptoethanol, 10 mM imidazole) was used. Moreover, 1 ml of Ni-NTA agarose (Qiagen) was used instead of amylose resin. Washing was performed with *E. coli* lysis buffer containing 20 mM imidazole. Proteins were eluted with 10 ml of elution buffer (50 mM Tris-HCl pH 8.0, 100 mM NaCl, 250 mM imidazole, 1 mM β -mercaptoethanol).

2.2.3.10. *In vitro* transcription and translation and *in vitro* binding assays

For *in vitro* binding assays, XIAP, RAE1, FBXO45 and MYCBP2(1951-2950) cDNA sequences in pCMV-3Tag1A backbones were transcribed and translated *in vitro* using the TNT T3 coupled reticulocyte system (Promega) according to the manufacturer's instructions. The proteins were synthesized in the presence of 20 μ Ci [³⁵S]-methionine so that synthesized proteins were radioactively labelled. 20 μ l of the *in vitro* translated proteins were incubated with 10 μ g of MBP-FBXW7 α -N167 or MBP alone coupled to 10 μ l of amylose beads in a final volume of 500 μ l NP40 lysis buffer on a rotating wheel at 4°C for 2 h. The beads were washed five times with 800 μ l of NP40 lysis buffer. Finally, the beads were incubated with 30 μ l of 2x Laemmli buffer at 95°C for 5 min. Input and pull-down samples were analyzed by SDS-PAGE and stained with Colloidal Coomassie. The gel was then incubated with Amersham Amplify Fluorographic reagent (GE Healthcare) for 30 min with gentle shaking. Afterwards, the gel was dried at 80°C for 1 h in a vacuum dryer and analyzed by autoradiography.

2.2.3.11. Pull-down assay with recombinant proteins

In order to analyze the direct interaction between FBXW7 α -N167 and XIAP, a pull-down assay with recombinant MBP-FBXW7 α -N167 and His-XIAP was performed. 10 μ g of either MBP alone or MBP-FBXW7 α -N167 were incubated with 10 μ g of His-XIAP in a total volume of 500 μ l NP40 lysis buffer on a rotating wheel at 4°C for 1 h. 10 μ l of amylose beads were added to each reaction and the reactions were incubated on a rotating wheel at 4°C for 2 h. The beads were washed five times with 800 μ l of NP40 lysis buffer. Finally, the beads were incubated with 30 μ l of 2x Laemmli buffer at 95°C for 5 min and 25 μ l of the supernatant were analyzed by SDS-PAGE and Western blotting.

3. Results

3.1. Identification of novel FBXW7 α interaction partners

3.1.1. Identification of FBXW7 α interaction partners by Flag-FBXW7 α immunoprecipitation and mass spectrometry analysis

In order to identify novel interaction partners of FBXW7, a screen based on immunoprecipitation and mass spectrometry analysis was performed. For this approach, HEK-293T cells were transfected with a plasmid encoding Flag-FBXW7 α . The resulting cell extracts were then used for an immunoprecipitation directed against the Flag tag. The immunoprecipitated proteins were eluted by competition with Flag peptide. The eluates were finally analyzed by Western blotting in order to evaluate the quality of the immunoprecipitation experiment. As shown in Fig. 5A, Flag-FBXW7 α was successfully immunoprecipitated. In addition, MYC was specifically found in co-immunoprecipitation with Flag-FBXW7 α , whereas it was not detected in the control. This was expected since MYC is a known substrate of FBXW7 (Yada et al., 2004). Next, the samples were analyzed by SDS-PAGE and Coomassie staining for subsequent mass spectrometry analysis.

Several protein bands were specifically stained in the Flag-FBXW7 α immunoprecipitation sample, whereas they were not detectable in the control lane (Fig. 5B). Consistently, mass spectrometry analysis detected numerous proteins that specifically co-immunoprecipitated with Flag-FBXW7 α . A selection of these proteins is shown in Fig. 5C. Among the identified proteins were several known interaction partners of FBXW7. Apart from FBXW7 itself, the whole SCF complex (CUL1, SKP1 and RBX1) was identified. Also NEDD8, a small ubiquitin-like protein that serves as a CUL1 modification and stimulates SCF activity (Freed et al., 1999; Osaka et al., 1998; Read et al., 2000), was found. Moreover, some well-characterized FBXW7 substrates were detected, as for example MYC (Yada et al., 2004), NOTCH (Hubbard et al., 1997), MED13/MED13L (Davis et al., 2013), Aurora B (Teng et al., 2012) and mTOR (Mao et al., 2008). Finally, ARIH1 was identified as an FBXW7 interacting protein. ARIH1 is an E3 ligase that has been shown to cooperate with many Cullin-RING E3 ligases for the ubiquitylation of their substrates (Scott et al., 2016). The identification of several known FBXW7 interaction partners suggests that

the screen was successful and that it is a good source for the identification of putative novel FBXW7 regulators.

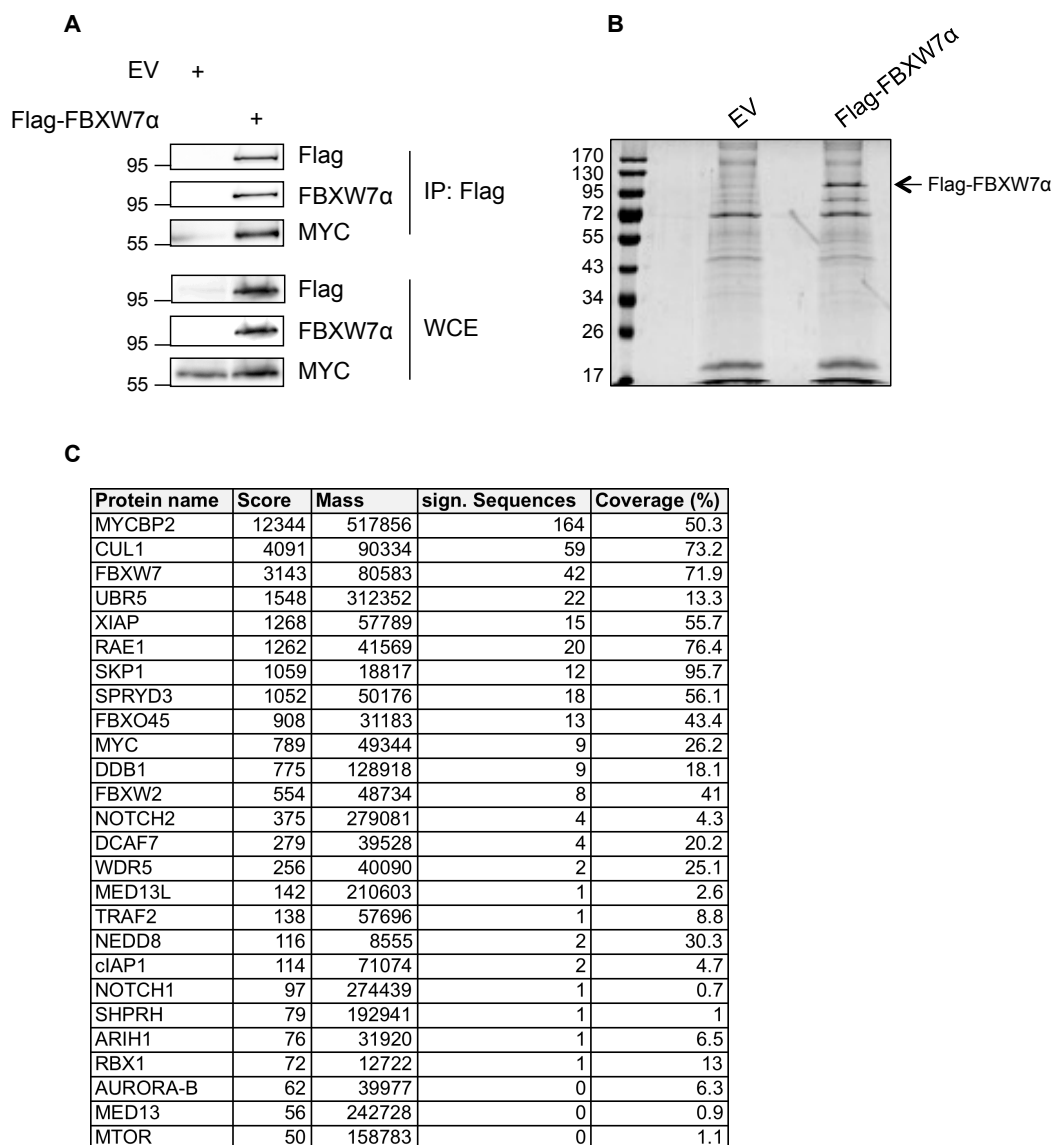


Fig. 5: Immunoprecipitation and mass spectrometry identify putative novel FBXW7 α interaction partners.

A: HEK-293T cells were transfected for 24 h with a construct encoding Flag-FBXW7 α or with an empty vector (EV) as a control. 5 h before harvesting, the cells were treated with MG132 in order to inhibit proteasomal degradation. Flag-FBXW7 α was immunoprecipitated from the cell extracts with α -Flag M2 agarose beads. Immunoprecipitated proteins were eluted from the beads by competition with Flag peptide. Eluted proteins were analyzed by Western blotting using α -Flag, α -FBXW7 α and α -MYC antibodies. WCE: Whole cell extract. **B:** Immunoprecipitated proteins from A were additionally analyzed by SDS-PAGE and stained by Colloidal Coomassie. The position of the Flag-FBXW7 α protein band is marked by an arrow. Whole lanes were cut out from the gel and analyzed by mass spectrometry. **C:** Selection of proteins that were specifically identified in co-immunoprecipitation with Flag-FBXW7 α . For each protein, the MASCOT score, the mass, the number of significant sequences and the coverage are specified.

3.1.2. WDR5 is a putative substrate of FBXW7

Before the mass spectrometry results were analyzed for putative regulators of FBXW7, WDR5 was analyzed in more detail. WDR5 is part of a histone-lysine methyltransferase complex that is involved in the regulation of transcription (Rao and Dou, 2015). Interestingly, WDR5 has been described to cooperate with MYC in oncogenic pathways (Thomas et al., 2015). It is therefore interesting that WDR5 was also identified as a putative interaction partner by mass spectrometry (Fig. 5C).

Because WDR5 cooperates with MYC, it was analyzed as a putative FBXW7 substrate. In order to confirm the interaction between WDR5 and FBXW7 α , cell extracts were prepared from HCT116 cells. As a control, HCT116 cells, where *FBXW7* had been inactivated by homologous recombination (HCT116 *FBXW7*^{-/-}), were used (Rajagopalan et al., 2004). The cell extracts were used for immunoprecipitations directed against endogenous FBXW7 α . The immunoprecipitates were analyzed by Western blotting. As expected, FBXW7 α could only be detected in the immunoprecipitate from HCT116 *FBXW7*^{+/+} cells, but not from HCT116 *FBXW7*^{-/-} cells (Fig. 6A). The known FBXW7 α substrates MYC and Cyclin E were specifically identified in co-immunoprecipitation with FBXW7 α . Interestingly, WDR5 was also found to co-immunoprecipitate with FBXW7 α (Fig. 6A), hence confirming the interaction between FBXW7 α and WDR5.

In order to analyze putative effects of FBXW7 α on WDR5 protein levels, whole cell extracts of HCT116 *FBXW7*^{+/+} and HCT116 *FBXW7*^{-/-} were subjected to Western blot analysis. Interestingly, WDR5 protein levels were increased in the absence of FBXW7 (Fig. 6B).

In order to confirm this result, an siRNA-mediated downregulation of FBXW7 was performed in HeLa cells. As shown in Fig. 6C, WDR5 protein levels were increased upon downregulation of FBXW7.

In summary, FBXW7 α interacts with WDR5 *in vivo* and negatively regulates WDR5 protein levels. Therefore, WDR5 is a promising candidate to be a novel FBXW7 substrate, but further validation will be required. As the main focus of this study is the characterization of FBXW7 regulation, only putative regulators of FBXW7 will be analyzed from here on.

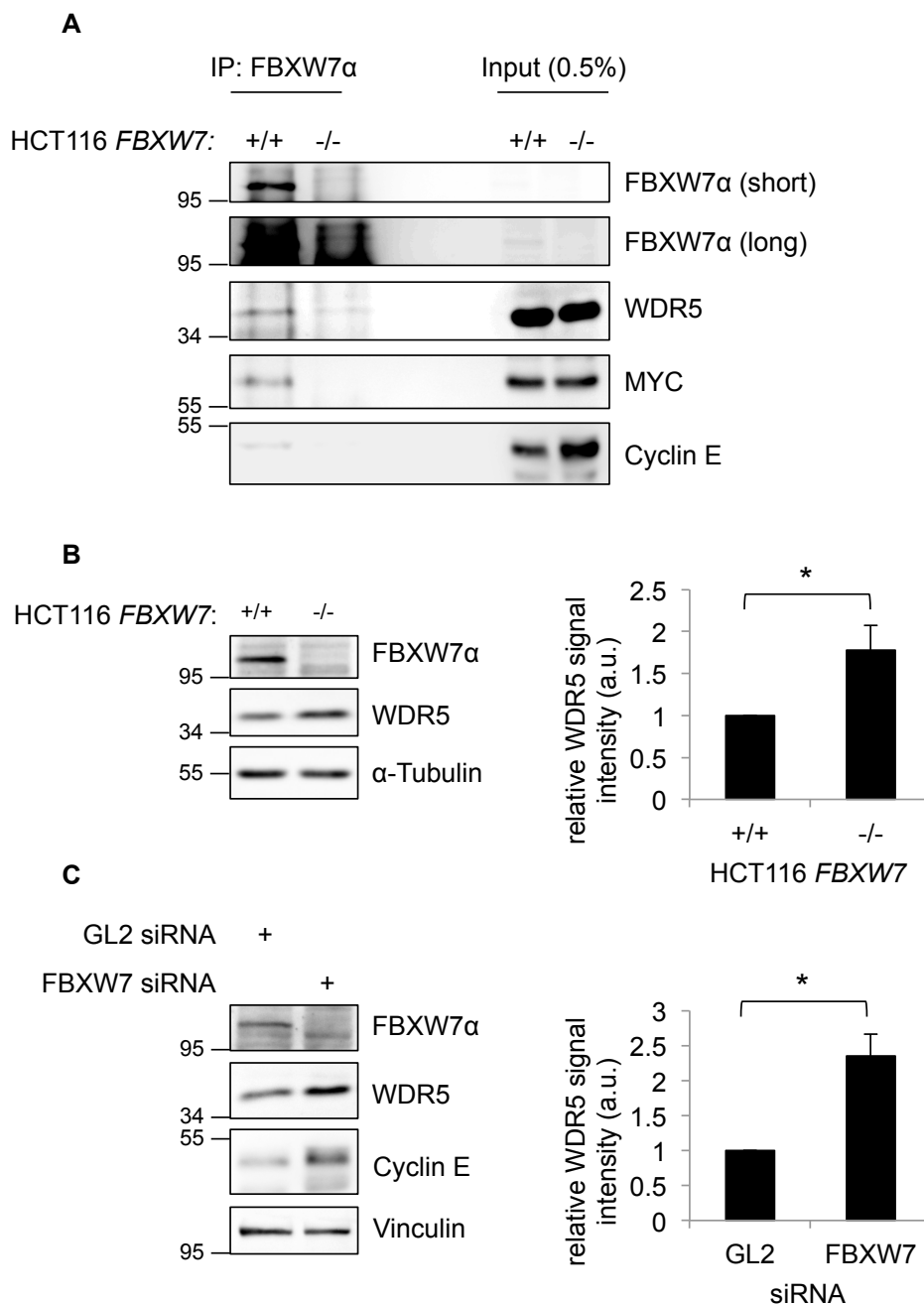


Fig. 6: WDR5 is a putative novel substrate of FBXW7.

A: FBXW7 α and WDR5 interact *in vivo*. Endogenous FBXW7 α was immunoprecipitated from HCT116 cells. HCT116 FBXW7 $^{-/-}$ cells were used as a control. Immunoprecipitates were analyzed by Western blotting with α -FBXW7 α , α -WDR5, α -MYC and α -Cyclin E antibodies. FBXW7 α signals were obtained after short and long exposure times. **B-C:** WDR5 protein levels increase upon depletion of FBXW7. WDR5 protein levels were analyzed by Western blotting in HCT116 FBXW7 $^{-/-}$ cells (B) and after siRNA-mediated downregulation (30 nM siRNA for 72 h) of FBXW7 in HeLa cells (C). In B, HCT116 FBXW7 $^{+/+}$ cells were used as a control, whereas firefly luciferase (GL2) siRNA was used as a control in C. For each blot, quantifications of relative WDR5 signal intensities are shown. Relative WDR5 signals in the HCT116 FBXW7 $^{+/+}$ or GL2 controls were set to 1. Average signal intensities and standard deviations from n=3 experiments were calculated. Statistical significance was analyzed by a two-tailed, unpaired t-test with unequal variance. * p<0.05.

3.1.3. Analysis of putative FBXW7 regulators

Among the proteins that were identified as putative interaction partners of FBXW7 α by mass spectrometry (Fig. 5C), there were several proteins with known E3 ligase activity. These E3 ligases were considered as putative regulators of FBXW7 protein levels.

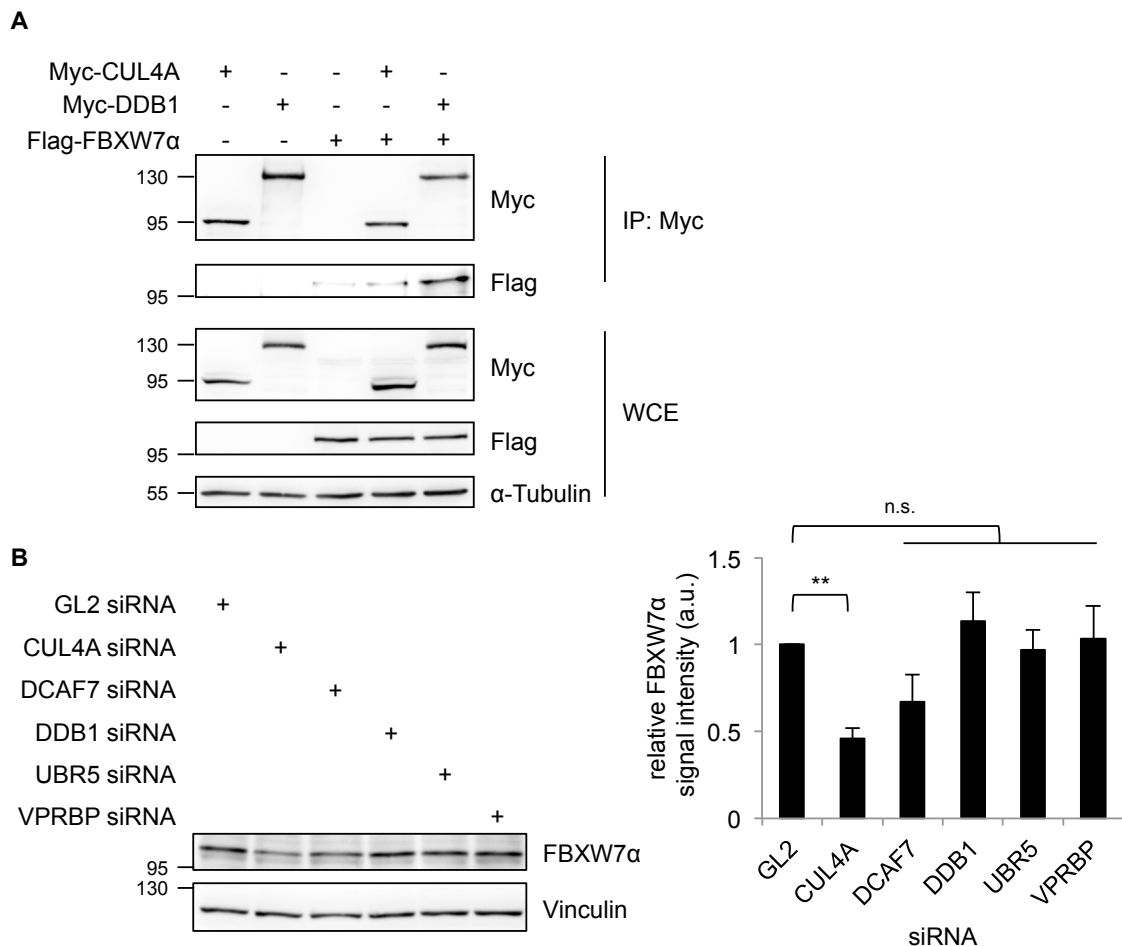


Fig. 7: Analysis of CUL4A, DCAF7, DDB1, UBR5 and VPRBP as putative FBXW7 α regulators.

A: Myc-DDB1 interacts with Flag-FBXW7 α . Flag-FBXW7 α was co-expressed with Myc-DDB1 or Myc-CUL4A in HEK-293T cells for 24 h. The resulting cell extracts were used for immunoprecipitations with α -Myc antibodies. Immunoprecipitates were analyzed by Western blotting with α -Myc, α -Flag and α -Tubulin antibodies. Tubulin was used as a loading control. **B:** FBXW7 α protein levels do not increase upon siRNA-mediated downregulation of putative regulators. HeLa cells were transfected with 30 nM of the indicated siRNAs for 72 h. Cell extracts were analyzed by Western blotting with α -FBXW7 α and α -Vinculin antibodies. Vinculin was used as a loading control. Quantifications of relative FBXW7 α protein levels are shown. Relative FBXW7 α signal intensity in the GL2 control was set to 1. Average signal intensities and standard deviations from $n=3$ experiments were calculated. Statistical significance was analyzed by a two-tailed, unpaired t-test with unequal variance. ** $p < 0.01$, n.s.: not significant.

DDB1 is a component of Cullin4-RING E3 ligases (CRL4s). It serves as an adaptor protein between the central CUL4A/B subunit and the substrate recognition subunit, the DCAF protein (Lee and Zhou, 2007). DDB1 was identified as a putative FBXW7 α interaction partner (Fig. 5C). In order to confirm the interaction between FBXW7 α and DDB1, an immunoprecipitation experiment was performed. Hence, Flag-FBXW7 α and Myc-DDB1 were overexpressed in HEK-293T cells. The cell extracts were used for an immunoprecipitation directed against the Myc tag. The immunoprecipitates were analyzed by Western blotting. Fig. 7A shows that the interaction between DDB1 and FBXW7 α could be confirmed. CUL4A, another subunit of the CRL4 complex, did not interact with FBXW7 α .

Next, FBXW7 α protein levels were analyzed upon siRNA-mediated downregulation of DDB1. Depletion of an FBXW7 α regulator is expected to cause an increase in FBXW7 α protein levels. However, there was no change in FBXW7 α protein levels upon downregulation of DDB1 (Fig. 7B). CUL4A depletion did not cause any increase in FBXW7 α protein levels either. Instead, it led to a decrease in FBXW7 α protein levels. DCAF7 is a DCAF protein that was also identified in the screen as a putative interaction partner of FBXW7 α (Fig. 5C). Thus, its effects on FBXW7 α protein levels were tested in the same experiment, but no increase in FBXW7 α protein levels was observed (Fig. 7B). DDB1 is not only found as a subunit of CRL4s, but it can also form complexes with other proteins. It was shown to form an alternative E3 ligase complex with VPRBP and UBR5 (Maddika and Chen, 2009), which was also found as a putative FBXW7 α interaction partner in the screen (Fig. 5C). However, similar to DDB1 depletion, siRNA-mediated downregulation of UBR5 or VPRBP did not cause any increase in FBXW7 α protein levels (Fig. 7B). Together, these results suggest that CRL4 and DDB1-UBR5-VPRBP E3 ligase complexes do not regulate FBXW7 α protein levels.

In additional experiments, further putative FBXW7 α regulators from the screen were analyzed in respect to their effects on FBXW7 α protein levels. However, siRNA-mediated downregulation of FBXW2, TRAF2, SHPRH, XIAP or cIAP1 did not cause any increase in FBXW7 α protein levels (Fig. 8A-B).

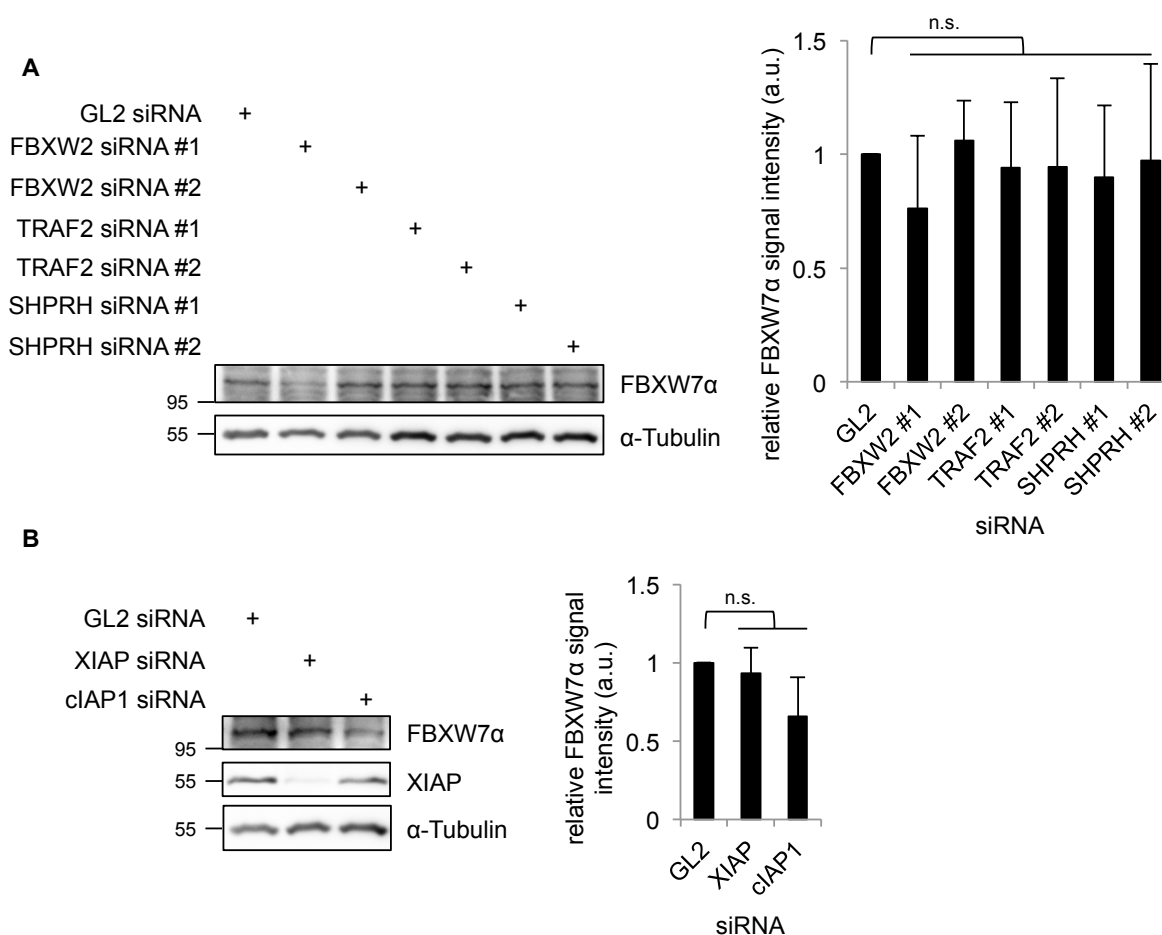


Fig. 8: Analysis of FBXW2, TRAF2, SHPRH, XIAP and cIAP1 as putative FBXW7α regulators.

A-B: FBXW7α protein levels do not increase upon siRNA-mediated downregulation of putative regulators. HeLa cells were transfected with 30 nM of the indicated siRNAs for 72 h. Cell extracts were analyzed by Western blotting with α-FBXW7α, α-XIAP and α-Tubulin antibodies. Tubulin was used as a loading control. Quantifications of relative FBXW7α protein levels are shown. Relative FBXW7α signal intensity in the GL2 control was set to 1. Average signal intensities and standard deviations from n=3 experiments were calculated. Statistical significance was analyzed by a two-tailed, unpaired t-test with unequal variance. n.s.: not significant.

3.2. Characterization of XIAP as a novel interaction partner of FBXW7α

3.2.1. XIAP interacts with FBXW7α *in vivo*

Depletion of XIAP did not cause an increase in FBXW7α protein levels (Fig. 8B). However, XIAP has been described as an inhibitor of apoptosis protein that is frequently found overexpressed in human cancers (reviewed by Gyrd-Hansen and Meier, 2010). Since an interaction between an oncoprotein and a tumor suppressor protein seems likely, it could be meaningful to study the interaction between XIAP and FBXW7α in more detail.

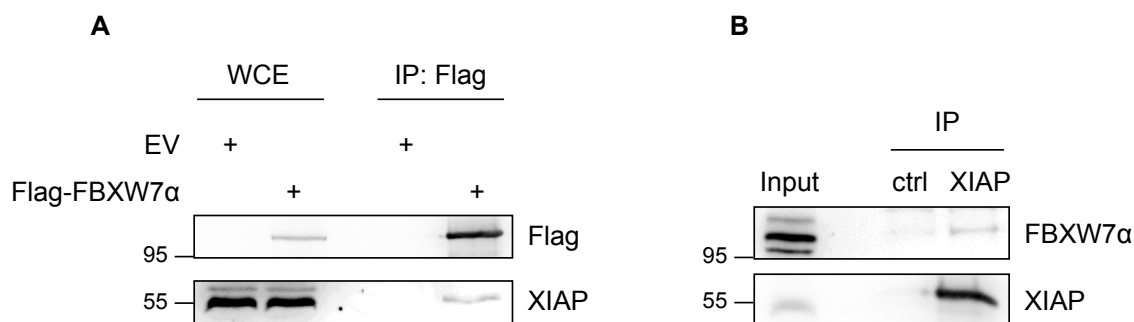


Fig. 9: *In vivo* interaction between FBXW7 α and XIAP.

A: Flag-FBXW7 α interacts with endogenous XIAP in HEK-293T cells. Flag-FBXW7 α was overexpressed in HEK-293T cells for 24 h. An empty vector (EV) was used as a control. The corresponding cell extracts were used for an immunoprecipitation directed against the Flag tag. Immunoprecipitates were analyzed by Western blotting with α -Flag and α -XIAP antibodies. **B:** Endogenous FBXW7 α interacts with endogenous XIAP in HeLa cells. Endogenous XIAP was immunoprecipitated from HeLa cell extracts. Mouse IgG was used for a control immunoprecipitation (ctrl). Immunoprecipitates were analyzed by Western blotting with FBXW7 α and XIAP antibodies.

In order to confirm the interaction between XIAP and FBXW7 α , Flag-FBXW7 α was overexpressed in HEK-293T cells. An immunoprecipitation directed against the Flag tag was performed. Endogenous XIAP was found in co-immunoprecipitation with Flag-FBXW7 α (Fig. 9A). It was also tested whether an interaction between the endogenous proteins exists. HeLa cell extracts were used for an immunoprecipitation directed against endogenous XIAP. Endogenous FBXW7 α co-immunoprecipitated with endogenous XIAP (Fig. 9B). These results show that XIAP and FBXW7 α interact *in vivo*, thus confirming the results from the screen (Fig. 5C).

3.2.2. XIAP specifically interacts with FBXW7 α

In order to test the specificity of the interaction between XIAP and FBXW7 α , it was compared with the interaction between XIAP and other F-box proteins (FBXW5, SKP2 and FBXO28), a substrate recognition subunit of the CRL4 complex (DCAF5) and two other proteins that have no E3 ligase activity (PLK4 and MISP). Flag-tagged versions of these proteins were overexpressed in HEK-293T cells and immunoprecipitated from the corresponding cell extracts via their Flag tags. The immunoprecipitates were analyzed for the presence of endogenous XIAP by Western blotting (Fig. 10). XIAP could only clearly be detected in co-immunoprecipitation with Flag-FBXW7 α , suggesting that the interaction between these two proteins is specific.

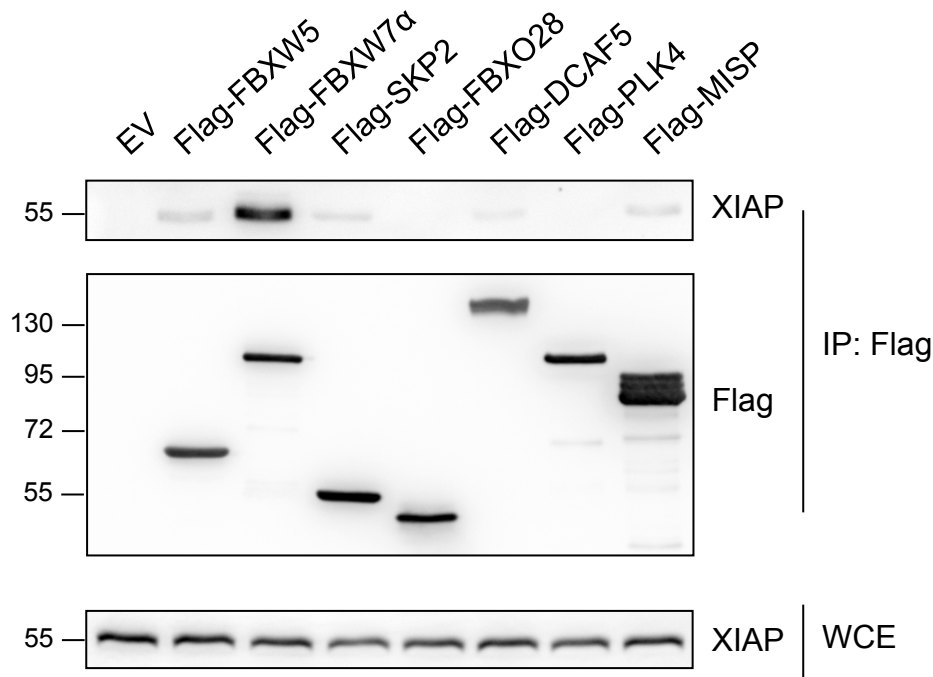


Fig. 10: Specific interaction of XIAP with FBXW7 α .

Flag-tagged FBXW7 α , FBXW5, SKP2, FBXO28, DCAF5, PLK4 and MISP proteins were overexpressed in HEK-293T cells for 24 h. An empty vector (EV) was used as a control. Cell extracts were used for immunoprecipitations with α -Flag agarose beads. Immunoprecipitates were analyzed by Western blotting with α -XIAP and α -Flag antibodies.

3.2.3. The interaction between FBXW7 α and XIAP does not require the F-box or WD40 domains of FBXW7 α

FBXW7 α interacts with SKP1 via its F-box domain, thereby enabling the incorporation of FBXW7 α into the SCF complex (reviewed by Davis et al., 2014; Welcker and Clurman, 2008). In order to exclude that the observed interaction between FBXW7 α and XIAP is indirectly mediated by other SCF subunits, an FBXW7 α mutant with a deletion of the F-box was generated (FBXW7 α Δ F-box). Flag-FBXW7 α or Flag-FBXW7 α Δ F-box were then co-expressed with HA-XIAP in HEK-293T cells and the different Flag-FBXW7 α proteins were immunoprecipitated via their Flag tag. As expected, endogenous SKP1 did not interact with the Flag-FBXW7 α Δ F-box mutant, whereas it clearly bound to Flag-FBXW7 α . HA-XIAP, on the other hand, was found in co-immunoprecipitation with both Flag-FBXW7 α and Flag-FBXW7 α Δ F-box proteins (Fig. 11A). This shows that the interaction between XIAP and FBXW7 α is independent of the incorporation of FBXW7 α into the SCF complex by its F-box domain.

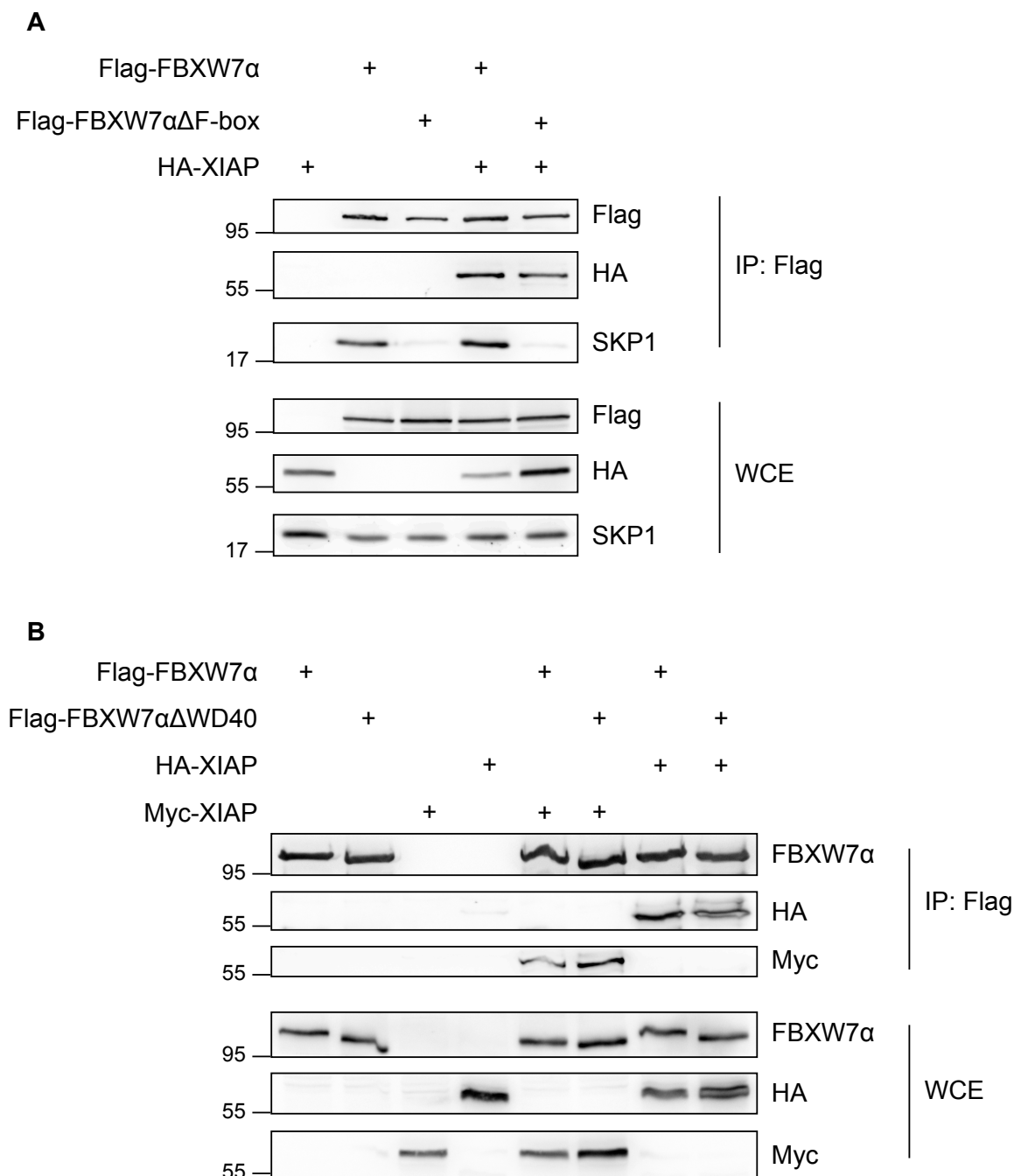


Fig. 11: Interaction between FBXW7 α and XIAP does not depend on F-box and WD40 domains of FBXW7 α .

A: Flag-FBXW7 α or Flag-FBXW7 α Δ F-box were overexpressed together with HA-XIAP in HEK-293T cells for 24 h. Cell extracts were used for immunoprecipitations with α -Flag agarose beads. Immunoprecipitates were analyzed by Western blotting with α -Flag, α -HA and α -SKP1 antibodies. **B:** Flag-FBXW7 α or Flag-FBXW7 α Δ WD40 were co-expressed with HA-XIAP or Myc-XIAP in HEK-293T cells for 24 h. Cell extracts were used for immunoprecipitations with α -Flag agarose beads. Immunoprecipitates were analyzed by Western blotting with α -FBXW7 α , α -HA and α -Myc antibodies.

FBXW7 α binds to its substrates through a WD40 repeat domain. The mutation of three amino acid residues within the WD40 repeat domain (S462A/T463V/R465A) has been shown to abolish FBXW7 α substrate binding and turnover (Busino et al., 2012; Hao et al., 2007). The corresponding WD40 mutant of FBXW7 α (FBXW7 α Δ WD40) was used to test whether XIAP binds to the same domain of FBXW7 α as its substrates. HEK-293T cells were transfected with constructs encoding either Flag-FBXW7 α or Flag-FBXW7 α Δ WD40. In addition, the cells were transiently transfected with HA-XIAP or Myc-XIAP constructs. Immunoprecipitations directed against the Flag tag revealed that HA-XIAP as well as Myc-XIAP bound to both the wild-type and Δ WD40 versions of FBXW7 α (Fig. 11B). In conclusion, the binding site of XIAP within FBXW7 α is different from the domain that is bound by FBXW7 α substrates, indicating that XIAP is not a direct substrate of FBXW7 α .

3.2.4. XIAP interacts with the N-terminal domain of FBXW7 α

FBXW7 contains several well-characterized protein domains (Fig. 4). Apart from the F-box and WD40 repeat domains, which have already been analyzed in Fig. 11, FBXW7 contains a dimerization domain as well as an isoform specific N-terminal domain that mediates isoform localizations (reviewed by Davis et al., 2014; Welcker and Clurman, 2008). In order to analyze the functional importance of the interaction between XIAP and FBXW7 α , it is interesting to further characterize the binding site of XIAP within FBXW7 α . For this purpose, Flag-tagged truncated versions of FBXW7 α were generated (Fig. 12) and used for interaction studies along with HA-tagged or endogenous XIAP.

As controls, the interactions of SKP1 (SCF subunit, expected to bind to the F-box domain) and MYC (known FBXW7 substrate, expected to bind to the WD40 domain) with the truncated FBXW7 α versions were analyzed. As expected, SKP1 only bound to FBXW7 α versions that contained the F-box domain (Flag-FBXW7 α -FL and Flag-FBXW7 α -N515), whereas the absence of the F-box domain (as in Flag-FBXW7 α -N283, Flag-FBXW7 α -C322 and Flag-FBXW7 α Δ F-box) prevented SKP1 binding (Fig. 13A). On the other hand, MYC only interacted with FBXW7 α fragments that contained a functional WD40 domain (Flag-FBXW7 α -FL, Flag-FBXW7 α -C322 and Flag-FBXW7 α Δ F-box), whereas a partial or complete loss of the WD40 domain (as in Flag-FBXW7 α -N283 and Flag-FBXW7 α -N515) abolished the MYC interaction (Fig. 13A).

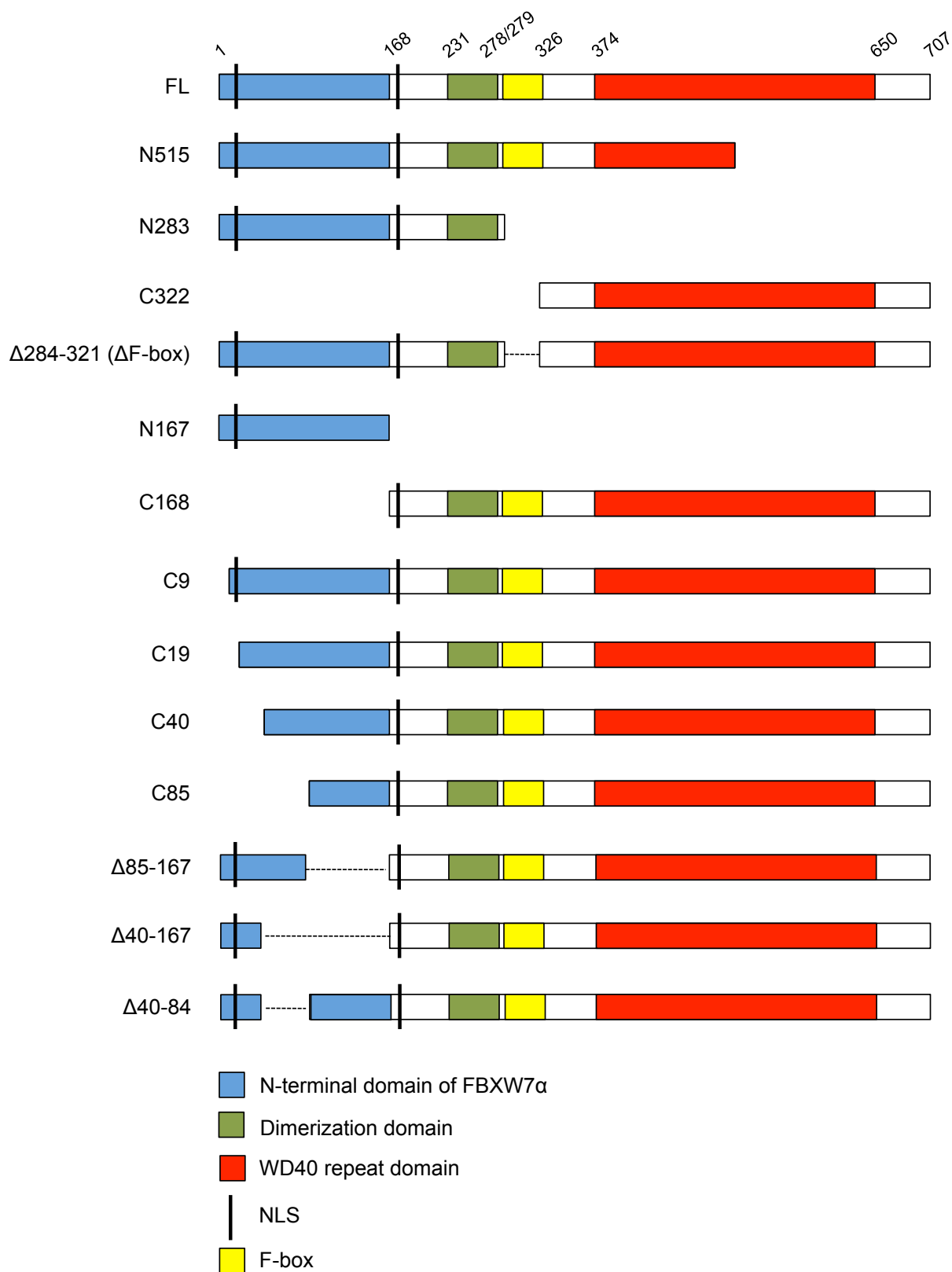


Fig. 12: Overview of Flag-tagged FBXW7 α mutants.

Illustration of truncations and deletions in FBXW7 α versions used in this study. Positions of N-terminal domain (blue), dimerization domain (green), F-box domain (yellow), WD40 domain (red) and NLS motifs (black bar) are indicated.

HA-XIAP was found to co-immunoprecipitate with Flag-FBXW7 α -FL and Flag-FBXW7 α Δ F-box (as already observed in Fig. 11A). In addition, HA-XIAP interacted with the N-terminal fragments Flag-FBXW7 α -N283 and Flag-FBXW7 α -N515, whereas no interaction could be detected with the C-terminal fragment Flag-FBXW7 α -C322. Consistent with the results presented in Fig. 11, this indicates that neither the F-box domain nor the WD40 domain are required for the interaction with XIAP. The Flag-FBXW7 α -N283 truncated version only contains the isoform specific N-terminal domain and the dimerization domain of FBXW7 α . As XIAP shows a clear interaction with Flag-FBXW7 α -N283 (Fig. 13A), this suggests that one of these domains could be responsible for mediating the interaction with XIAP.

In order to confirm these results and further differentiate the importance of the isoform specific N-terminus and the dimerization domain for the interaction with XIAP, additional truncated FBXW7 α versions were analyzed for their interactions with endogenous XIAP. Immunoprecipitations of the Flag-tagged truncated FBXW7 α versions revealed that endogenous XIAP only interacted with the N-terminal fragments of FBXW7 α (Flag-FBXW7 α -N167 and Flag-FBXW7 α -N283), whereas no interaction was observed with the C-terminal fragments (Flag-FBXW7 α -C168 and Flag-FBXW7 α -C322). Despite great experimental efforts to increase the expression levels of the Flag-FBXW7 α -N167 fragment, it showed lower protein levels compared to the other FBXW7 α versions. Nevertheless, this fragment showed a clear interaction with XIAP, similar to Flag-FBXW7 α -FL and Flag-FBXW7 α -N283 (Fig. 13B). Interestingly, Flag-FBXW7 α -N167 represents the isoform specific N-terminal domain of FBXW7 α . In conclusion, XIAP binds to FBXW7 α via its α -isoform specific N-terminus.

FBXW7 α contains two nuclear localization signals (NLS). One NLS is located between the N-terminal domain and the dimerization domain, whereas the second NLS is localized within the α -isoform specific N-terminal domain (Welcker et al., 2004). In order to test whether XIAP binds to this NLS motif within the N-terminal domain, additional truncated FBXW7 α versions were generated (Fig. 12) and then analyzed for their interactions with endogenous XIAP. As expected and already observed in previous experiments (Fig. 13B), Flag-FBXW7 α -C168 did not bind to XIAP. All the other truncated versions, however, were able to interact with XIAP (Flag-FBXW7 α -C9, Flag-FBXW7 α -C19, Flag-FBXW7 α -C40 and Flag-FBXW7 α -C85), suggesting that XIAP does not bind to the NLS sequence within the N-terminal

domain of FBXW7 α (Fig. 13C). Instead, the data generated show that the XIAP binding site is localized between amino acid residues 85 and 167 of FBXW7 α .

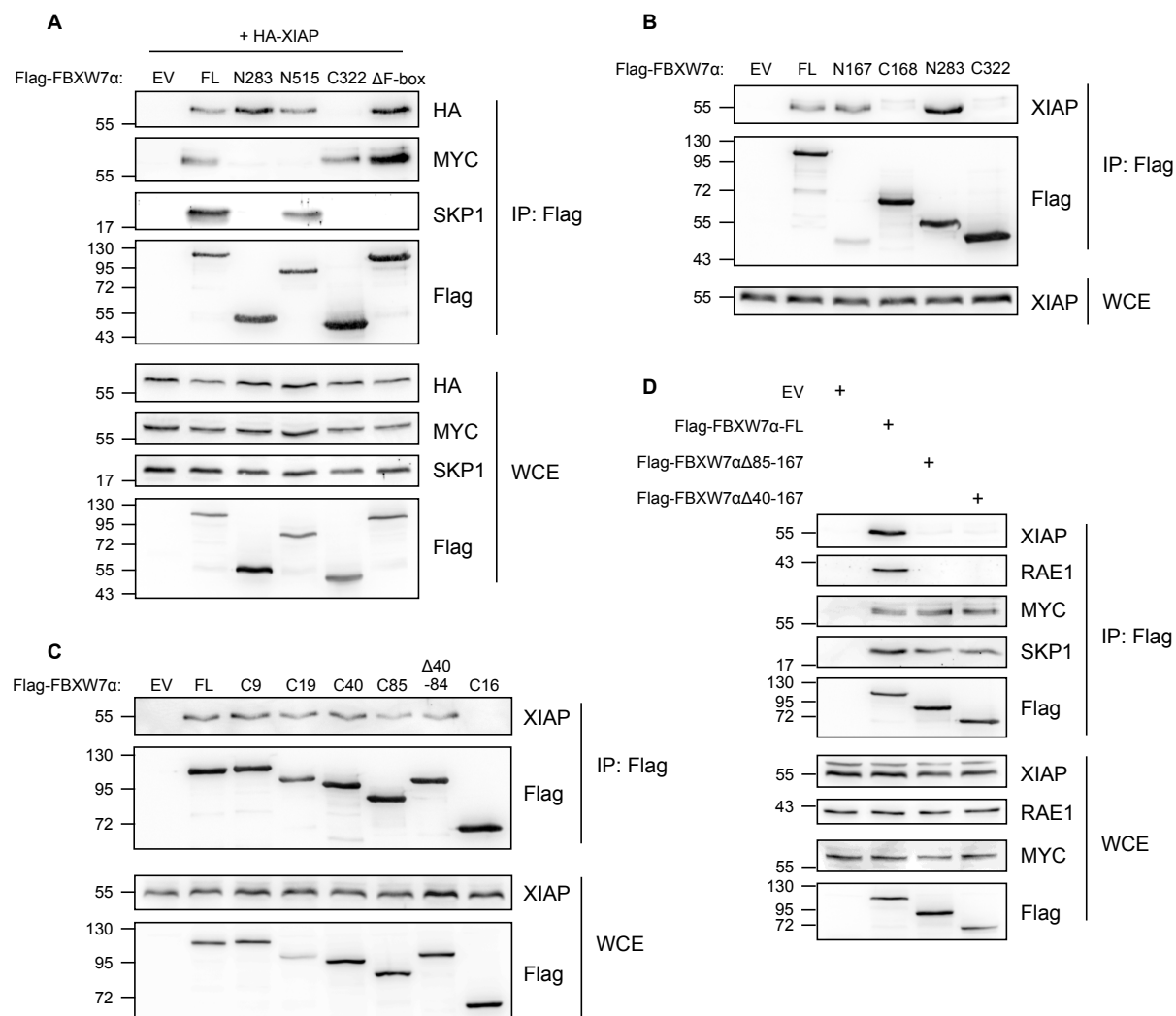


Fig. 13: N-terminal domain of FBXW7 α is required for the interaction with XIAP.

A-D: The indicated Flag-tagged versions of FBXW7 α were overexpressed either alone (B-D) or together with HA-XIAP (A) in HEK-293T cells for 24 h. Cell extracts were used for immunoprecipitations with α -Flag agarose beads. Immunoprecipitates were analyzed by Western blotting with α -XIAP, α -HA, α -Flag, α -SKP1, α -MYC or α -RAE1 antibodies.

In order to confirm this finding, the amino acid residues 85-167 were deleted from the Flag-FBXW7 α protein sequence. This deletion mutant (Flag-FBXW7 α Δ 85-167) was then immunoprecipitated from HEK-293T cell extracts. As expected, XIAP was not detected in co-immunoprecipitation with Flag-FBXW7 α Δ 85-167, although MYC and SKP1 clearly bound to the deletion mutant (Fig. 13D). Another deletion mutant, where the residues 40-167 had been deleted (Flag-FBXW7 α Δ 40-167), showed similar results (Fig. 13D). On the other hand, XIAP still bound to a mutant with a

deletion of only residues 40-84 (Flag-FBXW7 α Δ 40-84, Fig. 13C). In summary, these results confirm that XIAP binds to a region between amino acid residues 85 and 167 within the N-terminal domain of FBXW7 α .

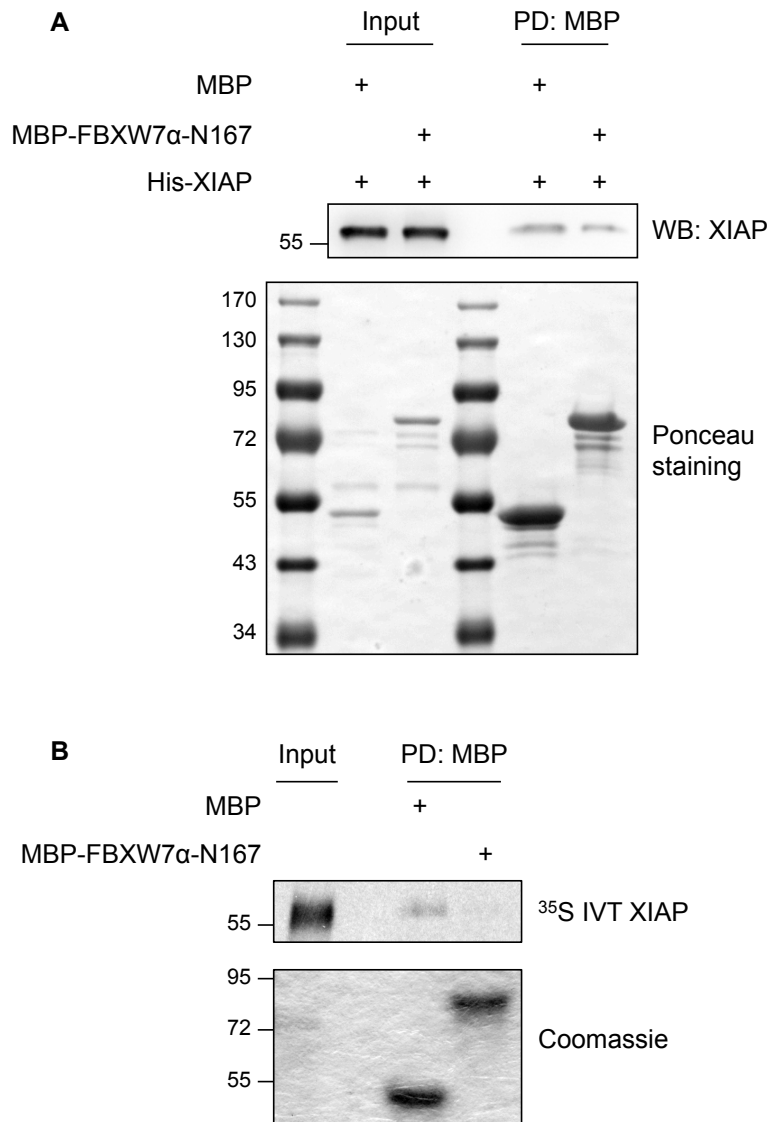


Fig. 14: FBXW7 α does not form a complex with XIAP *in vitro*.

A-B: Either MBP alone or MBP-FBXW7 α -N167 were incubated with recombinant His-XIAP (A) or with *in vitro* translated, [³⁵S]-methionine labelled XIAP (B). MBP was pulled down with amylose beads. Pull-down samples were analyzed by Western blotting with α -XIAP antibodies (A) or SDS-PAGE and Colloidal Coomassie staining (B). *In vitro* translated XIAP was detected by autoradiography.

3.2.5. XIAP does not interact with the N-terminus of FBXW7 α *in vitro*

In order to test whether XIAP directly binds to the N-terminal domain of FBXW7 α , an *in vitro* pull-down assay was performed with recombinant proteins. An MBP-tagged version of the FBXW7 α specific N-terminal domain (MBP-FBXW7 α -N167) was

purified from *E. coli* and incubated with a bacterially purified His-tagged XIAP version. As a control, His-XIAP was incubated with the MBP tag alone. MBP and MBP-FBXW7 α -N167 were then pulled down with amylose beads. The pull-down samples were analyzed for the presence of His-XIAP by Western blotting. As shown in Fig. 14A, His-XIAP was not found to be enriched in the MBP-FBXW7 α -N167 pull-down. In order to confirm this finding, MBP-FBXW7 α -N167 was incubated with *in vitro* translated XIAP. Again, an MBP pull-down was performed. However, *in vitro* translated XIAP was not detected in the MBP-FBXW7 α -N167 pull-down sample (Fig. 14B). These results therefore suggest that the interaction between FBXW7 α and XIAP is not direct, but is instead mediated by one or several additional proteins.

3.3. RAE1, FBXO45 and MYCBP2 form a complex with FBXW7 α and XIAP

3.3.1. Identification of XIAP interaction partners

As XIAP is not a direct interaction partner of FBXW7 α (Fig. 14), a screen for XIAP interaction partners was performed in order to identify the protein(s) that mediate the indirect interaction between FBXW7 α and XIAP. Flag-XIAP was overexpressed in HEK-293T cells and immunoprecipitated from the corresponding cell extracts with α -Flag agarose beads. Immunoprecipitated proteins were eluted from the beads by competition with excess Flag peptide. The immunoprecipitate was analyzed for the presence of expected interaction partners by Western blotting (Fig. 15A). As expected, XIAP was specifically detected in the Flag-XIAP immunoprecipitate. Caspase-3, a known interaction partner of XIAP (Deveraux et al., 1997), was also found in co-immunoprecipitation with Flag-XIAP. Moreover, FBXW7 α was found to interact with Flag-XIAP.

For mass spectrometry analysis, the immunoprecipitates were analyzed by SDS-PAGE and Colloidal Coomassie staining (Fig. 15B). Several protein bands were specifically detected in the Flag-XIAP immunoprecipitate, but not in the control. Consistently, mass spectrometry analysis identified proteins that specifically co-immunoprecipitated with Flag-XIAP (Fig. 15C). Apart from XIAP itself, HTRA2 was identified in the Flag-XIAP co-immunoprecipitate. HTRA2 is a known XIAP interaction partner that was shown to inhibit XIAP (Suzuki et al., 2001). Although FBXW7 α had been shown to interact with Flag-XIAP by Western blot analysis (Fig. 15A), it was not detected by mass spectrometry. Additional proteins that were identified as putative

interaction partners of Flag-XIAP were MYCBP2, RAE1, FBXO45 and SPRYD3 (Fig. 15C). Interestingly, these proteins had also been identified as putative FBXW7 α interaction partners (Fig. 5C).

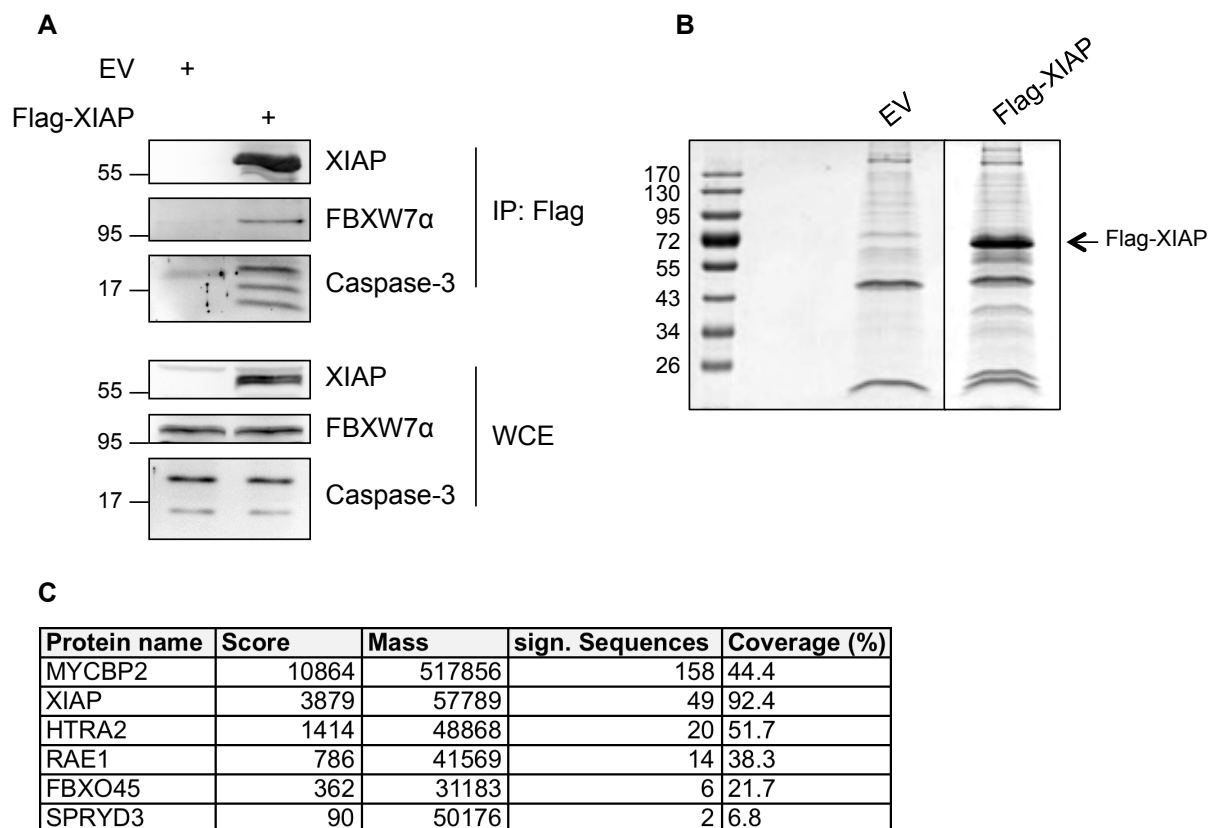


Fig. 15: Identification of XIAP interaction partners.

A-B: Flag-XIAP was overexpressed in HEK-293T cells for 24 h. An empty vector (EV) was transfected as a control. Cell extracts were used for immunoprecipitations with α -Flag agarose beads. Immunoprecipitated proteins were eluted by competition with Flag peptide and analyzed by Western blotting (A) or by SDS-PAGE and Colloidal Coomassie staining (B). The gel from B was analyzed by mass spectrometry. **C:** Selection of proteins that were specifically identified in the Flag-XIAP immunoprecipitate by mass spectrometry. For each identified protein, the MASCOT score, the protein mass, the number of significant sequences and the coverage is specified.

3.3.2. XIAP and RAE1 bind to a similar domain within the N-terminus of FBXW7 α

RAE1 is a protein that was identified as a putative interaction partner of both FBXW7 α (Fig. 5C) and XIAP (Fig. 15C). Therefore, it is a candidate protein that could be responsible for mediating the indirect interaction between FBXW7 α and XIAP. RAE1 has originally been described as an mRNA export factor in yeast (Brown et al., 1995). In vertebrates, it has been further characterized as a regulator of mitotic

spindle assembly and was also found to inhibit APC/C activity (Blower et al., 2005; Jeganathan et al., 2005).

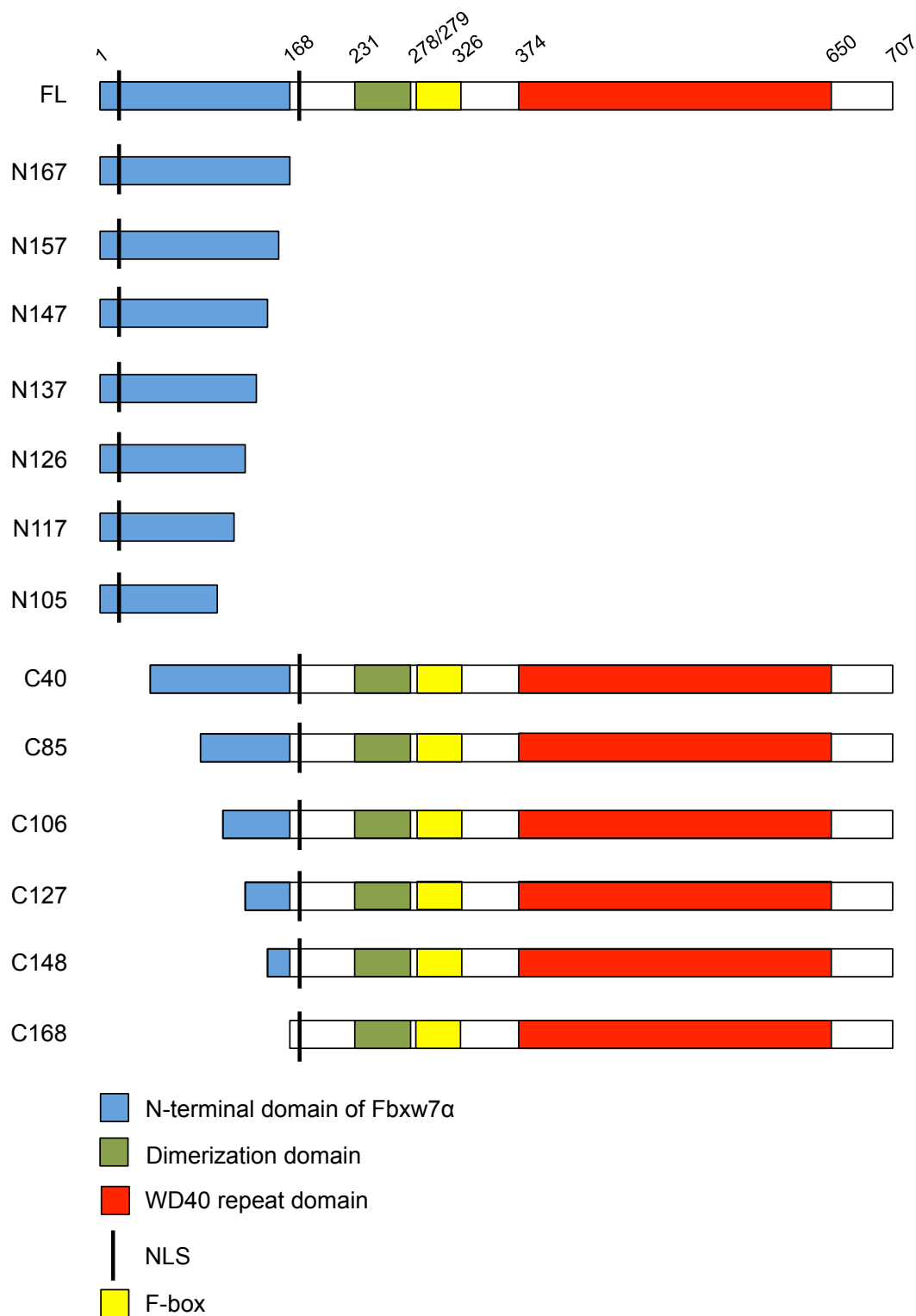


Fig. 16: Overview of N- and C-terminal truncated versions of Flag-FBXW7α for the characterization of the XIAP/RAE1 binding site within the N-terminal domain.

Overview of additional truncated FBXW7α versions. Positions of N-terminal domain (blue), dimerization domain (green), F-box domain (yellow), WD40 domain (red) and NLS motifs (black bar) are indicated.

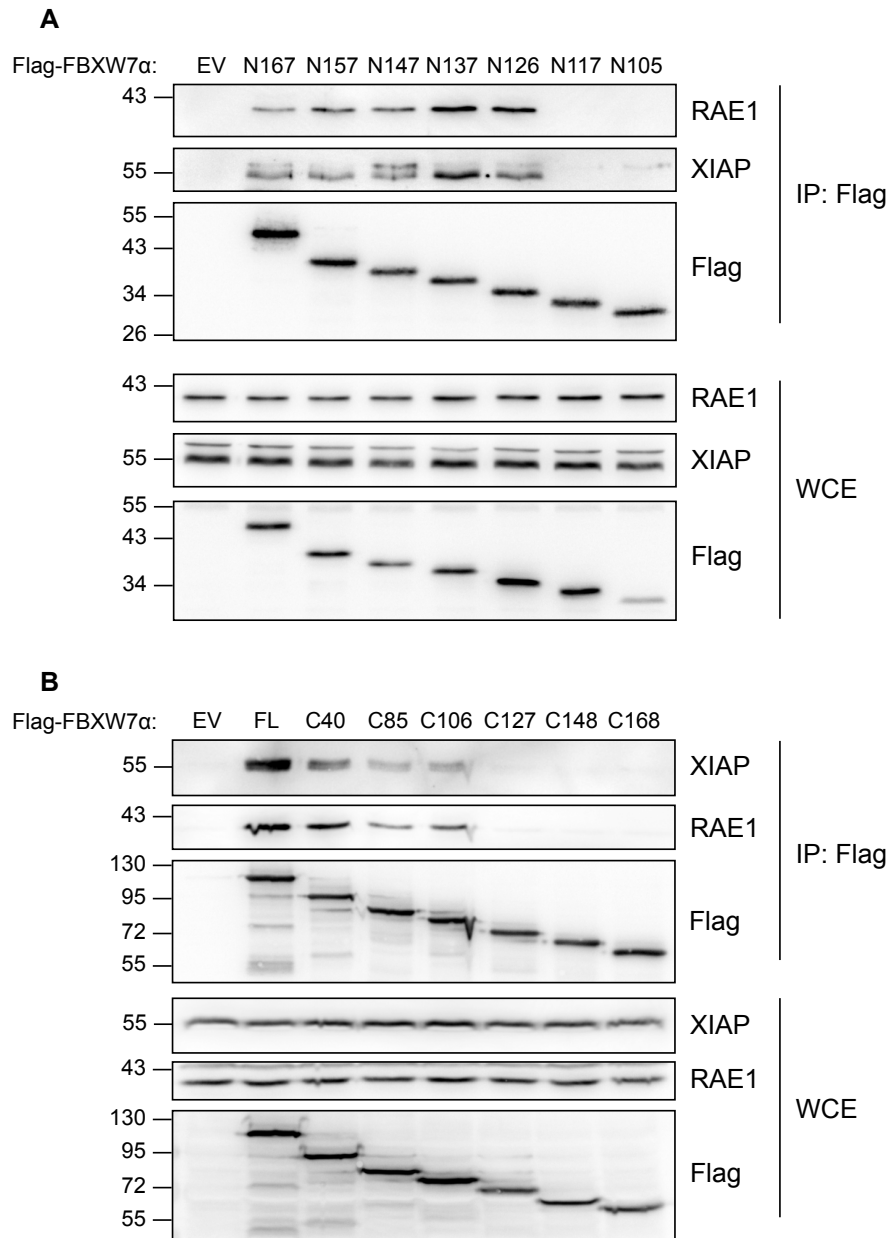


Fig. 17: A short motif within the N-terminal domain of FBXW7 α is required for the interaction with XIAP and RAE1.

A-B: The indicated Flag-tagged truncated versions of FBXW7 α were overexpressed in HEK-293T cells for 24 h. Cell extracts were used for immunoprecipitations directed against the Flag tag. Immunoprecipitates were analyzed by Western blotting with α -RAE1, α -XIAP and α -Flag antibodies.

A protein that forms a link between FBXW7 α and XIAP would be expected to bind to the same FBXW7 α domain as XIAP. In order to test this hypothesis, the interaction between FBXW7 α and RAE1 was analyzed. For this analysis, Flag-tagged deletion mutants of FBXW7 α , which had already been used to analyze the interaction with XIAP, were immunoprecipitated. Similar to XIAP, RAE1 did not co-immunoprecipitate

with the deletion mutants (Flag-FBXW7 α Δ 85-167 and Flag-FBXW7 α Δ 40-167), whereas it was clearly detected in co-immunoprecipitation with the full-length version of Flag-FBXW7 α (Fig. 13D). This result indicates that RAE1 binds to a similar domain within the N-terminus of FBXW7 α as XIAP.

In order to confirm that RAE1 and XIAP bind to the same region of the N-terminal FBXW7 α domain, the RAE1 binding site within FBXW7 α was characterized in more detail. For this purpose, additional truncated versions of Flag-FBXW7 α were generated. Both N-terminal and C-terminal truncations were analyzed in order to narrow down the XIAP and RAE1 binding sites within the N-terminal domain of FBXW7 α (Fig. 16). Interestingly, XIAP and RAE1 showed a similar binding behaviour to the different truncated versions of Flag-FBXW7 α . On the one hand, residues 127-167 were not required for the interaction with FBXW7 α because a truncated version of FBXW7 α that only contained the residues 1-126 (Flag-FBXW7 α -N126) was still able to bind both XIAP and RAE1. Shorter versions (Flag-FBXW7 α -N117 and Flag-FBXW7 α -N105), however, did not bind XIAP nor RAE1 (Fig. 17A). On the other hand, residues 1-105 of FBXW7 α are not essential for the interactions with XIAP and RAE1. A truncated version that lacks these residues (Flag-FBXW7 α -C106) is able to bind XIAP and RAE1, although the interaction is weaker than the interaction with the full-length version of Flag-FBXW7 α (Fig. 17B). Truncated versions that lack residues 1-126 (Flag-FBXW7 α -C127, Flag-FBXW7 α -C148 and Flag-FBXW7 α -C168), however, were not found to interact with XIAP and RAE1. This result is consistent with the finding that residues 1-126 are sufficient for the interaction with XIAP and RAE1 (Fig. 17A). In summary, these results suggest that a sequence motif between residues 106 and 126 is essential for the interaction with both XIAP and RAE1.

In order to confirm this finding, a Flag-tagged mutant of FBXW7 α was generated, where residues 106-126 were deleted (Flag-FBXW7 α Δ 106-126, Fig. 18A). Immunoprecipitation of this deletion mutant revealed that XIAP and RAE1 were not able to bind to Flag-FBXW7 α when residues 106-126 were deleted, whereas they clearly bound to the full-length version of Flag-FBXW7 α (Fig. 18B). As expected, SKP1 bound to both full-length Flag-FBXW7 and Flag-FBXW7 α Δ 106-126. In summary, this confirms that a motif between residues 106 and 126 in the N-terminal domain of FBXW7 α is required for the interaction with XIAP and RAE1.

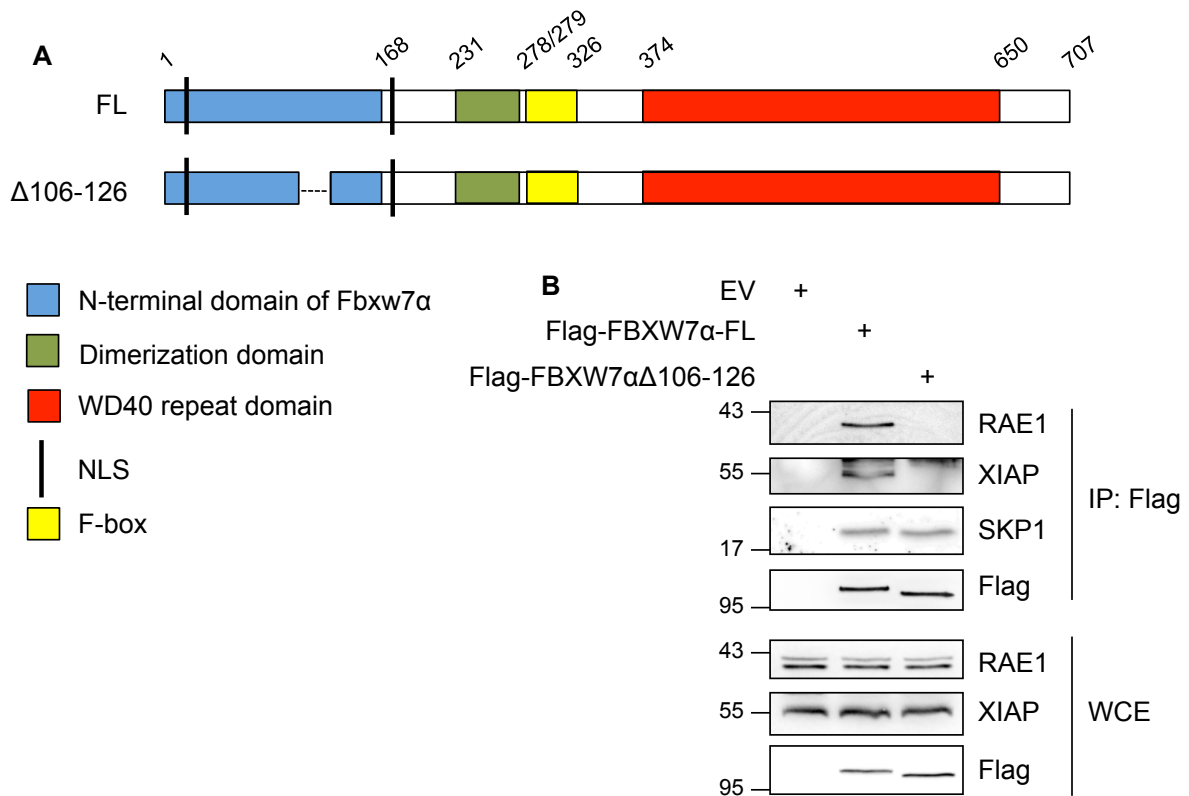


Fig. 18: Deletion of amino acid residues 106-126 of FBXW7α abolishes the interactions with XIAP and RAE1.

A: Illustration of the Flag-FBXW7αΔ106-126 mutant with a deletion of amino acid residues 106-126 in the N-terminal domain. **B:** Flag-FBXW7αΔ106-126 does not interact with XIAP or RAE1. Flag-FBXW7α-FL and Flag-FBXW7αΔ106-126 were overexpressed in HEK-293T cells for 24 h. An empty vector (EV) was transfected as a control. Cell extracts were used for immunoprecipitations with α-Flag agarose beads. Immunoprecipitates were analyzed by Western blotting with α-RAE1, α-XIAP, α-SKP1 and α-Flag antibodies.

3.3.3. Amino acid residues 106-126 of FBXW7α contain a negatively charged sequence motif that is highly conserved among vertebrates

As a short sequence between amino acid residues 106 and 126 of FBXW7α was shown to be required for the interaction with both XIAP and RAE1, this part of FBXW7α was analyzed in more detail. As shown in Fig. 19A, FBXW7α(106-126) contains a high percentage of negatively charged residues (D and E residues). Interestingly, comparison of human FBXW7α with homologues from other vertebrate species shows that the overrepresentation of negatively charged residues is conserved among vertebrates (Fig. 19A). In general, Fig. 19B shows that the N-terminal domain of FBXW7α (residues 1-167) is less conserved among vertebrates than the part of FBXW7α that is shared with the β- and γ-isoforms (residues 168-

empty vector had been transfected instead of the Flag-FBXW7 α construct. In addition, RAE1 was specifically detected in co-immunoprecipitation with Flag-FBXW7 α and XIAP. This confirms that FBXW7 α , XIAP and RAE1 form a complex.

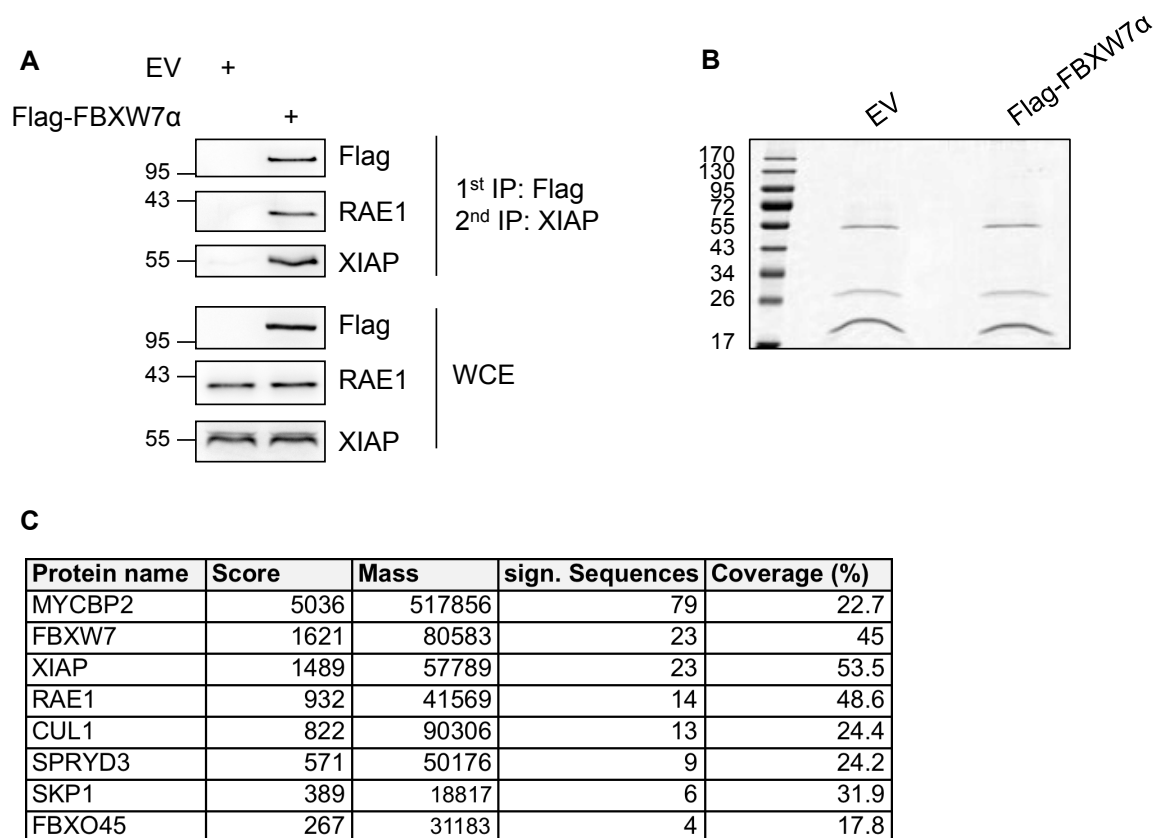


Fig. 20: Identification of FBXW7 α -XIAP complex components by a sequential immunoprecipitation approach.

A: RAE1 interacts with FBXW7 α -XIAP complex. Flag-FBXW7 α was overexpressed in HEK-293T cells for 24 h. Cell extracts were used for an immunoprecipitation with α -Flag agarose beads. Immunoprecipitated proteins were eluted by competition with Flag peptide. Eluates were used for a second immunoprecipitation with α -XIAP antibodies. Immunoprecipitates were analyzed by Western blotting with α -Flag, α -RAE1 and α -XIAP antibodies. **B:** Immunoprecipitates after sequential immunoprecipitation from A were analyzed by SDS-PAGE and stained by Colloidal Coomassie. **C:** Whole lanes were cut out from the gel in B and analyzed by mass spectrometry. The table shows a selection of the proteins that were specifically identified in the Flag-FBXW7 α -XIAP immunoprecipitate. For each identified protein, the MASCOT score, the protein mass, the number of significant sequences and the coverage are specified.

3.3.5. Identification of additional FBXW7 α -XIAP complex components

In order to test whether additional proteins interact with the FBXW7 α -XIAP complex apart from RAE1, the samples obtained after sequential immunoprecipitation were analyzed by SDS-PAGE and Colloidal Coomassie staining (Fig. 20B) as well as by

mass spectrometry. As expected, FBXW7, XIAP and RAE1 were identified by mass spectrometry (Fig. 20C). In addition, the SCF components CUL1 and SKP1 were detected. Moreover, MYCBP2, SPRYD3 and FBXO45 were found in co-immunoprecipitation with Flag-FBXW7 α /XIAP. Interestingly, these proteins had already been identified as putative interaction partners of Flag-FBXW7 α (Fig. 5C) as well as Flag-XIAP (Fig. 15C). This indicates that FBXW7 α could form a protein complex together with XIAP, RAE1, MYCBP2, SPRYD3 and FBXO45.

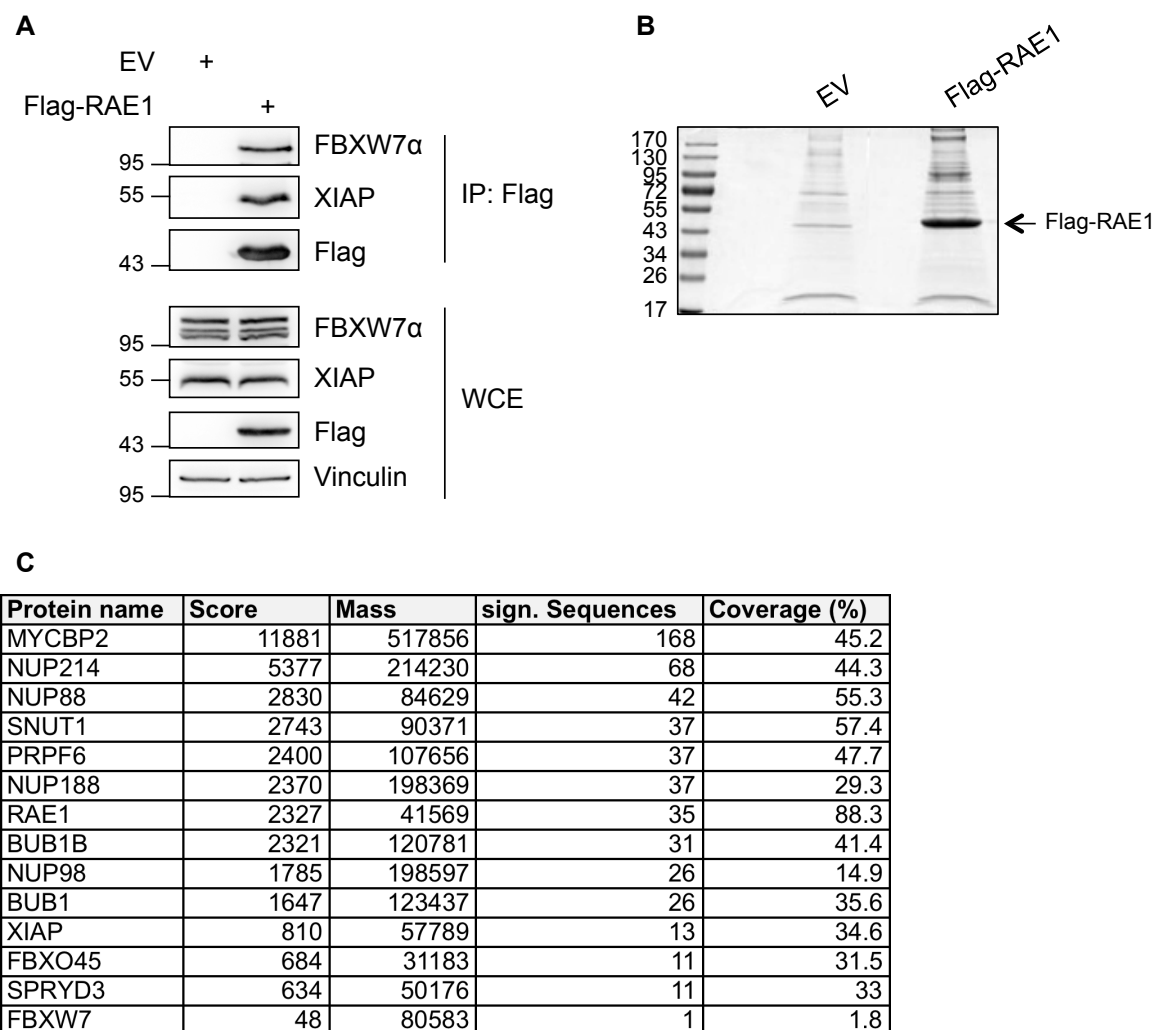


Fig. 21: Identification of RAE1 interaction partners.

A-B: Flag-RAE1 was overexpressed in HEK-293T cells for 24 h. An empty vector (EV) was transfected as a control. Cell extracts were used for an immunoprecipitation directed against the Flag tag. Immunoprecipitated proteins were eluted by competition with Flag peptide. Eluates were analyzed by Western blotting with α -FBXW7 α , α -XIAP, α -Flag and α -Vinculin antibodies (A) as well as by SDS-PAGE and Colloidal Coomassie staining (B). Whole lanes were cut out from the gel in B and analyzed by mass spectrometry. **C:** Selection of proteins that were specifically identified in the Flag-RAE1 immunoprecipitate by mass spectrometry. For each identified protein, the MASCOT score, the protein mass, the number of significant peptides and the coverage are specified.

3.3.6. Screen for RAE1 interaction partners

In order to confirm the results from the interaction studies, a screen for RAE1 interaction partners was performed. Flag-RAE1 was overexpressed in HEK-293T cells and immunoprecipitated from the cell extract with α -Flag resin. After elution by the addition of Flag peptide, immunoprecipitates were analyzed by Western blotting as well as SDS-PAGE for subsequent mass spectrometry analysis. As expected, FBXW7 α and XIAP were detected in co-immunoprecipitation with Flag-RAE1 by both Western blotting (Fig. 21A) and mass spectrometry analysis (Fig. 21C). Known interaction partners of RAE1, as BUB1/BUB1B and NUP98 (Pritchard et al., 1999; Wang et al., 2001), were identified by mass spectrometry, thus validating the screen. Importantly, MYCBP2, FBXO45 and SPRYD3 were identified as putative interaction partners of Flag-RAE1 (Fig. 21C), again confirming that these proteins could be additional components of the complex that contains FBXW7 α , XIAP and RAE1.

3.3.7. Both FBXO45 and MYCBP2 interact with the N-terminal domain of FBXW7 α

In order to verify that FBXO45 is an interaction partner of FBXW7 α , an immunoprecipitation experiment of Flag-FBXO45 was performed. As shown in Fig. 22A, FBXW7 α was found in co-immunoprecipitation with Flag-FBXO45. As expected, XIAP and RAE1 also interacted with Flag-FBXO45.

To test whether FBXO45 interacts with the same motif of FBXW7 α as XIAP and RAE1, the deletion mutant Flag-FBXW7 α Δ 106-126 was immunoprecipitated. Similar to XIAP and RAE1, endogenous FBXO45 was not detected in co-immunoprecipitation with Flag-FBXW7 α Δ 106-126, whereas it clearly interacted with the full-length version of Flag-FBXW7 α (Fig. 22B). This shows that FBXO45 interacts with a similar motif within FBXW7 α as XIAP and RAE1.

Also MYCBP2 was confirmed to interact with FBXW7 α as Myc-tagged MYCBP2 was detected in co-immunoprecipitation with Flag-FBXW7 α (Fig. 22C). However, it did not interact with Flag-FBXW7 α Δ 85-167, indicating that MYCBP2 also binds to the N-terminus of FBXW7 α (Fig. 22C).

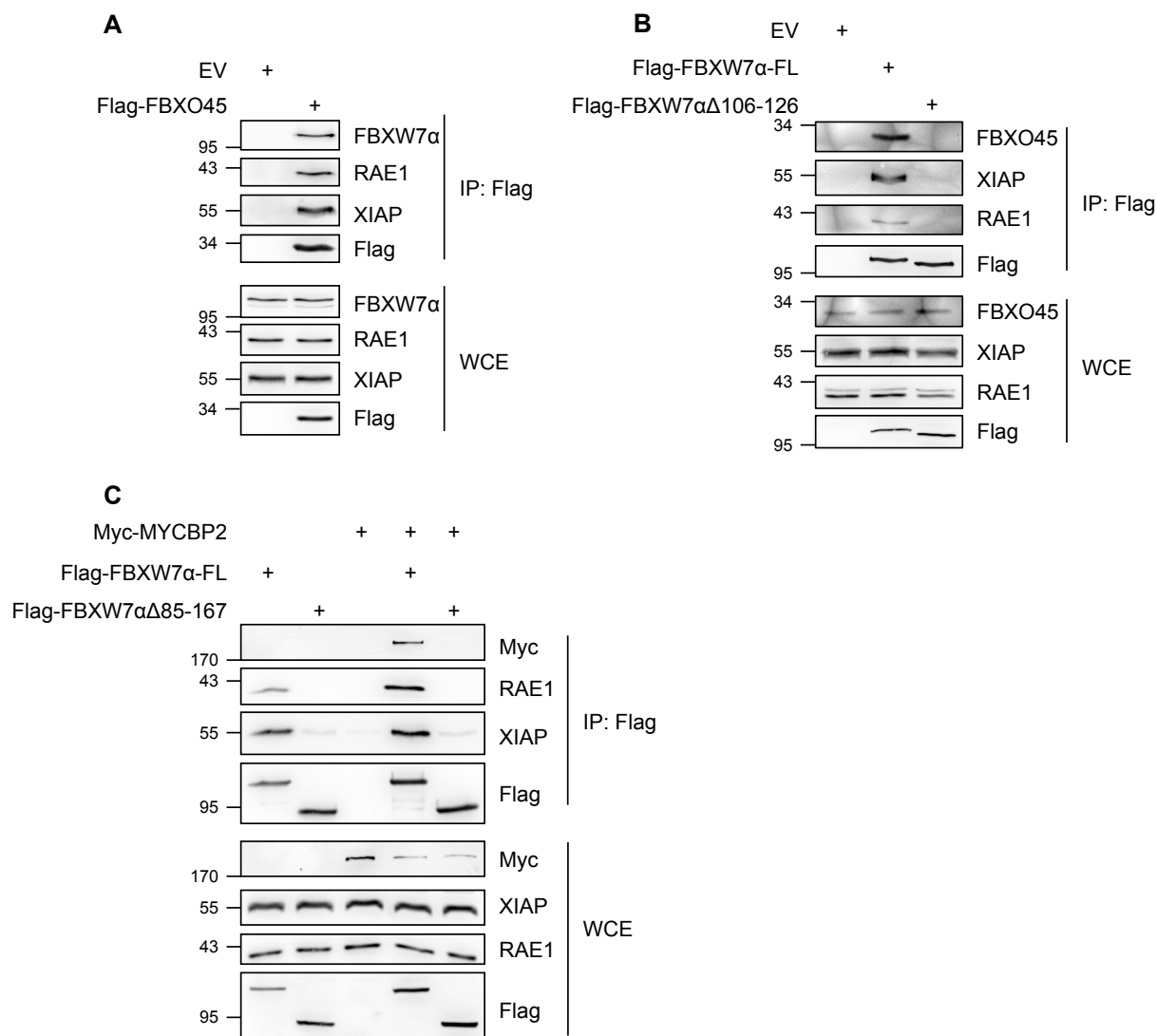


Fig. 22: FBXO45 and MYCBP2 interact with the N-terminal domain of FBXW7α.

A: Flag-FBXO45 interacts with endogenous FBXW7α. Flag-FBXO45 was overexpressed in HEK-293T cells for 24 h. Cell extracts were used for an immunoprecipitation directed against the Flag tag. Immunoprecipitates were analyzed by Western blotting with α-FBXW7α, α-RAE1, α-XIAP and α-Flag antibodies. **B:** FBXO45 interacts with the N-terminal domain of FBXW7α. Flag-FBXW7α-FL or Flag-FBXW7αΔ106-126 were overexpressed in HEK-293T cells for 24 h. Cell extracts were used for α-Flag immunoprecipitations. Immunoprecipitates were analyzed by Western blotting with α-FBXO45, α-XIAP, α-RAE1 and α-Flag antibodies. **C:** MYCBP2 interacts with the N-terminal domain of FBXW7α. Flag-FBXW7α-FL and Flag-FBXW7αΔ85-167 were overexpressed together with Myc-MYCBP2 in HEK-293T cells for 24 h. Cell extracts were used for immunoprecipitations with α-Flag agarose beads. Immunoprecipitates were analyzed by Western blotting with α-Myc, α-RAE1, α-XIAP and α-Flag antibodies.

3.3.8. FBXW7α and FBXO45 bind to the central domain of MYCBP2

MYCBP2 is a large protein of about 500 kDa that contains several characterized domains, such as an RCC1-like domain, two PHR domains, a central MYC-binding

domain and a C-terminal RING domain (Fig. 23) (reviewed by Grill et al., 2016). FBXO45 is a known interaction partner of MYCBP2 that has been shown to bind to the MYC-binding domain (Liao et al., 2004). Also RAE1 was shown to bind to a region close to the MYC-binding domain (Grill et al., 2012; Tian et al., 2011). In order to reproduce these data, Flag-tagged fragments of MYCBP2 were generated (Fig. 23). As expected, immunoprecipitations of these fragments revealed that Myc-FBXO45 (Fig. 24B) and endogenous RAE1 (Fig. 24A) bound to the Flag-MYCBP2(1951-2950) fragment containing the central MYC-binding domain. Moreover, endogenous FBXW7 α and XIAP bound to the Flag-MYCBP2(1951-2950) fragment (Fig. 24A).

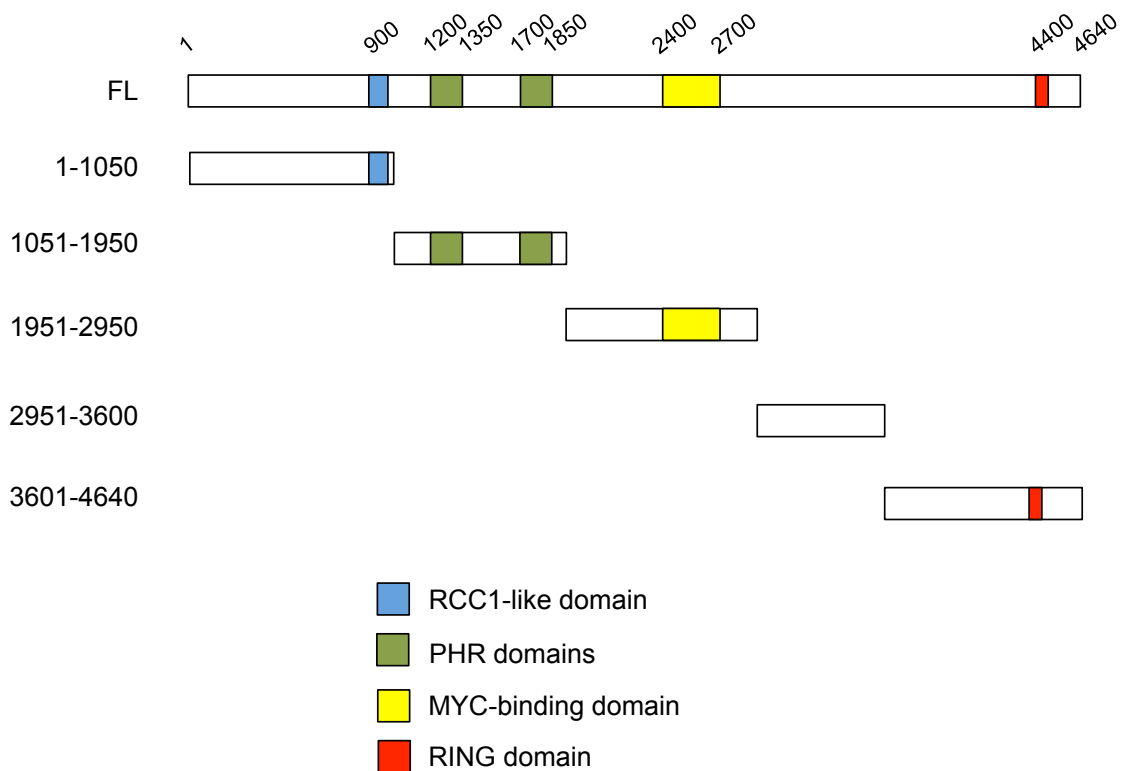


Fig. 23: Overview of Flag-tagged MYCBP2 fragments.

Illustration of MYCBP2 fragments. Positions of RCC1-like domain (blue), PHR domains (green), MYC-binding domain (yellow) and RING domain (red) are shown.

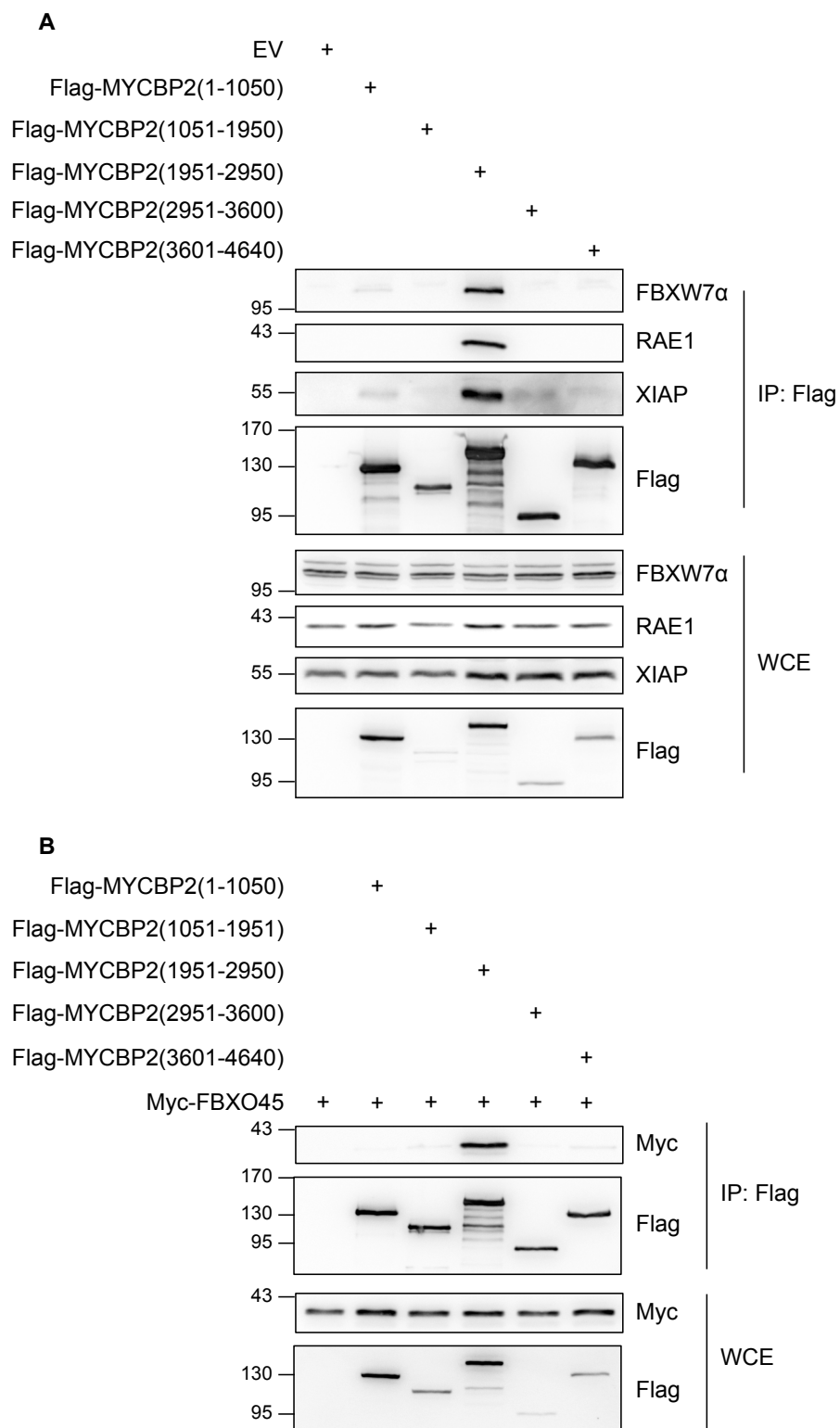


Fig. 24: FBXW7 α , XIAP, RAE1 and FBXO45 interact with the central domain of MYCBP2.

A-B: The indicated Flag-tagged MYCBP2 fragments were overexpressed alone (A) or together with Myc-FBXO45 (B) in HEK-293T cells for 24 h. Cell extracts were used for α -Flag immunoprecipitations. Immunoprecipitates were analyzed by Western blotting with α -FBXW7 α , α -RAE1, α -XIAP, α -Myc, and α -Flag antibodies.

3.3.9. FBXW7 α forms a complex with MYCBP2 and FBXO45

Both MYCBP2 and FBXO45 were identified as interaction partners of FBXW7 α , XIAP and RAE1 by mass spectrometry (Fig. 5C, 15C, 21C). They were also identified as interactors of the FBXW7 α -XIAP complex by sequential immunoprecipitation (Fig. 20C). Moreover, both MYCBP2 and FBXO45 bind to the same domain of FBXW7 α (Fig. 22B-C), whereas both FBXW7 α and FBXO45 bind to the same part of MYCBP2 (Fig. 24A-B). These findings suggest that FBXW7 α , MYCBP2 and FBXO45 could be part of a larger protein complex together with XIAP and RAE1. In order to confirm this, a two-step sequential immunoprecipitation was performed. HEK-293T cells were transfected with plasmids expressing either Flag-MYCBP2(1951-2950) and HA-FBXO45 or HA-FBXO45 alone. The first immunoprecipitation was directed against the Flag tag and precipitated proteins were eluted by competition with Flag peptide. Eluates were used for a second immunoprecipitation with α -HA resin. Analysis of immunoprecipitates by Western blotting (Fig. 25) revealed that FBXW7 α bound to the MYCBP2-FBXO45 complex. As expected, also RAE1 was found in this complex. In summary, this suggests that FBXW7 α , XIAP, RAE1, MYCBP2 and FBXO45 form a complex.

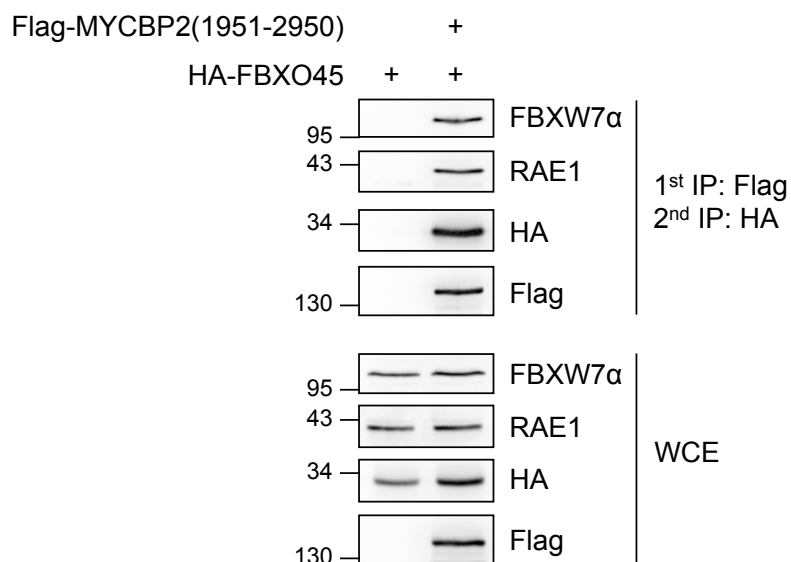


Fig. 25: FBXW7 α forms a complex with MYCBP2 and FBXO45.

Flag-MYCBP2(1951-2950) and HA-FBXO45 were co-expressed in HEK-293T cells for 24 h. Cell extracts were used for an immunoprecipitation with α -Flag agarose beads. Immunoprecipitated proteins were eluted by competition with Flag peptide. Eluates were used for a second immunoprecipitation directed against the HA tag. Immunoprecipitates obtained after the sequential immunoprecipitation were analyzed by Western blotting with α -FBXW7 α , α -RAE1, α -HA and α -Flag antibodies.

3.3.10. FBXO45 interacts with FBXW7 α *in vitro*

In order to find out which FBXW7 α interaction partner directly binds to FBXW7 α within the complex, *in vitro* pull-down assays were performed. As a direct interaction between FBXW7 α and XIAP had not been observed (Fig. 14), only MYCBP2, FBXO45 and RAE1 were analyzed regarding their interaction with FBXW7 α . Bacterially purified MBP or the MBP-tagged N-terminal domain of FBXW7 α (MBP-FBXW7 α -N167) were incubated with *in vitro* translated versions of FBXO45, RAE1 or the MYC-binding domain containing MYCBP2 fragment. A subsequent MBP pull-down with amylose beads revealed that only FBXO45 interacted with MBP-FBXW7 α -N167 *in vitro*, whereas RAE1 and the MYCBP2 fragment showed no interaction with the N-terminal domain of FBXW7 α (Fig. 26). This indicates that FBXW7 α is directly bound by FBXO45, whereas the interactions with the other complex components are possibly indirectly mediated by FBXO45.

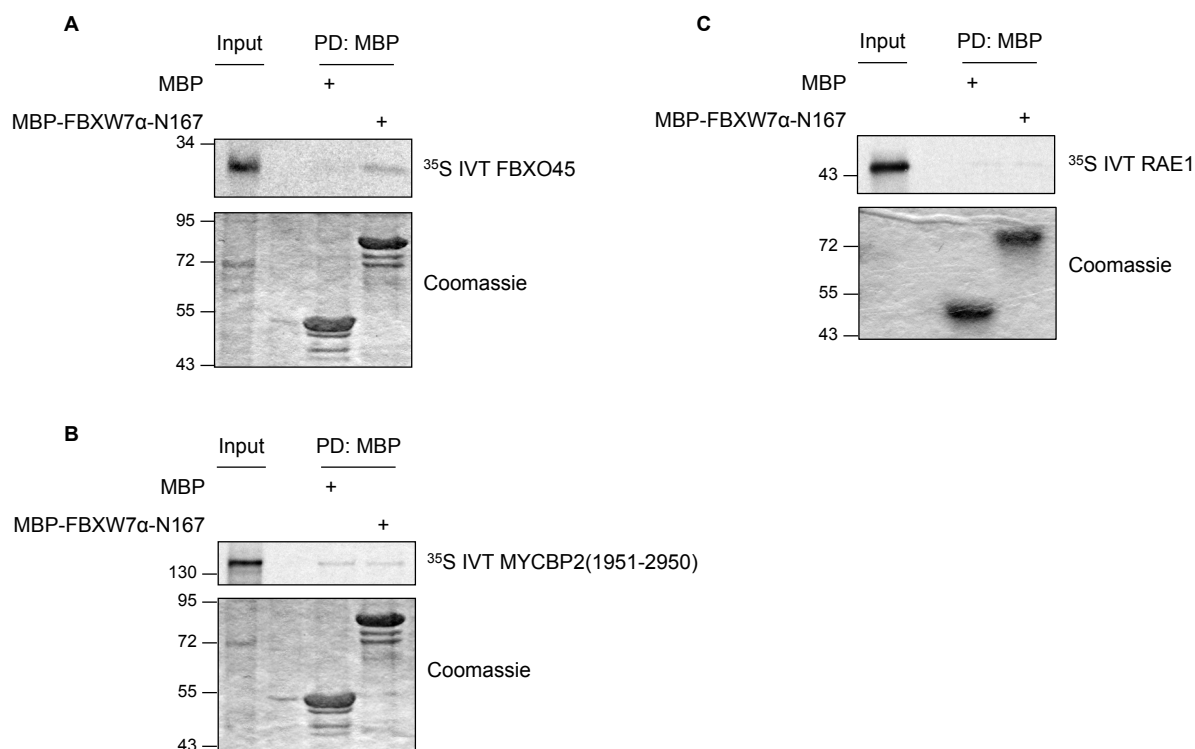


Fig. 26: FBXO45 directly interacts with the N-terminus of FBXW7 α .

A-C: Either MBP alone or MBP-FBXW7 α -N167 were incubated with *in vitro* translated and [³⁵S]-methionine containing FBXO45 (A), MYCBP2(1951-2950) (B) or RAE1 (C). MBP was pulled down with amylose beads. Pull-down samples were analyzed by SDS-PAGE and Colloidal Coomassie staining. *In vitro* translated proteins were detected by autoradiography.

3.3.11. FBXO45 specifically interacts with FBXW7 α

FBXO45 interacts with the N-terminal domain of FBXW7 α (Fig. 22B, 26A). This suggests that FBXO45 might specifically interact with the α -isoform of FBXW7 because the β - and γ -isoforms contain different N-termini. In order to exclude that there are other FBXO45 binding sites in FBXW7 β or FBXW7 γ , Flag-tagged versions of the three human FBXW7 isoforms were immunoprecipitated (Fig. 27). As expected, endogenous FBXO45 was only found in co-immunoprecipitation with Flag-FBXW7 α , but not with Flag-FBXW7 β or Flag-FBXW7 γ . This result confirms that FBXO45 specifically interacts with the FBXW7 α isoform.

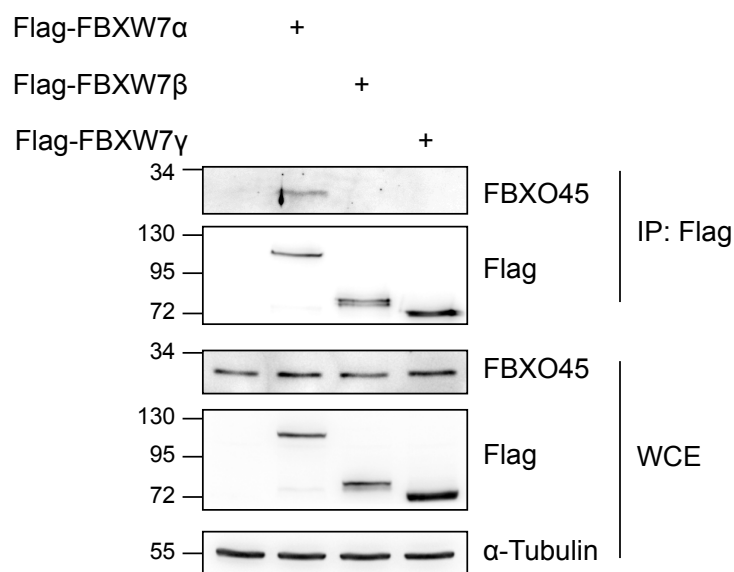


Fig. 27: FBXO45 specifically interacts with the α -isoform of FBXW7.

Flag-FBXW7 α , Flag-FBXW7 β or Flag-FBXW7 γ were overexpressed in HEK-293T cells for 24 h. FBXW7 isoforms were immunoprecipitated by their Flag tags. Immunoprecipitates were analyzed by Western blotting with α -FBXO45, α -Flag and α -Tubulin antibodies. Tubulin was used as a loading control.

3.4. Characterization of FBXO45 and MYCBP2 as novel regulators of FBXW7 α

3.4.1. FBXW7 α protein levels decrease during mitotic arrest

FBXW7 α is a nuclear protein (Kimura et al., 2003), whereas FBXO45 and MYCBP2 are mainly found in the cytosol (Chen et al., 2014; Pierre et al., 2004). Also XIAP is mainly localized in the cytosol (Liston et al., 2001). RAE1 shuttles between the nucleus and the cytosol (Kraemer and Blobel, 1997). It is therefore conceivable that

an effect of the identified complex on FBXW7 α protein levels can be observed in mitosis upon nuclear envelope breakdown.

In order to test whether there is a putative regulation of FBXW7 α protein levels during mitotic arrest, HeLa cells were treated with nocodazole for 2 h. Mitotic cells were then collected by a mitotic shake-off and further incubated with nocodazole. Cells were harvested at different time points after addition of nocodazole and cell extracts were analyzed by Western blotting. MCL1 is a known FBXW7 substrate that has been described to be degraded during mitotic arrest (Inuzuka et al., 2011; Wertz et al., 2011). As expected, this decrease in MCL1 protein levels could be confirmed (Fig. 28). Interestingly, FBXW7 α and MYC protein levels also decreased during mitotic arrest. This indicates that FBXW7 α protein levels are negatively regulated during mitotic arrest.

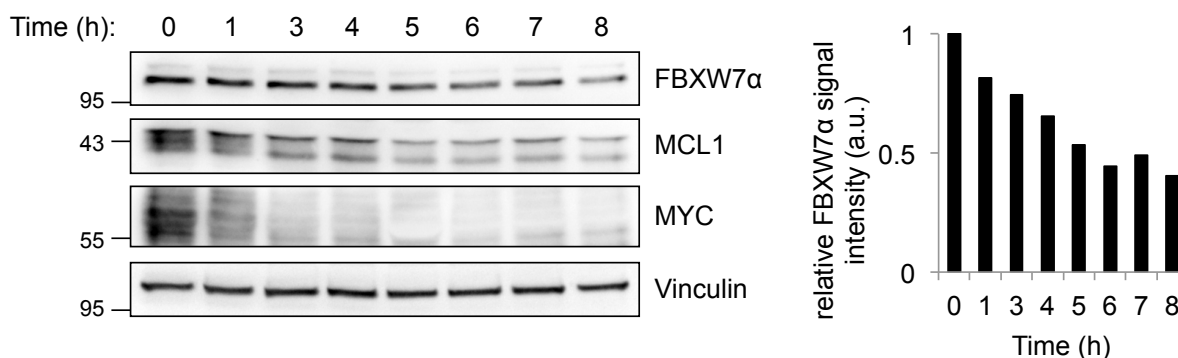


Fig. 28: FBXW7 α protein levels decrease during prolonged mitotic arrest.

HeLa cells were treated with 250 ng/mL nocodazole for 2 h. Mitotic cells were collected by mitotic shake-off and further incubated with 250 ng/mL nocodazole. The cells were harvested at different time points by a mitotic shake-off. Cell extracts were prepared and analyzed by Western blotting with α -FBXW7 α , α -MCL1, α -MYC and α -Vinculin antibodies. Vinculin was used as a loading control. Relative FBXW7 α signal intensities were quantified.

3.4.2. The FBXO45/MYCBP2 ubiquitin ligase regulates FBXW7 α protein levels

FBXO45 and MYCBP2 have been shown to form an E3 ubiquitin ligase complex that mediates the proteasomal degradation of several substrates. Since I could observe a binding of FBXO45 and MYCBP2 with FBXW7 α , it is conceivable that FBXW7 α is a substrate of the FBXO45/MYCBP2 ubiquitin ligase. It is possible that the decrease in FBXW7 α protein levels during mitotic arrest is mediated by this complex. In order to test this, FBXO45 and MYCBP2 were downregulated in HeLa cells by siRNA treatment. The cells were treated with nocodazole in order to arrest them in mitosis

and harvested by a mitotic shake-off. As a control, asynchronous cells were harvested. In subsequent Western blot analysis (Fig. 29A), Cyclin B1 protein levels served as a mitotic marker. As expected, Cyclin B1 levels were increased in nocodazole-treated cells compared to asynchronous cells, confirming the mitotic arrest upon nocodazole treatment. Interestingly, FBXO45 and MYCBP2 downregulation in nocodazole-arrested cells caused an increase in FBXW7 α protein levels compared to control cells, which had been treated with control siRNA directed against firefly luciferase GL2. This increase in FBXW7 α protein levels upon depletion of FBXO45 and MYCBP2 was not observed in asynchronous cells. These results suggest that the observed decrease in FBXW7 α protein levels during mitotic arrest (Fig. 28) is mediated by FBXO45 and MYCBP2. Moreover, as the effect was not observed in asynchronous cells, it is conceivable that the regulation of FBXW7 α by FBXO45 and MYCBP2 is specific for a prolonged mitotic arrest.

In order to further analyze the specificity of the impact of FBXO45 and MYCBP2 on FBXW7 α protein levels, the effect of FBXO45 and MYCBP2 was compared in a prolonged mitotic arrest and in unperturbed mitosis. For this purpose, mitotic cells were collected by mitotic shake-off after a release from a thymidine block and compared to nocodazole-treated cells (Fig. 29A). As expected, Cyclin B1 protein levels were increased in unperturbed mitotic cells compared to asynchronous cells. However, an increase in FBXW7 α protein levels upon depletion of FBXO45 and MYCBP2 could only be observed in nocodazole-treated cells, but not in mitotic cells after release from a thymidine block. This indicates that the effect of FBXO45 and MYCBP2 on FBXW7 α protein levels specifically occurs in a prolonged mitotic arrest, but not in unperturbed mitosis.

In order to exclude that the observed effects on FBXW7 α protein levels are caused by side-effects of the transfected siRNAs, siRNAs targeting different regions of FBXO45 and MYCBP2 mRNA were used (Fig. 29C). In mitotic HeLa cells, FBXW7 α protein levels increased upon FBXO45 or MYCBP2 downregulation mediated by different siRNAs. The downregulation of FBXO45 and MYCBP2 by the different siRNAs was confirmed by Western blotting (Fig. 29B-C).

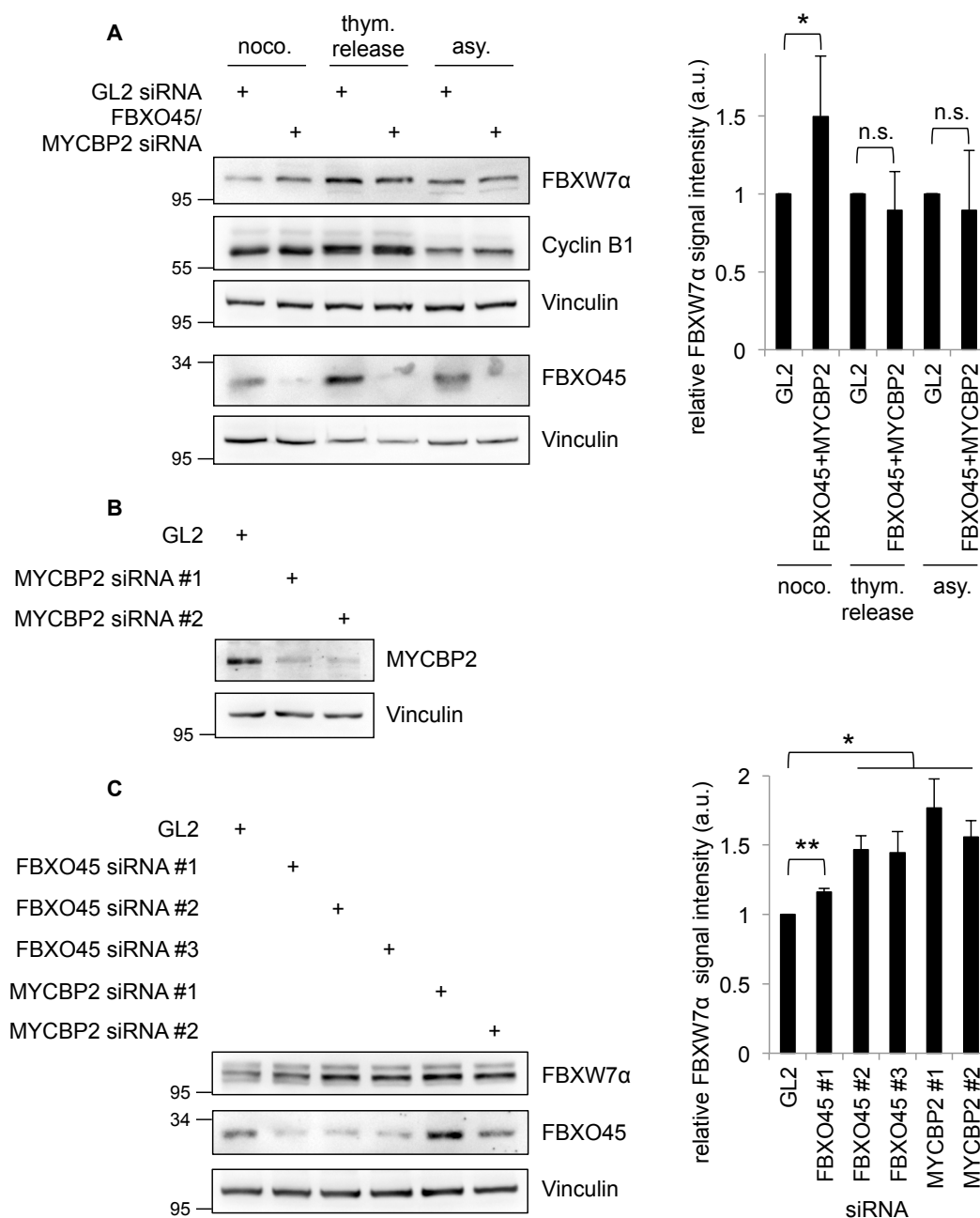


Fig. 29: FBXW7 α protein levels are negatively regulated by FBXO45 and MYCBP2 during prolonged mitotic arrest.

A: HeLa cells were transfected with 30 nM FBXO45 and MYCBP2 siRNAs for 72 h. GL2 siRNA was used as a control. The cells were arrested in mitosis by nocodazole (noco.) treatment (100 ng/mL for 17 h) and collected by a mitotic shake-off. Alternatively, mitotic cells were enriched after a release from a double-thymidine block (thym. release), followed by a mitotic shake-off when the cells reached the mitotic peak. The mitotic cells were compared with an asynchronous (asy.) cell population. Cell extracts were analyzed by Western blotting with α -FBXW7 α , α -Cyclin B1, α -FBXO45 and α -Vinculin antibodies. Vinculin was used as a loading control. A quantification of relative FBXW7 α signal intensities is shown. Relative FBXW7 α signals in the GL2 controls were set to 1. Average signal intensities and standard deviations from n=5 experiments were calculated. Statistical significance was analyzed by a two-tailed, unpaired t-test with unequal variance. * p<0.05; n.s.: not significant. **B:** HeLa

cells were transfected with 30 nM of different MYCBP2 siRNAs for 72 h. Cell extracts were analyzed by Western blotting with α -MYCBP2 and α -Vinculin antibodies. Vinculin was used as a loading control. **C:** HeLa cells were transfected with 30 nM of GL2, three different FBXO45 siRNAs or two different MYCBP2 siRNAs for 72 h. In addition, the cells were treated with 100 ng/mL nocodazole for 17 h before they were collected by a mitotic shake-off. Cell extracts were analyzed by Western blotting with α -FBXW7 α , α -FBXO45 and α -Vinculin antibodies. Vinculin was used as a loading control. Relative FBXW7 α signal intensities were quantified. Relative signal intensity in the GL2 control was set to 1. Average signal intensities and standard deviations from n=3 experiments were calculated. Statistical significance was analyzed by a two-tailed, unpaired t-test with unequal variance. * p<0.05; ** p<0.01.

3.4.3. FBXO45 and MYCBP2 promote the ubiquitylation of FBXW7 α

My results reveal that FBXO45 and MYCBP2 negatively regulate FBXW7 α protein levels during mitotic arrest (Fig. 29). In order to test whether this regulation is mediated by the ubiquitylation of FBXW7 α , HEK-293T cells were transfected with constructs encoding Myc-FBXO45 and HA-Ubiquitin. Additionally, cells were treated with nocodazole to arrest them in mitosis and with MG132 in order to inhibit the proteasome and to allow the accumulation of ubiquitylated proteins. Cell extracts were then used for immunoprecipitations directed against endogenous FBXW7 α . Western blot analysis of the FBXW7 α immunoprecipitates revealed that Myc-FBXO45 overexpression caused a strong, ladder-like HA signal pattern in co-immunoprecipitation with FBXW7 α (Fig. 30A). In contrast, HA signals could not be detected upon immunoprecipitation with a control antibody as well as in the absence of Myc-FBXO45 or HA-Ubiquitin. This indicates that FBXO45 promotes the ubiquitylation of FBXW7 α .

A similar experiment was performed in order to test a putative ubiquitylation of FBXW7 α by MYCBP2. Flag-FBXW7 α and Myc-MYCBP2 or Flag-FBXW7 α alone were overexpressed in HEK-293T cells. After treatment of the cells with nocodazole and MG132, the cells were harvested. Cell extracts were used for immunoprecipitations directed against the Flag tag. Immunoprecipitates were analyzed for the presence of endogenous Ubiquitin signals by Western blotting. As shown in Fig. 30B, overexpression of Myc-MYCBP2 caused an increase in the ubiquitylation pattern intensity in the Flag-FBXW7 α immunoprecipitate. This indicates that, in addition to FBXO45, also MYCBP2 promotes FBXW7 α ubiquitylation. Moreover, these results suggest that the regulation of FBXW7 α protein levels by FBXO45 and MYCBP2 depends on the ubiquitin-proteasome system.

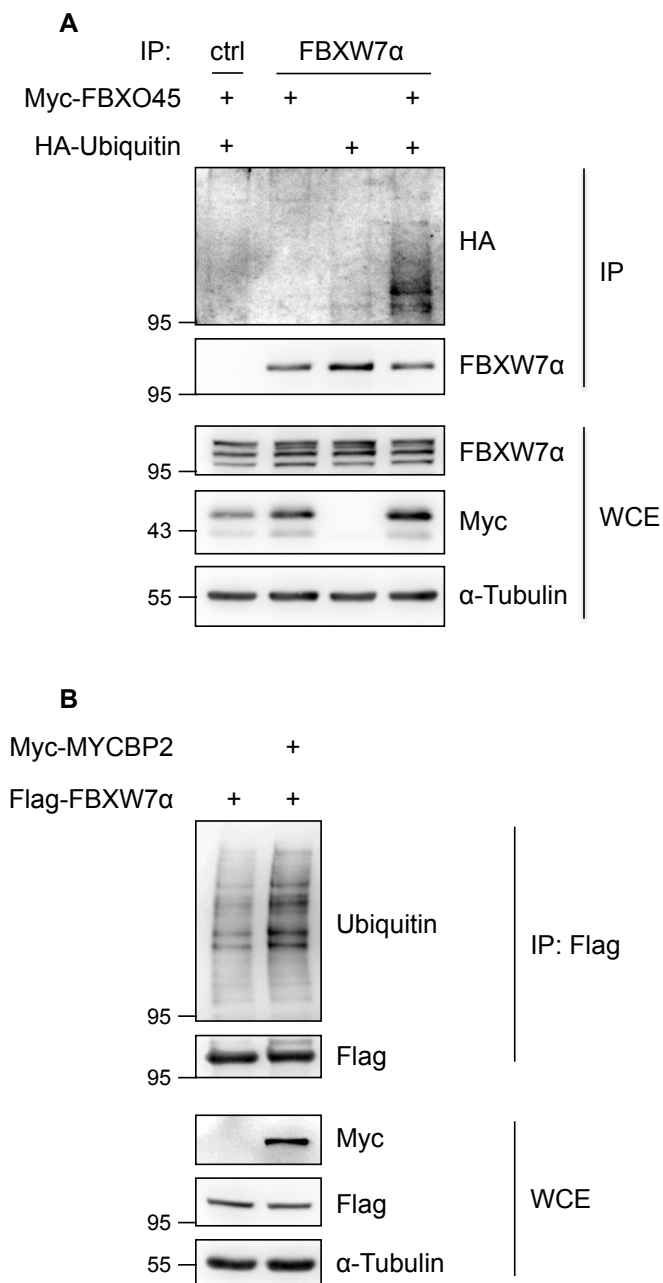


Fig. 30: FBXO45 and MYCBP2 promote the ubiquitylation of FBXW7 α .

A: Myc-FBXO45 and HA-Ubiquitin were overexpressed in HEK-293T cells for 48 h. 4 h before harvesting, cells were treated with MG132. Cell extracts were prepared and immunoprecipitations with FBXW7 α antibodies were performed. Rabbit IgG was used for a control immunoprecipitation. Immunoprecipitates were analyzed by Western blotting with α -HA, α -FBXW7 α , α -Myc and α -Tubulin antibodies. Tubulin was used as a loading control. **B:** Myc-MYCBP2 and Flag-FBXW7 α were overexpressed in HEK-293T cells for 48 h. 4 h before harvesting, cells were treated with MG132. Cell extracts were used for immunoprecipitations directed against the Flag tag. Immunoprecipitates were analyzed by Western blotting with α -Ubiquitin, α -Flag, α -Myc and α -Tubulin antibodies. Tubulin was used as a loading control.

3.4.4. FBXO45 mediates FBXW7 α destabilization during mitotic arrest

Proteins that are regulated by the ubiquitin-proteasome system are stabilized upon depletion of their upstream E3 ubiquitin ligases. In order to determine protein stability experimentally, synthesis of new proteins needs to be inhibited. The inhibition of cellular protein synthesis can be achieved by treatment of the cells with cycloheximide, an inhibitor of translation produced by the bacterium *Streptomyces griseus*.

In order to study the effect of FBXO45 on FBXW7 α protein stability during mitotic arrest, cells were transfected with GL2 or FBXO45 siRNA. In addition, cells were treated with nocodazole. Mitotic cells were collected by a mitotic shake-off and further incubated with nocodazole and cycloheximide. Cells were then harvested at different time points and cell extracts were prepared. Western blot analysis of the extracts revealed that FBXW7 α was readily degraded in the control cells. Upon downregulation of FBXO45, however, FBXW7 α was clearly stabilized (Fig. 31). This suggests that FBXO45 destabilizes FBXW7 α , thus confirming that FBXO45 promotes the degradation of FBXW7 α .

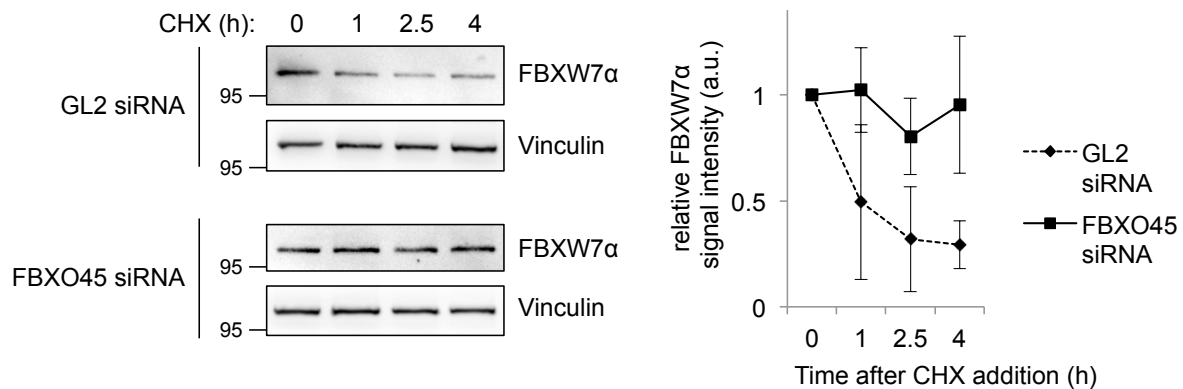


Fig. 31: FBXW7 α is stabilized upon siRNA-mediated downregulation of FBXO45.

HeLa cells were transfected with 30 nM GL2 or FBXO45 siRNA for 72 h. 17 h before harvesting, the cells were treated with 100 ng/mL nocodazole. Mitotic cells were collected by a mitotic shake-off and further incubated with 100 ng/mL nocodazole and 100 μ g/mL cycloheximide (CHX). The cells were harvested at different time points after the addition of cycloheximide by a mitotic shake-off. Cell extracts were analyzed by Western blotting with α -FBXW7 α and α -Vinculin antibodies. Vinculin was used as a loading control. Relative FBXW7 α signal intensities were quantified and average signal intensities as well as standard deviations from n=3 independent experiments are shown.

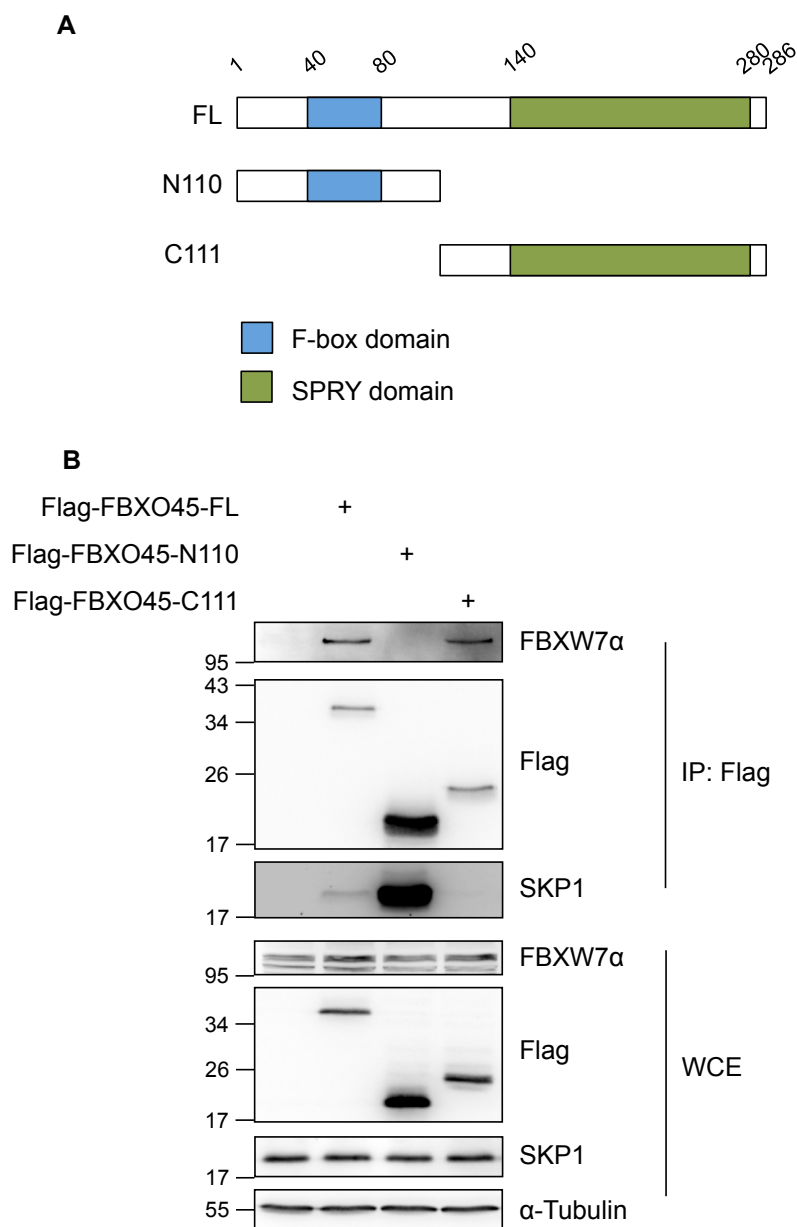


Fig. 32: FBXW7 α interacts with the C-terminus of FBXO45.

A: Overview of truncated FBXO45 versions. Positions of F-box domain (blue) and SPRY domain (green) are illustrated. **B:** The indicated Flag-tagged FBXO45 versions were overexpressed in HEK-293T cells for 24 h. Cell extracts were used for α -Flag immunoprecipitations. Immunoprecipitates were analyzed by Western blotting with α -FBXW7 α , α -Flag, α -SKP1 and α -Tubulin antibodies. Tubulin was used as a loading control.

3.4.5. FBXW7 α interacts with the C-terminus of FBXO45

FBXO45 contains two well-characterized domains, an N-terminal F-box domain and a C-terminal SPRY domain. The SPRY domain has been shown to mediate FBXO45 substrate binding (Chen et al., 2014; Kugler et al., 2010). As previous results suggest that FBXW7 α is a substrate of FBXO45, it was analyzed whether FBXW7 α interacts

with the SPRY domain containing C-terminus of FBXO45. In order to test this, Flag-tagged versions of an N-terminal (Flag-FBXO45-N110) and a C-terminal FBXO45 fragment (Flag-FBXO45-C111) were generated (Fig. 32A). The FBXO45 fragments as well as a full-length version of FBXO45 were overexpressed in HEK-293T cells. The cell extracts were used for immunoprecipitations with α -Flag agarose beads. As expected, SKP1 only interacted with the full-length version of FBXO45 and the Flag-FBXO45-N110 fragment, which contains the F-box domain (Fig. 32B). In contrast, FBXW7 α was only detected in co-immunoprecipitation with the full-length version of FBXO45 and the Flag-FBXO45-C111 fragment, which contains the SPRY domain (Fig. 32B). These results indicate that the interaction between FBXW7 α and FBXO45 depends on the SPRY domain of FBXO45, thus further supporting the finding that FBXW7 α is a novel FBXO45 substrate.

3.4.6. FBXO45 and MYCBP2 promote mitotic slippage

FBXW7 has been described to regulate mitotic cell fate. In cells that have been treated with antimicrotubule drugs in order to arrest them in mitosis, FBXW7 promotes mitotic cell death (Wertz et al., 2011). This function is consistent with the role of FBXW7 as a tumor suppressor protein as cancer cells are often able to evade mitotic cell death, thereby causing chemoresistance.

As FBXO45 and MYCBP2 mediate the degradation of FBXW7 α during mitotic arrest, they are expected to have a negative effect on mitotic cell death, thus promoting mitotic slippage. In order to test this, siRNA-mediated downregulation of FBXW7, FBXO45, MYCBP2 or FBXO45 in combination with MYCBP2 were performed in U2OS cells. The cells were treated with nocodazole and the mitotic cell fate was analyzed by live-cell imaging (Fig. 33A).

As expected, siRNA-mediated downregulation of FBXW7 caused a significant increase in mitotic slippage from about $61\pm 9\%$ in the control to about $74\pm 4\%$. FBXO45 downregulation led to a slight decrease in mitotic slippage to about $54\pm 14\%$, whereas MYCBP2 downregulation reduced mitotic slippage to about $51\pm 8\%$. However, these differences were not significant. On the other hand, co-depletion of FBXO45 and MYCBP2 caused a significant reduction of mitotic slippage to about $43\pm 10\%$ (Fig. 33B).

In summary, these results show that FBXW7 and FBXO45/MYCBP2 have opposing effects on mitotic cell fate. This is consistent with our model that FBXW7 α protein levels are regulated by the FBXO45/MYCBP2 ubiquitin ligase.

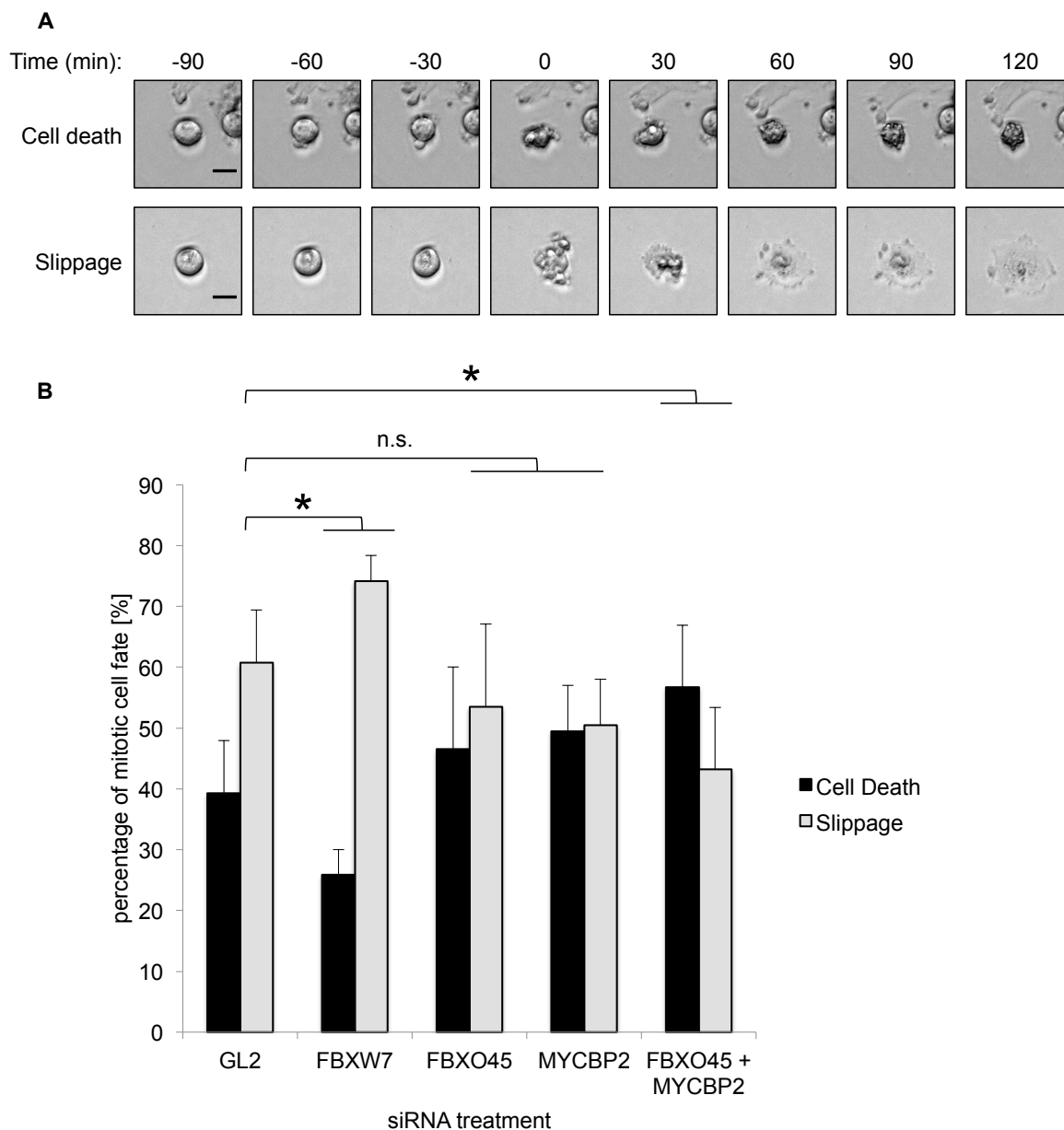


Fig. 33: FBXO45 and MYCBP2 promote mitotic slippage.

A-B: U2OS cells were transfected with 30 nM GL2, FBXW7, FBXO45 or MYCBP2 siRNA for 72 h and treated with 250 ng/mL nocodazole. 4 h after nocodazole addition, cells were analyzed by live-cell imaging. Representative images from live-cell imaging are shown in A. Time point 0 marks induction of mitotic cell death or mitotic slippage. Scale bars: 20 μ m. Percentages of cells undergoing mitotic cell death or mitotic slippage were quantified and are presented in B. Cells from n=4 independent experiments were analyzed. In each experiment, 50-80 cells were quantified. Statistical significance was analyzed by a two-tailed, unpaired t-test. * $p < 0.05$; n.s.: not significant.

4. Discussion

4.1. Identification of novel FBXW7 α interaction partners

FBXW7 is a well-characterized tumor suppressor protein with a broad spectrum of known interaction partners. So far, most studies have focused on the identification and characterization of downstream FBXW7 substrates, whereas upstream ubiquitin ligases regulating FBXW7 protein levels remain to be identified. In addition to auto-ubiquitylation, Parkin is the only E3 that has been described to regulate FBXW7 protein stability and this regulation is specific for the FBXW7 β isoform (Ekholm-Reed et al., 2013; Galan and Peter, 1999). Because FBXW7 exerts crucial functions within the cell, I hypothesized that FBXW7 protein levels need to be tightly controlled by different upstream ubiquitin ligases. It is for this reason that I performed a screen for novel FBXW7 interaction partners in order to identify ubiquitin ligases that are involved in the regulation of FBXW7. For the screen, which was based on immunoprecipitation and mass spectrometry analysis, I chose FBXW7 α as the bait protein because Parkin was already described as a regulator of the FBXW7 β isoform and because FBXW7 α is the most ubiquitously expressed isoform with broad functions in different tissues (Matsumoto et al., 2006; Spruck et al., 2002).

The fact that there are already many known FBXW7 interaction partners was used to validate the screen. Several known FBXW7 interaction partners were identified by mass spectrometry (Fig. 5), including the SCF components CUL1, SKP1 and RBX1, the CRL regulators NEDD8 and ARIH1 as well as the FBXW7 substrates MYC, NOTCH1/NOTCH2, MED13/MED13L, Aurora-B and mTOR (Davis et al., 2013; Feldman et al., 1997; Freed et al., 1999; Hubbard et al., 1997; Mao et al., 2008; Osaka et al., 1998; Read et al., 2000; Scott et al., 2016; Teng et al., 2012; Yada et al., 2004).

Also other screens for interaction partners that were performed in this study could be validated in this manner. For XIAP, the known interaction partner HTRA2 was identified, whereas mass spectrometry detected NUP98 and BUB1/BUB1B in the RAE1 screen (Pritchard et al., 1999; Suzuki et al., 2001; Wang et al., 2001).

4.2. WDR5 is a putative FBXW7 substrate

Apart from focusing on FBXW7 regulators, I performed an initial characterization of WDR5 as a putative FBXW7 substrate. WDR5 is an interesting candidate because it

was identified in the screen (Fig. 5C) and has important functions as part of a histone methyltransferase complex and as a mitotic regulator of spindle assembly (Ali et al., 2017; Rao and Dou, 2015). Interestingly, WDR5 was described to cooperate with MYC, which is a known substrate of FBXW7. MYC was shown to directly interact and to colocalize with WDR5 on chromatin. MYC mutants that cannot interact with WDR5 partly lose their oncogenic potential, which supports an oncogenic role of WDR5 in MYC-mediated transcription (Thomas et al., 2015). Moreover, the MYC-WDR5 axis was found to support pancreatic cancer cell proliferation and to protect cancer cells from DNA damage (Carugo et al., 2016). In addition, WDR5 was found to interact and cooperate with NMYC, an oncogenic member of the MYC protein family and a known substrate of FBXW7, in neuroblastoma (Otto et al., 2009; Sun et al., 2015; Yada et al., 2004). FBXW7 has already been shown to regulate important pathways by mediating the degradation of several pathway components. For example, FBXW7 controls the NOTCH pathway by regulating NOTCH and its activator Presenilin (Hubbard et al., 1997; Li et al., 2002; Wu et al., 1998). Therefore, it is conceivable that FBXW7 could regulate the important oncogenic MYC pathway via both MYC and WDR5. Interestingly, analysis of the human WDR5 protein sequence reveals that WDR5 contains a motif (PTPSSS, amino acids 17-22), which nicely matches the CPD consensus motif (Table 1).

WDR5 protein levels were already shown to be regulated by the ubiquitin system. CUL4B-DDB1 was suggested as a ubiquitin ligase for WDR5 in the regulation of neuronal gene expression (Nakagawa and Xiong, 2011).

Initial experiments presented in this thesis showed an endogenous interaction between FBXW7 α and WDR5 (Fig. 6A). Moreover, depletion of FBXW7 caused an increase in WDR5 protein levels (Fig. 6B-C), supporting a putative regulation of WDR5 by FBXW7.

However, I cannot exclude that the observed interaction between FBXW7 and WDR5 is indirectly mediated by MYC. Additionally, the effects on WDR5 protein levels could be indirect. Indeed, the transcription of the *WDR5* gene was shown to be upregulated by the FBXW7 substrate NMYC (Sun et al., 2015). Therefore, further experiments will be required in order to validate the direct regulation of WDR5 protein levels by FBXW7.

4.3. Analysis of putative FBXW7 α regulators

Ubiquitin ligases that had been identified as putative FBXW7 α interaction partners by mass spectrometry (Fig. 5C) were considered as putative regulators of FBXW7 α protein levels. Their effects on FBXW7 α protein levels were analyzed by siRNA-mediated downregulation of the corresponding E3s in HeLa cells. None of the analyzed siRNAs had a positive effect on FBXW7 α protein levels (Fig. 7B, 8A-B). There are several possible explanations for this observation. First, the experiment was performed with an asynchronous cell population under standard growth conditions. It is possible that the putative regulators only show an effect on FBXW7 protein levels in a specific context, for example in a specific cell-cycle stage or upon activation by a specific stimulus. Second, the putative ubiquitylation of FBXW7 by the candidate E3s does not necessarily have to cause proteasomal degradation of FBXW7. Depending on the type of ubiquitylation, there are alternative effects apart from degradation. For example, FBXW7 ubiquitin ligase activity or localization could be changed upon ubiquitylation (reviewed by Dikic et al., 2009). Third, the analyzed ubiquitin ligases could be FBXW7 substrates instead of FBXW7 regulators. Finally, the putative interactions between FBXW7 and the analyzed ubiquitin ligases could be indirect or unspecific.

It is for these reasons that I decided to choose only one ubiquitin ligase (XIAP) from the list of putative FBXW7 regulators in order to study the interaction as well as putative effects on FBXW7 in more detail.

4.4. XIAP, RAE1, FBXO45, MYCBP2 and SPRYD3 form a complex with FBXW7 α

As described above, I decided to characterize the interaction between XIAP and FBXW7 α in more detail. I chose XIAP for further characterization because it is a well-characterized protein with oncogenic functions, which is considered as a promising target in cancer therapy (reviewed by Fulda and Vucic, 2012). An interaction of an oncoprotein with a tumor suppressor protein seems likely. Moreover, XIAP was identified with one of the highest MASCOT scores in the screen for FBXW7 α interaction partners (Fig. 5C).

In the course of this project, XIAP was shown to interact with the N-terminal domain of the FBXW7 α isoform *in vivo* (Fig. 13). XIAP could not be shown to directly bind the N-terminal domain of FBXW7 α (Fig. 14), which rules out that there is a direct effect of XIAP on FBXW7 α . Therefore, additional screens based on immunoprecipitation and

mass spectrometry were performed in order to identify the protein(s) that indirectly mediate the interaction between XIAP and FBXW7 α . Interestingly, the screen for XIAP interaction partners identified RAE1, FBXO45, MYCBP2 and SPRYD3 with high MASCOT scores (Fig. 15C), which had already been identified in the screen for FBXW7 α interaction partners (Fig. 5C). Detailed interaction studies revealed that RAE1 interacted with the same part of the N-terminal FBXW7 α domain as XIAP (Fig. 17, 18). Moreover, sequential immunoprecipitation suggested that FBXW7 α , XIAP and RAE1 form a complex (Fig. 20A). In order to identify putative additional components of this complex, the samples obtained after sequential immunoprecipitation were analyzed by mass spectrometry. Interestingly, FBXO45, MYCBP2 and SPRYD3 were also identified in this screen (Fig. 20C). These results were supported by another screen for RAE1 interaction partners, where XIAP, FBXO45, MYCBP2, SPRYD3 and FBXW7 were identified (Fig. 21C). Finally, FBXO45 and MYCBP2 bound to the same part of the N-terminal FBXW7 α domain as XIAP and RAE1 (Fig. 22B-C). An additional sequential immunoprecipitation approach revealed that FBXW7 α , FBXO45 and MYCBP2 form a complex (Fig. 25). Taken together, these results strongly suggest that FBXW7 α , XIAP, RAE1, FBXO45, MYCBP2 and SPRYD3 are found in a complex *in vivo*.

Importantly, this conclusion is supported by the literature. On the one hand, FBXO45 is a known interaction partner of MYCBP2 (Liao et al., 2004; Saiga et al., 2009; Wu et al., 2007). Also RAE1 was shown to interact with MYCBP2 (Grill et al., 2012; Tian et al., 2011). On the other hand, several published screens found putative interactions between some of the complex components identified in this study. A published screen for FBXW7 α interaction partners identified MYCBP2, FBXO45, RAE1 and SPRYD3 (Kourtis et al., 2015). The authors suggested an indirect interaction between FBXW7 α and FBXO45/MYCBP2 via the SCF complex without showing any experimental evidence for this. However, the results obtained in the presented thesis do not support this speculation. The F-box domain of FBXW7 α was not required for the interaction with FBXO45 and MYCBP2. Instead, FBXO45 and MYCBP2 (as well as XIAP and RAE1) bound to the N-terminal domain of FBXW7 α (Fig. 22B-C). Moreover, FBXO45 interacted with the N-terminal domain of FBXW7 α *in vitro* (Fig. 26A).

Yet another published screen for protein interaction networks identified putative interactions between FBXW7 and MYCBP2, FBXO45 as well as RAE1 (Huttlin et al.,

2017). In summary, these published data support the interactions that are characterized in the presented thesis.

4.5. FBXO45 and MYCBP2 promote the degradation of FBXW7 α during mitotic arrest

Putative direct interactions between the N-terminal domain of FBXW7 α and XIAP, RAE1, FBXO45 as well as MYCBP2 were analyzed (Fig. 14, 26). Only FBXO45 bound to the N-terminal FBXW7 α domain *in vitro* (Fig. 26A). FBXO45 has been described to form a ubiquitin ligase complex with MYCBP2 (Liao et al., 2004; Saiga et al., 2009; Wu et al., 2007). Therefore, I focused on the analysis of FBXO45/MYCBP2-mediated effects on FBXW7 α protein levels in this thesis. Interestingly, FBXO45 and MYCBP2 specifically regulated FBXW7 α protein levels in a mitotic arrest, whereas no effects were observed in unperturbed mitosis or in asynchronous cells (Fig. 29A). The presented data in this thesis suggest that the negative regulation of FBXW7 α protein levels by FBXO45/MYCBP2 depends on the ubiquitin-proteasome system based on the following observations: (1) Overexpression of both FBXO45 and MYCBP2 induce an increased ubiquitylation of FBXW7 α (Fig. 30) and (2) siRNA-mediated downregulation of FBXO45 increased the stability of FBXW7 α protein in a cycloheximide experiment (Fig. 31).

Interestingly, several links between MYCBP2 and FBXW7 substrates have been described in the literature. MYCBP2 was originally identified as a MYC interaction partner (Guo et al., 1998). MYCBP2 binds to a region of MYC that contains the CPD motif, which is recognized and bound by FBXW7 (Yada et al., 2004). MYC and FBXO45 bind to the same domain of MYCBP2 (Saiga et al., 2009). A MYCBP2 fragment that contains the MYC- and FBXO45-binding domains interacts with FBXW7 α (Fig. 24). Therefore, although the interaction between MYC and MYCBP2 was shown *in vitro*, it is possible that the interaction could partly be mediated by FBXW7 α *in vivo*.

Other publications described a positive effect of MYCBP2 on mTOR signaling and a link between MYCBP2 and the circadian regulator REV-ERB α (Han et al., 2008; Maeurer et al., 2009; Murthy et al., 2004; Yin et al., 2010). However, the effects of MYCBP2 on REV-ERB α have only been observed in combination with another ubiquitin ligase called HUWE1. Therefore, the specific role of MYCBP2 in the regulation of REV-ERB α remains elusive.

4.6. Degradation of FBXW7 α by FBXO45/MYCBP2 might promote resistance to spindle poisons

Spindle poisons, such as nocodazole, vincristine or paclitaxel (Taxol), are drugs that prevent the assembly (nocodazole, vincristine) or the disassembly (paclitaxel) of microtubules (reviewed by Field et al., 2014). By preventing normal microtubule dynamics, spindle poisons inhibit spindle function and chromosome segregation during mitosis. Treatment with spindle poisons therefore activates the spindle assembly checkpoint (SAC) and the corresponding cells arrest in mitosis. Cells that have been arrested in mitosis after treatment with spindle poisons frequently undergo mitotic cell death. It is for this reason that spindle poisons, for example paclitaxel and vincristine, are widely used in chemotherapy in order to prevent proliferation of cancer cells and to induce cancer cell death (reviewed by Topham and Taylor, 2013). However, cells that are arrested in mitosis do not always undergo mitotic cell death. Alternatively, cells can perform mitotic slippage, which means that they exit from mitosis without completing a normal cell division, resulting in tetraploid cells. Mitotic slippage is a problem with respect to chemotherapy as cancer cells are often able to evade mitotic cell death by performing mitotic slippage. Mitotic slippage can therefore promote chemoresistance of cancer cells. Resistance to drugs is a big problem in chemotherapy and often impairs their result. In addition, the formation of tetraploid cells by mitotic slippage supports aneuploidy and cancer formation (reviewed by Topham and Taylor, 2013).

The decision whether a cell undergoes mitotic cell death or mitotic slippage depends on the balance between different signals. On the one hand, there are death signals that result in the activation of caspases. On the other hand, Cyclin B gets slowly degraded during mitotic arrest, promoting the exit from mitosis (Brito and Rieder, 2006). Originally, residual APC/C activity has been thought to mediate the degradation of Cyclin B while the SAC is active. However, this view is challenged by the discovery of a CRL2 complex that degrades Cyclin B during mitotic arrest (Balachandran et al., 2016). If one of the opposing signals, caspase activation or Cyclin B degradation, reaches a specific threshold, mitotic cell death or mitotic slippage will be induced (Topham and Taylor, 2013).

Several oncoproteins and tumor suppressors are involved in the regulation of mitotic cell fate. For example, MCL1 is an inhibitor of apoptosis and a key regulator of cell death signals during mitotic arrest. MCL1 is unstable during mitotic arrest, allowing

death signals to increase with time. Overexpression of MCL1 in cancer delays the increase in death signals, thereby promoting mitotic slippage (Schwickart et al., 2010). Two different ubiquitin ligases have been shown to promote the degradation of MCL1 during mitotic arrest. On the one hand, the APC/C causes a decrease in MCL1 protein levels in prolonged mitosis (Harley et al., 2010). On the other hand, the SCF-FBXW7 complex was identified as a regulator of MCL1 both in interphase and in mitosis (Inuzuka et al., 2011; Wertz et al., 2011). Indeed, deletion of FBXW7 was found to promote mitotic slippage, which is consistent with its function to mediate the degradation of MCL1, thereby promoting cell death signals during mitotic arrest (Wertz et al., 2011). The promotion of mitotic cell death by FBXW7 is also consistent with its role as a tumor suppressor, as it counteracts cancer cell death evasion.

In the presented thesis, the effect of FBXW7 on mitotic cell fate was confirmed. As expected, siRNA-mediated downregulation of FBXW7 promoted mitotic slippage (Fig. 33). As FBXO45 and MYCBP2 promoted the degradation of FBXW7 α specifically during mitotic arrest, it was conceivable that they would indirectly also affect mitotic cell fate. Indeed, siRNA-mediated downregulation of FBXO45 and MYCBP2 promoted mitotic cell death (Fig. 33), which is consistent with their roles as negative regulators of FBXW7 α protein levels. In conclusion, it is possible that FBXO45 and MYCBP2 are involved in the regulation of cell death signals during mitotic arrest, thereby modulating the balance between mitotic cell death and mitotic slippage. Overexpression of FBXO45 and MYCBP2 in cancer might promote mitotic slippage, thereby supporting resistance of cancer cells to spindle poisons.

Consistent with this putative oncogenic function of the FBXO45/MYCBP2 complex, FBXO45 amplification is frequently found in different cancer types (cBioPortal for Cancer Genomics, Cerami et al., 2012; Gao et al., 2013). Moreover, FBXO45 was already described to have a negative effect on apoptosis by the regulation of p73 and PAR4 (Chen et al., 2014; Peschiaroli et al., 2009).

4.7. Different FBXW7 substrates could mediate the effect of FBXO45/MYCBP2 on mitotic cell fate

As described above, FBXW7 is thought to induce mitotic cell death by promoting the degradation of MCL1 (Wertz et al., 2011). However, the exact role of FBXW7 in mitotic MCL1 degradation is still under debate because the APC/C-CDC20 has been shown to regulate MCL1 in the same cellular context (Harley et al., 2010). It is

possible to argue that the SCF-FBXW7 complex could be solely responsible for MCL1 ubiquitylation during prolonged mitotic arrest with active SAC signaling because the APC/C should be inhibited under these conditions. However, the APC/C is able to promote the degradation of specific substrates, for example Cyclin A, independently from SAC activation (den Elzen and Pines, 2001; Geley et al., 2001). It is therefore still unclear whether the APC/C and the SCF-FBXW7 complex cooperate or compete regarding mitotic degradation of MCL1. Furthermore, it is possible that the effect of FBXW7 on mitotic cell fate is mediated by additional substrates apart from MCL1.

Similar to FBXW7, MYC has been shown to promote mitotic cell death (Topham et al., 2015). At first glance, this suggests that MYC cannot be the FBXW7 substrate mediating the effects of FBXW7 on mitotic cell fate. However, the pro-apoptotic function of MYC mainly stems from an apoptotic transcription program that is induced upon MYC overexpression during interphase (Topham et al., 2015). It is possible that MYC could have other anti-apoptotic effects specifically during mitotic arrest that cannot be observed upon overexpression of MYC during the whole cell cycle. In this case, specific regulation of MYC by the FBXO45/MYCBP2-FBXW7 α axis during mitotic arrest would be able to affect only the mitotic function of MYC. Indeed, MYC protein levels were observed to decrease during prolonged mitotic arrest, similar to MCL1 protein levels (Fig. 28). Moreover, there is published experimental evidence that the effect of MYC on mitotic cell fate could be complex and multilayer. MYC negatively regulates the expression of the anti-apoptotic protein BCL-XL (Eischen et al., 2001). Consistent with the anti-survival function of MYC, overexpression of BCL-XL prevented mitotic cell death. However, prevention of mitotic cell death upon BCL-XL overexpression was much more efficient than upon MYC downregulation (Eichhorn et al., 2014; Topham et al., 2015). This suggests that MYC could have additional functions opposing its role as a promoter of mitotic cell death. Consistent with this, it was suggested that MYC has a stabilizing effect on MCL1 protein (Topham et al., 2015). Therefore, it could be intriguing to analyze whether the suggested effect of FBXW7 on MCL1 during mitotic arrest could be partly mediated by MYC.

Furthermore, cancer-specific Cyclin E isoforms and JUN have been suggested to promote mitotic slippage (Bagheri-Yarmand et al., 2010; Duan et al., 2007). In

summary, these findings suggest that other FBXW7 substrates apart from MCL1 could be involved in FBXW7 dependent regulation of mitotic cell fate.

4.8. A negatively charged motif within the N-terminal domain of FBXW7 α is recognized by FBXO45/MYCBP2

In this study, a short motif within the N-terminal domain of FBXW7 α , which is required for the interactions with XIAP, RAE1, FBXO45 and MYCBP2, was identified (Fig. 22). Interestingly, the motif is negatively charged because of its high content of acidic amino acid residues (glutamate and aspartate). Moreover, the motif is highly conserved among vertebrate orthologues of FBXW7 (Fig. 19).

FBXO45 is the direct interaction partner of FBXW7 α within the identified protein complex (Fig. 26A). An FBXO45 fragment containing the SPRY domain was shown to bind FBXW7 α (Fig. 32). The SPRY domain has already been shown to bind substrates of the FBXO45/MYCBP2 complex (Chen et al., 2014; Kugler et al., 2010). Sequence motifs within substrates that are recognized by SPRY domain containing proteins have only poorly been characterized so far. One of the only known sequence motifs that were shown to bind to SPRY domains was identified in the *Drosophila* protein VASA. The VASA motif (DINNNN) is recognized by the SPRY domain and SOCS box containing (SPSB) protein GUSTAVUS (Styhler et al., 2002). Human SPSB proteins have been shown to interact with a similar motif (ELNNNL) of the human protein PAR4 (Woo et al., 2006). Additional studies suggested that this motif of PAR4 is also recognized by the SPRY domain of FBXO45 and that FBXO45 binds to two similar motifs (DMNDNR and DVNDNP) within CDH2 (Chen et al., 2014; Chung et al., 2014). However, a similar motif is not included in the N-terminal FBXW7 α sequence that is required for the interaction with FBXO45 (Fig. 19).

Interestingly, however, there is another interaction between a SPRY domain and a sequence motif in the literature that has been characterized extensively. ASH2L and RBBP5, two components of a histone methyltransferase complex, interact via the SPRY domain of ASH2L. The motif in RBBP5, which interacts with the SPRY domain of ASH2L, has been identified in several publications (Cao et al., 2010; Zhang et al., 2015). Importantly, the RBBP5 motif contains a high percentage of negatively charged D and E residues, suggesting that SPRY domains might be able to bind acidic patches within protein sequences. This is consistent with the finding that the

FBXO45 binding motif within the N-terminal domain of FBXW7 α contains a cluster of acidic residues (Fig. 19).

4.9. Putative roles of RAE1, XIAP and SPRYD3 in the complex with FBXW7 α , FBXO45 and MYCBP2

RAE1, XIAP and SPRYD3 were identified as putative components of the complex with FBXW7 α , FBXO45 and MYCBP2. However, RAE1 and XIAP did not interact with FBXW7 α *in vitro* (Fig. 14, 26). The interaction between SPRYD3 and FBXW7 α has not been analyzed in this thesis. Therefore, the question remains what the roles of RAE1, XIAP and SPRYD3 could be in the complex.

RAE1 has been described as a conserved interaction partner of MYCBP2. It was shown to cooperate with MYCBP2, but the specific function of RAE1 in complex with MYCBP2 is not completely clear. *Drosophila* RAE1 was suggested to stabilize Highwire by preventing its autophagy-dependent degradation (Tian et al., 2011). On the other hand, another publication suggested that *C. elegans* RAE1 functions downstream of RPM-1 (Grill et al., 2012). In the same publication, the authors showed that binding of RAE1 to RPM-1 is required for RPM-1 function, whereas they did not observe an effect of RAE1 on RPM-1 protein levels. Therefore, it remains unclear whether RAE1 could have different roles in different organisms. Alternatively, RAE1 could act downstream of MYCBP2 and could simultaneously feed back on MYCBP2 protein levels or activity.

So far, XIAP has not been described as an interaction partner of FBXW7 α , FBXO45, MYCBP2, RAE1 or SPRYD3. Since FBXO45 and MYCBP2 had a specific effect on FBXW7 α protein levels during mitotic arrest, it is interesting to discuss the known mitotic functions of XIAP. XIAP was shown to be deubiquitylated and stabilized by USP9X during mitotic arrest. USP9X and XIAP promoted chemoresistance (Engel et al., 2016). On the other hand, XIAP gets phosphorylated by CDK1-Cyclin B1 during mitotic arrest, which prevents the anti-apoptotic activity of XIAP, thus promoting mitotic cell death induced by spindle poisons (Hou et al., 2017). The role of XIAP in the regulation of mitotic cell death could be a link to the FBXO45/MYCBP2-dependent degradation of FBXW7 α during mitotic arrest. XIAP could inhibit mitotic cell death not only by the inhibition of caspases or stimulation of NF- κ B signaling, but also by promoting the FBXO45/MYCBP2-dependent degradation of FBXW7 α . XIAP

could possibly promote the degradation of FBXW7 α by promoting FBXO45/MYCBP2 complex formation or by stimulating FBXO45/MYCBP2 ubiquitin ligase activity.

SPRYD3 is an uncharacterized protein whose cellular function is still unknown. It was identified as a putative interaction partner of FBXW7 α , FBXO45, MYCBP2, RAE1 and XIAP in this thesis. Interestingly, SPRYD3 contains a SPRY domain similar to FBXO45. The SPRY domain of FBXO45 was shown to bind substrates of the FBXO45/MYCBP2 complex (Chen et al., 2014; Kugler et al., 2010). Also FBXW7 α binds to an FBXO45 fragment that contains the SPRY domain (Fig. 32). Therefore, it is possible that SPRYD3 serves as an additional substrate recognition subunit in the complex with MYCBP2. Indeed, there is evidence in the literature that MYCBP2 could use additional substrate recognition subunits apart from FBXO45. For example, the MYCBP2 substrate TSC2 (Tuberin), a negative regulator of mTOR signaling, shows increased protein levels in mice with Phr mutation, but not in mice with a Fbxo45 deletion. Moreover, overexpression of Phr leads to an activation of mTOR signaling, which is not observed upon overexpression of Fbxo45 (Han et al., 2012).

If SPRYD3 served as an additional substrate recognition subunit for MYCBP2 complexes, it could be interchangeable with FBXO45 in MYCBP2 complexes. This would be comparable to the interchangeability of F-box proteins within the SCF complex. Interchangeability of substrate recognition subunits in MYCBP2 complexes would allow the targeting of different substrate subsets under different conditions, for example in different cell-cycle stages. On the other hand, SPRYD3 could cooperate with FBXO45 to specifically target substrate proteins for ubiquitylation by MYCBP2. This would be comparable with the F-box protein SKP2, which uses the cofactor CKS1 to bind its substrate p27 (Ganoth et al., 2001; Spruck et al., 2001).

4.10. Outlook and perspectives

4.10.1. WDR5 as a putative FBXW7 substrate

Initial experiments suggested that WDR5 could act as a substrate of FBXW7. However, it cannot be excluded that the observed interaction between FBXW7 and WDR5 as well as the effect of FBXW7 on WDR5 protein levels are indirect. Therefore, it will be important to show a direct interaction between FBXW7 and WDR5 *in vitro* in future experiments. Moreover, in order to exclude that the effects on WDR5 protein levels are indirectly caused by an increase in WDR5 transcript levels

upon FBXW7 depletion, cycloheximide chase experiments can be performed. These experiments will show whether FBXW7 affects the protein stability of WDR5.

All of the known FBXW7 substrates bind to the WD40 domain of FBXW7. Thus, it would be interesting to analyze whether WDR5 also binds to the WD40 domain of FBXW7. Recognition of WDR5 by the WD40 domain would support the putative role of WDR5 as an FBXW7 substrate. On the other hand, FBXW7 substrates contain a conserved sequence motif, the CDC4 phosphodegron or CPD (Table 1). As discussed above, WDR5 contains a putative CPD motif. In future experiments, it could be tested if point mutations within the putative CPD of WDR5 affect the interaction with FBXW7. Moreover, it would be interesting whether WDR5 mutations within the CPD have an effect on its stability or on a putative ubiquitylation by FBXW7.

4.10.2. Verification of the FBXW7 α regulation by FBXO45/MYCBP2

The obtained data in the presented thesis suggest that the FBXO45/MYCBP2 protein complex interacts with a negatively charged motif within the N-terminal domain of FBXW7 α (Fig. 19, 22). The binding of FBXW7 α by the FBXO45/MYCBP2 complex is mediated by a direct interaction between FBXW7 α and FBXO45 (Fig. 26A). In future experiments, it will be necessary to further confirm this interaction. It should be tested whether a deletion of the binding site within the N-terminal domain of FBXW7 α also prevents the *in vitro* interaction between FBXW7 α and FBXO45. Moreover, the *in vitro* interaction between FBXW7 α and FBXO45 could be confirmed in experiments that only analyze the interaction between recombinant, bacterially purified proteins instead of using *in vitro* transcription and translation approaches with rabbit reticulocyte extracts.

FBXO45 and MYCBP2 promoted the degradation of FBXW7 α upon nocodazole-mediated mitotic arrest (Fig. 29A). In this context, it would be interesting to analyze if the effect on FBXW7 α protein levels can also be observed upon treatment with other spindle poisons, for example paclitaxel or vincristine. These spindle poisons are frequently used in chemotherapy. The putative finding that FBXO45/MYCBP2 regulate the tumor suppressor FBXW7 α upon treatment with a broad spectrum of spindle poisons could impact our understanding of how chemoresistance might arise. Furthermore, the effects of FBXO45/MYCBP2 on FBXW7 α were specifically observed during mitotic arrest, while they were not detected during unperturbed

mitosis or in asynchronous cells (Fig. 29A). This regulation of FBXW7 α in a specific cell-cycle stage might be caused by a specific interaction between FBXO45/MYCBP2 and FBXW7 α during mitosis. Indeed, FBXO45 and MYCBP2 are mainly localized in the cytosol, whereas FBXW7 α resides in the nucleus (Chen et al., 2014; Kimura et al., 2003; Pierre et al., 2004). Nuclear breakdown during mitosis might promote the interaction between FBXO45/MYCBP2 and FBXW7 α . The transient interaction during unperturbed mitosis might not be long enough to cause visible effects on FBXW7 α protein levels. Alternatively, additional signals, such as posttranslational modifications of one of the interaction partners, might be required to induce the interaction. These signals might be specific for a mitotic arrest. In future experiments, it will be important to verify that FBXO45/MYCBP2 specifically interact with FBXW7 α during mitotic arrest.

The deletion mutant of FBXW7 α , which did not bind to FBXO45, XIAP, RAE1 or MYCBP2 (Fig. 22), could be analyzed in comparison to the wild-type version of FBXW7 α in future ubiquitylation assays and in cycloheximide chase experiments. The deletion mutant of FBXW7 α should not be ubiquitylated upon FBXO45/MYCBP2 overexpression and its stability should be increased compared to wild-type FBXW7 α . These experiments could support a direct effect of FBXO45/MYCBP2 on FBXW7 α ubiquitylation and stability.

Although most studies described FBXO45 in complex with MYCBP2, one publication suggested that FBXO45 can be incorporated into the canonical SCF complex in addition to its complex formation with MYCBP2 (Peschiaroli et al., 2009). In the presented thesis, I showed that FBXO45 and MYCBP2 form a complex with FBXW7 α (Fig. 25). Moreover, single analysis of only FBXO45 or only MYCBP2 revealed that they both promote the ubiquitylation and degradation of FBXW7 α (Fig. 29, 30). Nevertheless, it would be supportive to further verify that it is the complex formation between FBXO45 and MYCBP2 that is required for the degradation of FBXW7 α . In the literature, it has been shown that the ectopic overexpression of the MYCBP2 domain that contains the FBXO45 binding site is able to inhibit the downstream functions of the FBXO45/MYCBP2 complex (Sharma et al., 2014). Therefore, the corresponding MYCBP2 fragment could be used as a tool to study the dependency of FBXW7 α protein levels on FBXO45/MYCBP2 complex formation.

FBXW7 α binds to a fragment of FBXO45 that contains the SPRY domain (Fig. 32). Other substrates of FBXO45 have already been described to interact with the SPRY

domain (Chen et al., 2014; Kugler et al., 2010). As already discussed above, the SPRY domain of ASH2L binds a negatively charged motif of RBBP5, which is similar to the FBXO45 binding motif of FBXW7 α (Cao et al., 2010; Zhang et al., 2015). Because of these similarities between the ASH2L/RBBP5 and FBXO45/FBXW7 α interactions, it is possible that further details about the interaction between FBXO45 and FBXW7 α can be concluded from the ASH2L/RBBP5 complex. For example, specific residues within the SPRY domain of ASH2L were identified as important mediators of RBBP5 binding (Zhang et al., 2015). Sequence alignment of the ASH2L and FBXO45 SPRY domains could be used in order to identify corresponding residues in the FBXO45 SPRY domain that mediate the interaction with FBXW7 α . Point mutations of these residues could be introduced in the FBXO45 protein, which could serve as a dominant-negative mutant for further experiments.

4.10.3. Unraveling the roles of RAE1, XIAP and SPRYD3 in the complex

RAE1 and XIAP do not directly interact with FBXW7 α (Fig. 14, 26C). However, RAE1 is a known component of the FBXO45/MYCBP2 complex (Grill et al., 2012; Tian et al., 2011). XIAP has not been linked to the FBXO45/MYCBP2 complex so far, but it is a known regulator of mitotic cell fate (Engel et al., 2016; Hou et al., 2017). They were both identified in a complex with FBXO45/MYCBP2 and FBXW7 α (Fig. 21, 25). Therefore, it would be interesting to analyze putative functional links between RAE1, XIAP and FBXO45/MYCBP2. First, the direct interaction partners of RAE1 and XIAP in the complex should be identified. As RAE1 was suggested as a regulator of Highwire stability in *Drosophila* (Tian et al., 2011), putative effects of RAE1 on MYCBP2 protein levels could be analyzed. As XIAP is a well-characterized ubiquitin ligase, the effects of its ubiquitin ligase activity on the stabilities of other complex components or on FBXW7 α /FBXO45/MYCBP2 complex formation could be determined. As an alternative to siRNA-mediated downregulation of XIAP, cells could be treated with SMAC mimetics in order to inhibit the ubiquitin ligase activity of XIAP in future experiments (reviewed by Fulda and Vucic, 2012).

As already discussed above, SPRYD3 is an uncharacterized protein. But since both FBXO45 and SPRYD3 contain SPRY domains, SPRYD3 could fulfill a similar function as FBXO45 in the protein complex. In future experiments, the putative interactions between SPRYD3 and the other complex components should be verified. In addition, in order to determine whether SPRYD3 might cooperate with FBXO45 in

the regulation of FBXW7 α , siRNA-mediated downregulation of SPRYD3 and FBXO45 alone as well as co-depletion of SPRYD3 and FBXO45 could be compared with respect to their effects on FBXW7 α protein levels.

4.10.4. Identification of mitotic FBXW7 substrate(s)

As discussed above, regulation of FBXW7 α by FBXO45/MYCBP2 during mitotic arrest might affect mitotic cell fate (Fig. 33). In future experiments, it will be necessary to identify the FBXW7 α substrate(s) that mediate(s) the effect of FBXO45/MYCBP2 on mitotic cell fate. Overexpression of such a substrate should be able to rescue the increase in mitotic cell death observed upon downregulation of FBXO45 and MYCBP2. This kind of rescue experiment would also verify a direct link between FBXO45/MYCBP2 and FBXW7 α in the regulation of mitotic cell fate.

An alternative strategy to identify FBXW7 α substrates that are affected by FBXO45/MYCBP2 would be the analysis of different FBXW7 α substrate levels upon overexpression of FBXO45/MYCBP2 in mitotic cells. Because of the negative effect of FBXO45/MYCBP2 on FBXW7 α protein levels, downstream mitotic substrates of FBXW7 α should be upregulated in such an experiment.

Finally, substrates that are specifically targeted by FBXW7 α during mitotic arrest could be identified by immunoprecipitation combined with mass spectrometry analysis. Similar to a published screen for FBXW7 substrates (Busino et al., 2012), wild-type FBXW7 and a WD40 mutant of FBXW7 could be used as bait proteins for immunoprecipitations. Substrates should bind to the wild-type FBXW7, but not to the WD40 mutant. Immunoprecipitations could be performed with extracts from cells arrested in different cell-cycle stages or from asynchronous cells. FBXW7 α substrates that are specifically identified upon mitotic arrest would be promising candidates to mediate the effect of FBXW7 α on mitotic cell fate.

Altogether, the presented thesis identifies novel interaction partners of FBXW7 α . The FBXO45/MYCBP2 complex is identified as a regulator of FBXW7 α protein levels during mitotic arrest. This regulation contributes to our understanding of regulation mechanisms for the important tumor suppressor FBXW7. As FBXW7 is a known regulator of mitotic cell fate, its regulation during mitotic arrest has the potential to impact strategies for the efficient treatment of cancer cells with spindle poisons.

Future studies on the exact mechanism of FBXW7 α regulation by FBXO45/MYCBP2 and the roles of other FBXO45/MYCBP2 complex components will be required.

5. References

- Ali, A., Veeranki, S.N., Chinchole, A., and Tyagi, S. (2017). MLL/WDR5 Complex Regulates Kif2A Localization to Ensure Chromosome Congression and Proper Spindle Assembly during Mitosis. *Dev. Cell* **41**, 605–622.e7.
- Arabi, A., Ullah, K., Branca, R.M.M., Johansson, J., Bandarra, D., Haneklaus, M., Fu, J., Ariès, I., Nilsson, P., Den Boer, M.L., et al. (2012). Proteomic screen reveals Fbw7 as a modulator of the NF- κ B pathway. *Nat. Commun.* **3**, 976.
- Artavanis-Tsakonas, S., Rand, M.D., and Lake, R.J. (1999). Notch signaling: cell fate control and signal integration in development. *Science* **284**, 770–776.
- Babu, J.R., Jeganathan, K.B., Baker, D.J., Wu, X., Kang-Decker, N., and van Deursen, J.M. (2003). Rae1 is an essential mitotic checkpoint regulator that cooperates with Bub3 to prevent chromosome missegregation. *J. Cell Biol.* **160**, 341–353.
- Bagheri-Yarmand, R., Nanos-Webb, A., Biernacka, A., Bui, T., and Keyomarsi, K. (2010). Cyclin E deregulation impairs mitotic progression through premature activation of Cdc25C. *Cancer Res.* **70**, 5085–5095.
- Bai, C., Sen, P., Hofmann, K., Ma, L., Goebel, M., Harper, J.W., and Elledge, S.J. (1996). SKP1 connects cell cycle regulators to the ubiquitin proteolysis machinery through a novel motif, the F-box. *Cell* **86**, 263–274.
- Balachandran, R.S., Heighington, C.S., Starostina, N.G., Anderson, J.W., Owen, D.L., Vasudevan, S., and Kipreos, E.T. (2016). The ubiquitin ligase CRL2ZYG11 targets cyclin B1 for degradation in a conserved pathway that facilitates mitotic slippage. *J. Cell Biol.* **215**, 151–166.
- Balamurugan, K., Wang, J.-M., Tsai, H.-H., Sharan, S., Anver, M., Leighty, R., and Sterneck, E. (2010). The tumour suppressor C/EBP δ inhibits FBXW7 expression and promotes mammary tumour metastasis. *EMBO J.* **29**, 4106–4117.
- Bashir, T., Dorrello, N.V., Amador, V., Guardavaccaro, D., and Pagano, M. (2004). Control of the SCF(Skp2-Cks1) ubiquitin ligase by the APC/C(Cdh1) ubiquitin ligase. *Nature* **428**, 190–193.
- Bengoechea-Alonso, M.T., and Ericsson, J. (2010). Tumor suppressor Fbxw7 regulates TGF β signaling by targeting TGIF1 for degradation. *Oncogene* **29**, 5322–5328.
- Bhogaraju, S., Kalayil, S., Liu, Y., Bonn, F., Colby, T., Matic, I., and Dikic, I. (2016). Phosphoribosylation of Ubiquitin Promotes Serine Ubiquitination and Impairs Conventional Ubiquitination. *Cell* **167**, 1636–1649.e13.
- Blower, M.D., Nachury, M., Heald, R., and Weis, K. (2005). A Rae1-containing ribonucleoprotein complex is required for mitotic spindle assembly. *Cell* **121**, 223–234.

- Brito, D.A., and Rieder, C.L. (2006). Mitotic checkpoint slippage in humans occurs via cyclin B destruction in the presence of an active checkpoint. *Curr. Biol.* *CB 16*, 1194–1200.
- Brown, J.A., Bharathi, A., Ghosh, A., Whalen, W., Fitzgerald, E., and Dhar, R. (1995). A mutation in the *Schizosaccharomyces pombe* *rae1* gene causes defects in poly(A)⁺ RNA export and in the cytoskeleton. *J. Biol. Chem.* *270*, 7411–7419.
- Buetow, L., and Huang, D.T. (2016). Structural insights into the catalysis and regulation of E3 ubiquitin ligases. *Nat. Rev. Mol. Cell Biol.* *17*, 626–642.
- Busino, L., Millman, S.E., Scotto, L., Kyratsous, C.A., Basrur, V., O'Connor, O., Hoffmann, A., Elenitoba-Johnson, K.S., and Pagano, M. (2012). Fbxw7 α - and GSK3-mediated degradation of p100 is a pro-survival mechanism in multiple myeloma. *Nat. Cell Biol.* *14*, 375–385.
- Cao, F., Chen, Y., Cierpicki, T., Liu, Y., Basrur, V., Lei, M., and Dou, Y. (2010). An Ash2L/RbBP5 heterodimer stimulates the MLL1 methyltransferase activity through coordinated substrate interactions with the MLL1 SET domain. *PLoS One* *5*, e14102.
- Carrano, A.C., Eytan, E., Hershko, A., and Pagano, M. (1999). SKP2 is required for ubiquitin-mediated degradation of the CDK inhibitor p27. *Nat. Cell Biol.* *1*, 193–199.
- Carugo, A., Genovese, G., Seth, S., Nezi, L., Rose, J.L., Bossi, D., Cicalese, A., Shah, P.K., Viale, A., Pettazzoni, P.F., et al. (2016). In Vivo Functional Platform Targeting Patient-Derived Xenografts Identifies WDR5-Myc Association as a Critical Determinant of Pancreatic Cancer. *Cell Rep.* *16*, 133–147.
- Cassavaugh, J.M., Hale, S.A., Wellman, T.L., Howe, A.K., Wong, C., and Lounsbury, K.M. (2011). Negative regulation of HIF-1 α by an FBW7-mediated degradation pathway during hypoxia. *J. Cell. Biochem.* *112*, 3882–3890.
- Cerami, E., Gao, J., Dogrusoz, U., Gross, B.E., Sumer, S.O., Aksoy, B.A., Jacobsen, A., Byrne, C.J., Heuer, M.L., Larsson, E., et al. (2012). The cBio Cancer Genomics Portal: An Open Platform for Exploring Multidimensional Cancer Genomics Data. *Cancer Discov.* *2*, 401–404.
- Chen, X., Sahasrabudhe, A.A., Szankasi, P., Chung, F., Basrur, V., Rangnekar, V.M., Pagano, M., Lim, M.S., and Elenitoba-Johnson, K.S.J. (2014). Fbxo45-mediated degradation of the tumor-suppressor Par-4 regulates cancer cell survival. *Cell Death Differ.* *21*, 1535–1545.
- Chung, F.-Z., Sahasrabudhe, A.A., Ma, K., Chen, X., Basrur, V., Lim, M.S., and Elenitoba-Johnson, K.S.J. (2014). Fbxo45 inhibits calcium-sensitive proteolysis of N-cadherin and promotes neuronal differentiation. *J. Biol. Chem.* *289*, 28448–28459.
- Ciechanover, A., Hod, Y., and Hershko, A. (1978). A heat-stable polypeptide component of an ATP-dependent proteolytic system from reticulocytes. *Biochem. Biophys. Res. Commun.* *81*, 1100–1105.
- Ciechanover, A., Heller, H., Elias, S., Haas, A.L., and Hershko, A. (1980). ATP-dependent conjugation of reticulocyte proteins with the polypeptide required for protein degradation. *Proc. Natl. Acad. Sci. U. S. A.* *77*, 1365–1368.

References

- Ciechanover, A., Heller, H., Katz-Etzion, R., and Hershko, A. (1981). Activation of the heat-stable polypeptide of the ATP-dependent proteolytic system. *Proc. Natl. Acad. Sci. U. S. A.* *78*, 761–765.
- Cizmecioglu, O., Krause, A., Bahtz, R., Ehret, L., Malek, N., and Hoffmann, I. (2012). Plk2 regulates centriole duplication through phosphorylation-mediated degradation of Fbxw7 (human Cdc4). *J. Cell Sci.* *125*, 981–992.
- Clurman, B.E., Sheaff, R.J., Thress, K., Groudine, M., and Roberts, J.M. (1996). Turnover of cyclin E by the ubiquitin-proteasome pathway is regulated by cdk2 binding and cyclin phosphorylation. *Genes Dev.* *10*, 1979–1990.
- Cope, G.A., Suh, G.S.B., Aravind, L., Schwarz, S.E., Zipursky, S.L., Koonin, E.V., and Deshaies, R.J. (2002). Role of predicted metalloprotease motif of Jab1/Csn5 in cleavage of Nedd8 from Cul1. *Science* *298*, 608–611.
- Cunha-Ferreira, I., Rodrigues-Martins, A., Bento, I., Riparbelli, M., Zhang, W., Laue, E., Callaini, G., Glover, D.M., and Bettencourt-Dias, M. (2009). The SCF/Slimb ubiquitin ligase limits centrosome amplification through degradation of SAK/PLK4. *Curr. Biol. CB* *19*, 43–49.
- Davis, M.A., Larimore, E.A., Fissel, B.M., Swanger, J., Taatjes, D.J., and Clurman, B.E. (2013). The SCF-Fbw7 ubiquitin ligase degrades MED13 and MED13L and regulates CDK8 module association with Mediator. *Genes Dev.* *27*, 151–156.
- Davis, R.J., Welcker, M., and Clurman, B.E. (2014). Tumor suppression by the Fbw7 ubiquitin ligase: mechanisms and opportunities. *Cancer Cell* *26*, 455–464.
- Davis, R.J., Swanger, J., Hughes, B.T., and Clurman, B.E. (2017). The PP2A-B56 Phosphatase Opposes Cyclin E Autocatalytic Degradation via Site-Specific Dephosphorylation. *Mol. Cell. Biol.* *37*.
- Deveraux, Q.L., Takahashi, R., Salvesen, G.S., and Reed, J.C. (1997). X-linked IAP is a direct inhibitor of cell-death proteases. *Nature* *388*, 300–304.
- Dikic, I., Wakatsuki, S., and Walters, K.J. (2009). Ubiquitin-binding domains - from structures to functions. *Nat. Rev. Mol. Cell Biol.* *10*, 659–671.
- Dörr, A., Pierre, S., Zhang, D.D., Henke, M., Holland, S., and Scholich, K. (2015). MYCBP2 Is a Guanosine Exchange Factor for Ran Protein and Determines Its Localization in Neurons of Dorsal Root Ganglia. *J. Biol. Chem.* *290*, 25620–25635.
- Du, C., Fang, M., Li, Y., Li, L., and Wang, X. (2000). Smac, a mitochondrial protein that promotes cytochrome c-dependent caspase activation by eliminating IAP inhibition. *Cell* *102*, 33–42.
- Duan, L., Sterba, K., Kolomeichuk, S., Kim, H., Brown, P.H., and Chambers, T.C. (2007). Inducible overexpression of c-Jun in MCF7 cells causes resistance to vinblastine via inhibition of drug-induced apoptosis and senescence at a step subsequent to mitotic arrest. *Biochem. Pharmacol.* *73*, 481–490.
- Dulić, V., Lees, E., and Reed, S.I. (1992). Association of human cyclin E with a periodic G1-S phase protein kinase. *Science* *257*, 1958–1961.

- Durgan, J., and Parker, P.J. (2010). Regulation of the tumour suppressor Fbw7 α by PKC-dependent phosphorylation and cancer-associated mutations. *Biochem. J.* 432, 77–87.
- Eckelman, B.P., Salvesen, G.S., and Scott, F.L. (2006). Human inhibitor of apoptosis proteins: why XIAP is the black sheep of the family. *EMBO Rep.* 7, 988–994.
- Eichhorn, J.M., Alford, S.E., Sakurikar, N., and Chambers, T.C. (2014). Molecular analysis of functional redundancy among anti-apoptotic Bcl-2 proteins and its role in cancer cell survival. *Exp. Cell Res.* 322, 415–424.
- Eischen, C.M., Woo, D., Roussel, M.F., and Cleveland, J.L. (2001). Apoptosis triggered by Myc-induced suppression of Bcl-X(L) or Bcl-2 is bypassed during lymphomagenesis. *Mol. Cell. Biol.* 21, 5063–5070.
- Ekholm-Reed, S., Goldberg, M.S., Schlossmacher, M.G., and Reed, S.I. (2013). Parkin-dependent degradation of the F-box protein Fbw7 β promotes neuronal survival in response to oxidative stress by stabilizing Mcl-1. *Mol. Cell. Biol.* 33, 3627–3643.
- den Elzen, N., and Pines, J. (2001). Cyclin A is destroyed in prometaphase and can delay chromosome alignment and anaphase. *J. Cell Biol.* 153, 121–136.
- Enchev, R.I., Schulman, B.A., and Peter, M. (2015). Protein neddylation: beyond cullin-RING ligases. *Nat. Rev. Mol. Cell Biol.* 16, 30–44.
- Engel, K., Rudelius, M., Slawska, J., Jacobs, L., Ahangarian Abhari, B., Altmann, B., Kurutz, J., Rathakrishnan, A., Fernández-Sáiz, V., Brunner, A., et al. (2016). USP9X stabilizes XIAP to regulate mitotic cell death and chemoresistance in aggressive B-cell lymphoma. *EMBO Mol. Med.* 8, 851–862.
- Evans, T., Rosenthal, E.T., Youngblom, J., Distel, D., and Hunt, T. (1983). Cyclin: a protein specified by maternal mRNA in sea urchin eggs that is destroyed at each cleavage division. *Cell* 33, 389–396.
- Feldman, R.M., Correll, C.C., Kaplan, K.B., and Deshaies, R.J. (1997). A complex of Cdc4p, Skp1p, and Cdc53p/cullin catalyzes ubiquitination of the phosphorylated CDK inhibitor Sic1p. *Cell* 91, 221–230.
- Field, J.J., Kanakkanthara, A., and Miller, J.H. (2014). Microtubule-targeting agents are clinically successful due to both mitotic and interphase impairment of microtubule function. *Bioorg. Med. Chem.* 22, 5050–5059.
- Flotho, A., and Melchior, F. (2013). Sumoylation: a regulatory protein modification in health and disease. *Annu. Rev. Biochem.* 82, 357–385.
- Flügel, D., Görlach, A., and Kietzmann, T. (2012). GSK-3 β regulates cell growth, migration, and angiogenesis via Fbw7 and USP28-dependent degradation of HIF-1 α . *Blood* 119, 1292–1301.
- Freed, E., Lacey, K.R., Huie, P., Lyapina, S.A., Deshaies, R.J., Stearns, T., and Jackson, P.K. (1999). Components of an SCF ubiquitin ligase localize to the

References

- centrosome and regulate the centrosome duplication cycle. *Genes Dev.* **13**, 2242–2257.
- Fukushima, H., Matsumoto, A., Inuzuka, H., Zhai, B., Lau, A.W., Wan, L., Gao, D., Shaik, S., Yuan, M., Gygi, S.P., et al. (2012). SCF(Fbw7) modulates the NFκB signaling pathway by targeting NFκB2 for ubiquitination and destruction. *Cell Rep.* **1**, 434–443.
- Fulda, S., and Vucic, D. (2012). Targeting IAP proteins for therapeutic intervention in cancer. *Nat. Rev. Drug Discov.* **11**, 109–124.
- Galan, J.M., and Peter, M. (1999). Ubiquitin-dependent degradation of multiple F-box proteins by an autocatalytic mechanism. *Proc. Natl. Acad. Sci. U. S. A.* **96**, 9124–9129.
- Galan, J.M., Wiederkehr, A., Seol, J.H., Haguener-Tsapis, R., Deshaies, R.J., Riezman, H., and Peter, M. (2001). Skp1p and the F-box protein Rcy1p form a non-SCF complex involved in recycling of the SNARE Snc1p in yeast. *Mol. Cell. Biol.* **21**, 3105–3117.
- Ganoth, D., Bornstein, G., Ko, T.K., Larsen, B., Tyers, M., Pagano, M., and Hershko, A. (2001). The cell-cycle regulatory protein Cks1 is required for SCF(Skp2)-mediated ubiquitinylation of p27. *Nat. Cell Biol.* **3**, 321–324.
- Gao, J., Aksoy, B.A., Dogrusoz, U., Dresdner, G., Gross, B., Sumer, S.O., Sun, Y., Jacobsen, A., Sinha, R., Larsson, E., et al. (2013). Integrative analysis of complex cancer genomics and clinical profiles using the cBioPortal. *Sci. Signal.* **6**, p11.
- Geley, S., Kramer, E., Gieffers, C., Gannon, J., Peters, J.M., and Hunt, T. (2001). Anaphase-promoting complex/cyclosome-dependent proteolysis of human cyclin A starts at the beginning of mitosis and is not subject to the spindle assembly checkpoint. *J. Cell Biol.* **153**, 137–148.
- Glotzer, M., Murray, A.W., and Kirschner, M.W. (1991). Cyclin is degraded by the ubiquitin pathway. *Nature* **349**, 132–138.
- Goldenberg, S.J., Cascio, T.C., Shumway, S.D., Garbutt, K.C., Liu, J., Xiong, Y., and Zheng, N. (2004). Structure of the Cand1-Cul1-Roc1 complex reveals regulatory mechanisms for the assembly of the multisubunit cullin-dependent ubiquitin ligases. *Cell* **119**, 517–528.
- Grandori, C., Cowley, S.M., James, L.P., and Eisenman, R.N. (2000). The Myc/Max/Mad network and the transcriptional control of cell behavior. *Annu. Rev. Cell Dev. Biol.* **16**, 653–699.
- Grill, B., Chen, L., Tulgren, E.D., Baker, S.T., Bienvenut, W., Anderson, M., Quadroni, M., Jin, Y., and Garner, C.C. (2012). RAE-1, a novel PHR binding protein, is required for axon termination and synapse formation in *Caenorhabditis elegans*. *J. Neurosci. Off. J. Soc. Neurosci.* **32**, 2628–2636.
- Grill, B., Murphey, R.K., and Borgen, M.A. (2016). The PHR proteins: intracellular signaling hubs in neuronal development and axon degeneration. *Neural Develop.* **11**, 8.

- Guo, Q., Xie, J., Dang, C.V., Liu, E.T., and Bishop, J.M. (1998). Identification of a large Myc-binding protein that contains RCC1-like repeats. *Proc. Natl. Acad. Sci. U. S. A.* *95*, 9172–9177.
- Gyrd-Hansen, M., and Meier, P. (2010). IAPs: from caspase inhibitors to modulators of NF-kappaB, inflammation and cancer. *Nat. Rev. Cancer* *10*, 561–574.
- Han, S., Witt, R.M., Santos, T.M., Polizzano, C., Sabatini, B.L., and Ramesh, V. (2008). Pam (Protein associated with Myc) functions as an E3 ubiquitin ligase and regulates TSC/mTOR signaling. *Cell. Signal.* *20*, 1084–1091.
- Han, S., Kim, S., Bahl, S., Li, L., Burande, C.F., Smith, N., James, M., Beauchamp, R.L., Bhide, P., DiAntonio, A., et al. (2012). The E3 ubiquitin ligase protein associated with Myc (Pam) regulates mammalian/mechanistic target of rapamycin complex 1 (mTORC1) signaling in vivo through N- and C-terminal domains. *J. Biol. Chem.* *287*, 30063–30072.
- Hao, B., Oehlmann, S., Sowa, M.E., Harper, J.W., and Pavletich, N.P. (2007). Structure of a Fbw7-Skp1-cyclin E complex: multisite-phosphorylated substrate recognition by SCF ubiquitin ligases. *Mol. Cell* *26*, 131–143.
- Harley, M.E., Allan, L.A., Sanderson, H.S., and Clarke, P.R. (2010). Phosphorylation of Mcl-1 by CDK1-cyclin B1 initiates its Cdc20-dependent destruction during mitotic arrest. *EMBO J.* *29*, 2407–2420.
- Hartwell, L.H., Mortimer, R.K., Culotti, J., and Culotti, M. (1973). Genetic Control of the Cell Division Cycle in Yeast: V. Genetic Analysis of *cdc* Mutants. *Genetics* *74*, 267–286.
- Hershko, A., Ciechanover, A., and Rose, I.A. (1979). Resolution of the ATP-dependent proteolytic system from reticulocytes: a component that interacts with ATP. *Proc. Natl. Acad. Sci. U. S. A.* *76*, 3107–3110.
- Hershko, A., Ciechanover, A., Heller, H., Haas, A.L., and Rose, I.A. (1980). Proposed role of ATP in protein breakdown: conjugation of protein with multiple chains of the polypeptide of ATP-dependent proteolysis. *Proc. Natl. Acad. Sci. U. S. A.* *77*, 1783–1786.
- Hershko, A., Heller, H., Elias, S., and Ciechanover, A. (1983). Components of ubiquitin-protein ligase system. Resolution, affinity purification, and role in protein breakdown. *J. Biol. Chem.* *258*, 8206–8214.
- Hoeller, D., Hecker, C.-M., and Dikic, I. (2006). Ubiquitin and ubiquitin-like proteins in cancer pathogenesis. *Nat. Rev. Cancer* *6*, 776–788.
- Hofer-Warbinek, R., Schmid, J.A., Stehlik, C., Binder, B.R., Lipp, J., and de Martin, R. (2000). Activation of NF-kappa B by XIAP, the X chromosome-linked inhibitor of apoptosis, in endothelial cells involves TAK1. *J. Biol. Chem.* *275*, 22064–22068.
- Hou, Y., Allan, L.A., and Clarke, P.R. (2017). Phosphorylation of XIAP by CDK1-cyclin-B1 controls mitotic cell death. *J. Cell Sci.* *130*, 502–511.

References

- Hubbard, E.J., Wu, G., Kitajewski, J., and Greenwald, I. (1997). sel-10, a negative regulator of lin-12 activity in *Caenorhabditis elegans*, encodes a member of the CDC4 family of proteins. *Genes Dev.* *11*, 3182–3193.
- Huttlin, E.L., Bruckner, R.J., Paulo, J.A., Cannon, J.R., Ting, L., Baltier, K., Colby, G., Gebreab, F., Gygi, M.P., Parzen, H., et al. (2017). Architecture of the human interactome defines protein communities and disease networks. *Nature* *545*, 505–509.
- Inuzuka, H., Shaik, S., Onoyama, I., Gao, D., Tseng, A., Maser, R.S., Zhai, B., Wan, L., Gutierrez, A., Lau, A.W., et al. (2011). SCF(FBW7) regulates cellular apoptosis by targeting MCL1 for ubiquitylation and destruction. *Nature* *471*, 104–109.
- Jeganathan, K.B., Malureanu, L., and van Deursen, J.M. (2005). The Rae1-Nup98 complex prevents aneuploidy by inhibiting securin degradation. *Nature* *438*, 1036–1039.
- Jiang, X., Xing, H., Kim, T.-M., Jung, Y., Huang, W., Yang, H.W., Song, S., Park, P.J., Carroll, R.S., and Johnson, M.D. (2012). Numb regulates glioma stem cell fate and growth by altering epidermal growth factor receptor and Skp1-Cullin-F-box ubiquitin ligase activity. *Stem Cells Dayt. Ohio* *30*, 1313–1326.
- Jonas, S., and Izaurralde, E. (2015). Towards a molecular understanding of microRNA-mediated gene silencing. *Nat. Rev. Genet.* *16*, 421–433.
- Kanei-Ishii, C., Nomura, T., Takagi, T., Watanabe, N., Nakayama, K.I., and Ishii, S. (2008). Fbxw7 acts as an E3 ubiquitin ligase that targets c-Myb for nemo-like kinase (NLK)-induced degradation. *J. Biol. Chem.* *283*, 30540–30548.
- Kaplan, K.B., Hyman, A.A., and Sorger, P.K. (1997). Regulating the yeast kinetochore by ubiquitin-dependent degradation and Skp1p-mediated phosphorylation. *Cell* *91*, 491–500.
- Kimura, T., Gotoh, M., Nakamura, Y., and Arakawa, H. (2003). hCDC4b, a regulator of cyclin E, as a direct transcriptional target of p53. *Cancer Sci.* *94*, 431–436.
- Koepp, D.M., Schaefer, L.K., Ye, X., Keyomarsi, K., Chu, C., Harper, J.W., and Elledge, S.J. (2001). Phosphorylation-dependent ubiquitination of cyclin E by the SCFFbw7 ubiquitin ligase. *Science* *294*, 173–177.
- Koff, A., Giordano, A., Desai, D., Yamashita, K., Harper, J.W., Elledge, S., Nishimoto, T., Morgan, D.O., Franza, B.R., and Roberts, J.M. (1992). Formation and activation of a cyclin E-cdk2 complex during the G1 phase of the human cell cycle. *Science* *257*, 1689–1694.
- Komander, D., and Rape, M. (2012). The ubiquitin code. *Annu. Rev. Biochem.* *81*, 203–229.
- Komander, D., Clague, M.J., and Urbé, S. (2009). Breaking the chains: structure and function of the deubiquitinases. *Nat. Rev. Mol. Cell Biol.* *10*, 550–563.
- Kominami, K., Ochotorena, I., and Toda, T. (1998). Two F-box/WD-repeat proteins Pop1 and Pop2 form hetero- and homo-complexes together with cullin-1 in the fission

- yeast SCF (Skp1-Cullin-1-F-box) ubiquitin ligase. *Genes Cells Devoted Mol. Cell. Mech.* **3**, 721–735.
- Kotewicz, K.M., Ramabhadran, V., Sjoblom, N., Vogel, J.P., Haenssler, E., Zhang, M., Behringer, J., Scheck, R.A., and Isberg, R.R. (2017). A Single Legionella Effector Catalyzes a Multistep Ubiquitination Pathway to Rearrange Tubular Endoplasmic Reticulum for Replication. *Cell Host Microbe* **21**, 169–181.
- Kourtis, N., Moubarak, R.S., Aranda-Orgilles, B., Lui, K., Aydin, I.T., Trimarchi, T., Darvishian, F., Salvaggio, C., Zhong, J., Bhatt, K., et al. (2015). FBXW7 modulates cellular stress response and metastatic potential through HSF1 post-translational modification. *Nat. Cell Biol.* **17**, 322–332.
- Kraemer, D., and Blobel, G. (1997). mRNA binding protein mrnp 41 localizes to both nucleus and cytoplasm. *Proc. Natl. Acad. Sci. U. S. A.* **94**, 9119–9124.
- Kratz, A.-S., Richter, K.T., Schlosser, Y.T., Schmitt, M., Shumilov, A., Delecluse, H.-J., and Hoffmann, I. (2016). Fbxo28 promotes mitotic progression and regulates topoisomerase II α -dependent DNA decatenation. *Cell Cycle Georget. Tex* **15**, 3419–3431.
- Kugler, J.-M., Woo, J.-S., Oh, B.-H., and Lasko, P. (2010). Regulation of Drosophila vasa in vivo through paralogous cullin-RING E3 ligase specificity receptors. *Mol. Cell. Biol.* **30**, 1769–1782.
- Lee, J., and Zhou, P. (2007). DCAFs, the missing link of the CUL4-DDB1 ubiquitin ligase. *Mol. Cell* **26**, 775–780.
- Lerner, M., Lundgren, J., Akhoondi, S., Jahn, A., Ng, H.-F., Akbari Moqadam, F., Oude Vrielink, J.A.F., Agami, R., Den Boer, M.L., Grandér, D., et al. (2011). MiRNA-27a controls FBW7/hCDC4-dependent cyclin E degradation and cell cycle progression. *Cell Cycle Georget. Tex* **10**, 2172–2183.
- Li, J., Pauley, A.M., Myers, R.L., Shuang, R., Brashler, J.R., Yan, R., Buhl, A.E., Ruble, C., and Gurney, M.E. (2002). SEL-10 interacts with presenilin 1, facilitates its ubiquitination, and alters A-beta peptide production. *J. Neurochem.* **82**, 1540–1548.
- Liao, E.H., Hung, W., Abrams, B., and Zhen, M. (2004). An SCF-like ubiquitin ligase complex that controls presynaptic differentiation. *Nature* **430**, 345–350.
- Lipkowitz, S., and Weissman, A.M. (2011). RINGs of good and evil: RING finger ubiquitin ligases at the crossroads of tumour suppression and oncogenesis. *Nat. Rev. Cancer* **11**, 629–643.
- Liston, P., Fong, W.G., Kelly, N.L., Toji, S., Miyazaki, T., Conte, D., Tamai, K., Craig, C.G., McBurney, M.W., and Korneluk, R.G. (2001). Identification of XAF1 as an antagonist of XIAP anti-Caspase activity. *Nat. Cell Biol.* **3**, 128–133.
- Liu, J., Furukawa, M., Matsumoto, T., and Xiong, Y. (2002). NEDD8 modification of CUL1 dissociates p120(CAND1), an inhibitor of CUL1-SKP1 binding and SCF ligases. *Mol. Cell* **10**, 1511–1518.

References

- Liu, N., Li, H., Li, S., Shen, M., Xiao, N., Chen, Y., Wang, Y., Wang, W., Wang, R., Wang, Q., et al. (2010). The Fbw7/human CDC4 tumor suppressor targets proproliferative factor KLF5 for ubiquitination and degradation through multiple phosphodegron motifs. *J. Biol. Chem.* *285*, 18858–18867.
- Liu, Y.-C., Penninger, J., and Karin, M. (2005). Immunity by ubiquitylation: a reversible process of modification. *Nat. Rev. Immunol.* *5*, 941–952.
- Lu, D., Davis, M.P.A., Abreu-Goodger, C., Wang, W., Campos, L.S., Siede, J., Vigorito, E., Skarnes, W.C., Dunham, I., Enright, A.J., et al. (2012). MiR-25 regulates Wwp2 and Fbxw7 and promotes reprogramming of mouse fibroblast cells to iPSCs. *PLoS One* *7*, e40938.
- Lyapina, S., Cope, G., Shevchenko, A., Serino, G., Tsuge, T., Zhou, C., Wolf, D.A., Wei, N., Shevchenko, A., and Deshaies, R.J. (2001). Promotion of NEDD-CUL1 conjugate cleavage by COP9 signalosome. *Science* *292*, 1382–1385.
- Maddika, S., and Chen, J. (2009). Protein kinase DYRK2 is a scaffold that facilitates assembly of an E3 ligase. *Nat. Cell Biol.* *11*, 409–419.
- Maeurer, C., Holland, S., Pierre, S., Potstada, W., and Scholich, K. (2009). Sphingosine-1-phosphate induced mTOR-activation is mediated by the E3-ubiquitin ligase PAM. *Cell. Signal.* *21*, 293–300.
- Mao, J.-H., Perez-Losada, J., Wu, D., Delrosario, R., Tsunematsu, R., Nakayama, K.I., Brown, K., Bryson, S., and Balmain, A. (2004). Fbxw7/Cdc4 is a p53-dependent, haploinsufficient tumour suppressor gene. *Nature* *432*, 775–779.
- Mao, J.-H., Kim, I.-J., Wu, D., Climent, J., Kang, H.C., DelRosario, R., and Balmain, A. (2008). FBXW7 targets mTOR for degradation and cooperates with PTEN in tumor suppression. *Science* *321*, 1499–1502.
- Margottin-Goguet, F., Hsu, J.Y., Loktev, A., Hsieh, H.M., Reimann, J.D.R., and Jackson, P.K. (2003). Prophase destruction of Emi1 by the SCF(betaTrCP/Slimb) ubiquitin ligase activates the anaphase promoting complex to allow progression beyond prometaphase. *Dev. Cell* *4*, 813–826.
- Matsumoto, A., Onoyama, I., and Nakayama, K.I. (2006). Expression of mouse Fbxw7 isoforms is regulated in a cell cycle- or p53-dependent manner. *Biochem. Biophys. Res. Commun.* *350*, 114–119.
- Min, S.-H., Lau, A.W., Lee, T.H., Inuzuka, H., Wei, S., Huang, P., Shaik, S., Lee, D.Y., Finn, G., Balastik, M., et al. (2012). Negative regulation of the stability and tumor suppressor function of Fbw7 by the Pin1 prolyl isomerase. *Mol. Cell* *46*, 771–783.
- Moberg, K.H., Bell, D.W., Wahrer, D.C., Haber, D.A., and Hariharan, I.K. (2001). Archipelago regulates Cyclin E levels in *Drosophila* and is mutated in human cancer cell lines. *Nature* *413*, 311–316.
- Murthy, V., Han, S., Beauchamp, R.L., Smith, N., Haddad, L.A., Ito, N., and Ramesh, V. (2004). Pam and its ortholog highwire interact with and may negatively regulate the TSC1.TSC2 complex. *J. Biol. Chem.* *279*, 1351–1358.

- Nakagawa, T., and Xiong, Y. (2011). X-linked mental retardation gene CUL4B targets ubiquitylation of H3K4 methyltransferase component WDR5 and regulates neuronal gene expression. *Mol. Cell* **43**, 381–391.
- Nakata, K., Abrams, B., Grill, B., Goncharov, A., Huang, X., Chisholm, A.D., and Jin, Y. (2005). Regulation of a DLK-1 and p38 MAP kinase pathway by the ubiquitin ligase RPM-1 is required for presynaptic development. *Cell* **120**, 407–420.
- Nakayama, K.I., and Nakayama, K. (2006). Ubiquitin ligases: cell-cycle control and cancer. *Nat. Rev. Cancer* **6**, 369–381.
- Nakayama, K., Nagahama, H., Minamishima, Y.A., Matsumoto, M., Nakamichi, I., Kitagawa, K., Shirane, M., Tsunematsu, R., Tsukiyama, T., Ishida, N., et al. (2000). Targeted disruption of Skp2 results in accumulation of cyclin E and p27(Kip1), polyploidy and centrosome overduplication. *EMBO J.* **19**, 2069–2081.
- Nash, P., Tang, X., Orlicky, S., Chen, Q., Gertler, F.B., Mendenhall, M.D., Sicheri, F., Pawson, T., and Tyers, M. (2001). Multisite phosphorylation of a CDK inhibitor sets a threshold for the onset of DNA replication. *Nature* **414**, 514–521.
- Nateri, A.S., Riera-Sans, L., Da Costa, C., and Behrens, A. (2004). The ubiquitin ligase SCFFbw7 antagonizes apoptotic JNK signaling. *Science* **303**, 1374–1378.
- Ohsumi, Y. (2001). Molecular dissection of autophagy: two ubiquitin-like systems. *Nat. Rev. Mol. Cell Biol.* **2**, 211–216.
- Olson, B.L., Hock, M.B., Ekholm-Reed, S., Wohlschlegel, J.A., Dev, K.K., Kralli, A., and Reed, S.I. (2008). SCFCdc4 acts antagonistically to the PGC-1alpha transcriptional coactivator by targeting it for ubiquitin-mediated proteolysis. *Genes Dev.* **22**, 252–264.
- Osaka, F., Kawasaki, H., Aida, N., Saeki, M., Chiba, T., Kawashima, S., Tanaka, K., and Kato, S. (1998). A new NEDD8-ligating system for cullin-4A. *Genes Dev.* **12**, 2263–2268.
- Otto, T., Horn, S., Brockmann, M., Eilers, U., Schüttrumpf, L., Popov, N., Kenney, A.M., Schulte, J.H., Beijersbergen, R., Christiansen, H., et al. (2009). Stabilization of N-Myc is a critical function of Aurora A in human neuroblastoma. *Cancer Cell* **15**, 67–78.
- Peschiaroli, A., Scialpi, F., Bernassola, F., Pagano, M., and Melino, G. (2009). The F-box protein FBXO45 promotes the proteasome-dependent degradation of p73. *Oncogene* **28**, 3157–3166.
- Petroski, M.D., and Deshaies, R.J. (2005). Function and regulation of cullin-RING ubiquitin ligases. *Nat. Rev. Mol. Cell Biol.* **6**, 9–20.
- Pierce, N.W., Lee, J.E., Liu, X., Sweredoski, M.J., Graham, R.L.J., Larimore, E.A., Rome, M., Zheng, N., Clurman, B.E., Hess, S., et al. (2013). Cand1 promotes assembly of new SCF complexes through dynamic exchange of F box proteins. *Cell* **153**, 206–215.

References

- Pierre, S.C., Häusler, J., Birod, K., Geisslinger, G., and Scholich, K. (2004). PAM mediates sustained inhibition of cAMP signaling by sphingosine-1-phosphate. *EMBO J.* **23**, 3031–3040.
- Po, M.D., Hwang, C., and Zhen, M. (2010). PHRs: bridging axon guidance, outgrowth and synapse development. *Curr. Opin. Neurobiol.* **20**, 100–107.
- Pritchard, C.E., Fornerod, M., Kasper, L.H., and van Deursen, J.M. (1999). RAE1 is a shuttling mRNA export factor that binds to a GLEBS-like NUP98 motif at the nuclear pore complex through multiple domains. *J. Cell Biol.* **145**, 237–254.
- Puklowski, A., Homsí, Y., Keller, D., May, M., Chauhan, S., Kossatz, U., Grünwald, V., Kubicka, S., Pich, A., Manns, M.P., et al. (2011). The SCF-FBXW5 E3-ubiquitin ligase is regulated by PLK4 and targets HsSAS-6 to control centrosome duplication. *Nat. Cell Biol.* **13**, 1004–1009.
- Qiu, J., Sheedlo, M.J., Yu, K., Tan, Y., Nakayasu, E.S., Das, C., Liu, X., and Luo, Z.-Q. (2016). Ubiquitination independent of E1 and E2 enzymes by bacterial effectors. *Nature* **533**, 120–124.
- Radtke, F., Schweisguth, F., and Pear, W. (2005). The Notch “gospel.” *EMBO Rep.* **6**, 1120–1125.
- Rajagopalan, H., Jallepalli, P.V., Rago, C., Velculescu, V.E., Kinzler, K.W., Vogelstein, B., and Lengauer, C. (2004). Inactivation of hCDC4 can cause chromosomal instability. *Nature* **428**, 77–81.
- Rao, R.C., and Dou, Y. (2015). Hijacked in cancer: the KMT2 (MLL) family of methyltransferases. *Nat. Rev. Cancer* **15**, 334–346.
- Read, M.A., Brownell, J.E., Gladysheva, T.B., Hottelot, M., Parent, L.A., Coggins, M.B., Pierce, J.W., Podust, V.N., Luo, R.S., Chau, V., et al. (2000). Nedd8 modification of cul-1 activates SCF(beta(TrCP))-dependent ubiquitination of IkkappaBalpha. *Mol. Cell. Biol.* **20**, 2326–2333.
- Reiterer, V., Figueras-Puig, C., Le Guerroue, F., Confalonieri, S., Vecchi, M., Jalapothu, D., Kanse, S.M., Deshaies, R.J., Di Fiore, P.P., Behrens, C., et al. (2017). The pseudophosphatase STYX targets the F-box of FBXW7 and inhibits SCFFBXW7 function. *EMBO J.* **36**, 260–273.
- Rotin, D., and Kumar, S. (2009). Physiological functions of the HECT family of ubiquitin ligases. *Nat. Rev. Mol. Cell Biol.* **10**, 398–409.
- Saiga, T., Fukuda, T., Matsumoto, M., Tada, H., Okano, H.J., Okano, H., and Nakayama, K.I. (2009). Fbxo45 forms a novel ubiquitin ligase complex and is required for neuronal development. *Mol. Cell. Biol.* **29**, 3529–3543.
- Sancho, R., Blake, S.M., Tendeng, C., Clurman, B.E., Lewis, J., and Behrens, A. (2013). Fbw7 repression by hes5 creates a feedback loop that modulates Notch-mediated intestinal and neural stem cell fate decisions. *PLoS Biol.* **11**, e1001586.
- Sancho, R., Gruber, R., Gu, G., and Behrens, A. (2014). Loss of Fbw7 reprograms adult pancreatic ductal cells into α , δ , and β cells. *Cell Stem Cell* **15**, 139–153.

- Schülein, C., Eilers, M., and Popov, N. (2011). PI3K-dependent phosphorylation of Fbw7 modulates substrate degradation and activity. *FEBS Lett.* **585**, 2151–2157.
- Schülein-Völk, C., Wolf, E., Zhu, J., Xu, W., Taranets, L., Hellmann, A., Jänicke, L.A., Diefenbacher, M.E., Behrens, A., Eilers, M., et al. (2014). Dual regulation of Fbw7 function and oncogenic transformation by Usp28. *Cell Rep.* **9**, 1099–1109.
- Schwickart, M., Huang, X., Lill, J.R., Liu, J., Ferrando, R., French, D.M., Maecker, H., O'Rourke, K., Bazan, F., Eastham-Anderson, J., et al. (2010). Deubiquitinase USP9X stabilizes MCL1 and promotes tumour cell survival. *Nature* **463**, 103–107.
- Scott, D.C., Rhee, D.Y., Duda, D.M., Kelsall, I.R., Olszewski, J.L., Paulo, J.A., de Jong, A., Ova, H., Alpi, A.F., Harper, J.W., et al. (2016). Two Distinct Types of E3 Ligases Work in Unison to Regulate Substrate Ubiquitylation. *Cell* **166**, 1198–1214.e24.
- Seol, J.H., Shevchenko, A., Shevchenko, A., and Deshaies, R.J. (2001). Skp1 forms multiple protein complexes, including RAVE, a regulator of V-ATPase assembly. *Nat. Cell Biol.* **3**, 384–391.
- Sharma, J., Baker, S.T., Turgeon, S.M., Gurney, A.M., Opperman, K.J., and Grill, B. (2014). Identification of a peptide inhibitor of the RPM-1 · FSN-1 ubiquitin ligase complex. *J. Biol. Chem.* **289**, 34654–34666.
- Shaulian, E., and Karin, M. (2002). AP-1 as a regulator of cell life and death. *Nat. Cell Biol.* **4**, E131-136.
- Singer, J.D., Gurian-West, M., Clurman, B., and Roberts, J.M. (1999). Cullin-3 targets cyclin E for ubiquitination and controls S phase in mammalian cells. *Genes Dev.* **13**, 2375–2387.
- Skaar, J.R., Pagan, J.K., and Pagano, M. (2013). Mechanisms and function of substrate recruitment by F-box proteins. *Nat. Rev. Mol. Cell Biol.* **14**, 369–381.
- Skowyra, D., Craig, K.L., Tyers, M., Elledge, S.J., and Harper, J.W. (1997). F-box proteins are receptors that recruit phosphorylated substrates to the SCF ubiquitin-ligase complex. *Cell* **91**, 209–219.
- Smit, J.J., and Sixma, T.K. (2014). RBR E3-ligases at work. *EMBO Rep.* **15**, 142–154.
- Song, Y., Lai, L., Chong, Z., He, J., Zhang, Y., Xue, Y., Xie, Y., Chen, S., Dong, P., Chen, L., et al. (2017). E3 ligase FBXW7 is critical for RIG-I stabilization during antiviral responses. *Nat. Commun.* **8**, 14654.
- Spruck, C., Strohmaier, H., Watson, M., Smith, A.P., Ryan, A., Krek, T.W., and Reed, S.I. (2001). A CDK-independent function of mammalian Cks1: targeting of SCF(Skp2) to the CDK inhibitor p27Kip1. *Mol. Cell* **7**, 639–650.
- Spruck, C.H., Strohmaier, H., Sangfelt, O., Müller, H.M., Hubalek, M., Müller-Holzner, E., Marth, C., Widschwendter, M., and Reed, S.I. (2002). hCDC4 gene mutations in endometrial cancer. *Cancer Res.* **62**, 4535–4539.

References

- Strohmaier, H., Spruck, C.H., Kaiser, P., Won, K.A., Sangfelt, O., and Reed, S.I. (2001). Human F-box protein hCdc4 targets cyclin E for proteolysis and is mutated in a breast cancer cell line. *Nature* **413**, 316–322.
- Styhler, S., Nakamura, A., and Lasko, P. (2002). VASA localization requires the SPRY-domain and SOCS-box containing protein, GUSTAVUS. *Dev. Cell* **3**, 865–876.
- Sun, Y., Bell, J.L., Carter, D., Gherardi, S., Poulos, R.C., Milazzo, G., Wong, J.W.H., Al-Awar, R., Tee, A.E., Liu, P.Y., et al. (2015). WDR5 Supports an N-Myc Transcriptional Complex That Drives a Protumorigenic Gene Expression Signature in Neuroblastoma. *Cancer Res.* **75**, 5143–5154.
- Sundqvist, A., Bengoechea-Alonso, M.T., Ye, X., Lukiyanchuk, V., Jin, J., Harper, J.W., and Ericsson, J. (2005). Control of lipid metabolism by phosphorylation-dependent degradation of the SREBP family of transcription factors by SCF(Fbw7). *Cell Metab.* **1**, 379–391.
- Suzuki, Y., Nakabayashi, Y., and Takahashi, R. (2001a). Ubiquitin-protein ligase activity of X-linked inhibitor of apoptosis protein promotes proteasomal degradation of caspase-3 and enhances its anti-apoptotic effect in Fas-induced cell death. *Proc. Natl. Acad. Sci. U. S. A.* **98**, 8662–8667.
- Suzuki, Y., Imai, Y., Nakayama, H., Takahashi, K., Takio, K., and Takahashi, R. (2001b). A serine protease, HtrA2, is released from the mitochondria and interacts with XIAP, inducing cell death. *Mol. Cell* **8**, 613–621.
- Tang, X., Orlicky, S., Lin, Z., Willems, A., Neculai, D., Ceccarelli, D., Mercurio, F., Shilton, B.H., Sicheri, F., and Tyers, M. (2007). Suprafacial orientation of the SCFCdc4 dimer accommodates multiple geometries for substrate ubiquitination. *Cell* **129**, 1165–1176.
- Teng, C.-L., Hsieh, Y.-C., Phan, L., Shin, J., Gully, C., Velazquez-Torres, G., Skerl, S., Yeung, S.-C.J., Hsu, S.-L., and Lee, M.-H. (2012). FBXW7 is involved in Aurora B degradation. *Cell Cycle Georget. Tex* **11**, 4059–4068.
- Thomas, L.R., Wang, Q., Grieb, B.C., Phan, J., Foshage, A.M., Sun, Q., Olejniczak, E.T., Clark, T., Dey, S., Lorey, S., et al. (2015). Interaction with WDR5 promotes target gene recognition and tumorigenesis by MYC. *Mol. Cell* **58**, 440–452.
- Thompson, B.J., Buonamici, S., Sulis, M.L., Palomero, T., Vilimas, T., Basso, G., Ferrando, A., and Aifantis, I. (2007). The SCFFBW7 ubiquitin ligase complex as a tumor suppressor in T cell leukemia. *J. Exp. Med.* **204**, 1825–1835.
- Tian, X., Li, J., Valakh, V., DiAntonio, A., and Wu, C. (2011). Drosophila Rae1 controls the abundance of the ubiquitin ligase Highwire in post-mitotic neurons. *Nat. Neurosci.* **14**, 1267–1275.
- Topham, C.H., and Taylor, S.S. (2013). Mitosis and apoptosis: how is the balance set? *Curr. Opin. Cell Biol.* **25**, 780–785.
- Topham, C., Tighe, A., Ly, P., Bennett, A., Sloss, O., Nelson, L., Ridgway, R.A., Huels, D., Littler, S., Schandl, C., et al. (2015). MYC Is a Major Determinant of Mitotic Cell Fate. *Cancer Cell* **28**, 129–140.

- Tron, A.E., Arai, T., Duda, D.M., Kuwabara, H., Olszewski, J.L., Fujiwara, Y., Bahamon, B.N., Signoretti, S., Schulman, B.A., and DeCaprio, J.A. (2012). The glomovenous malformation protein Glomulin binds Rbx1 and regulates cullin RING ligase-mediated turnover of Fbw7. *Mol. Cell* **46**, 67–78.
- Tsvetkov, L.M., Yeh, K.H., Lee, S.J., Sun, H., and Zhang, H. (1999). p27(Kip1) ubiquitination and degradation is regulated by the SCF(Skp2) complex through phosphorylated Thr187 in p27. *Curr. Biol. CB* **9**, 661–664.
- Wang, X., Babu, J.R., Harden, J.M., Jablonski, S.A., Gazi, M.H., Lingle, W.L., de Groen, P.C., Yen, T.J., and van Deursen, J.M. (2001). The mitotic checkpoint protein hBUB3 and the mRNA export factor hRAE1 interact with GLE2p-binding sequence (GLEBS)-containing proteins. *J. Biol. Chem.* **276**, 26559–26567.
- Wang, Z., Liu, Y., Zhang, P., Zhang, W., Wang, W., Curr, K., Wei, G., and Mao, J.-H. (2013). FAM83D promotes cell proliferation and motility by downregulating tumor suppressor gene FBXW7. *Oncotarget* **4**, 2476–2486.
- Wang, Z., Liu, P., Inuzuka, H., and Wei, W. (2014). Roles of F-box proteins in cancer. *Nat. Rev. Cancer* **14**, 233–247.
- Wei, W., Ayad, N.G., Wan, Y., Zhang, G.-J., Kirschner, M.W., and Kaelin, W.G. (2004). Degradation of the SCF component Skp2 in cell-cycle phase G1 by the anaphase-promoting complex. *Nature* **428**, 194–198.
- Wei, W., Jin, J., Schlisio, S., Harper, J.W., and Kaelin, W.G. (2005). The v-Jun point mutation allows c-Jun to escape GSK3-dependent recognition and destruction by the Fbw7 ubiquitin ligase. *Cancer Cell* **8**, 25–33.
- Welcker, M., and Clurman, B.E. (2007). Fbw7/hCDC4 dimerization regulates its substrate interactions. *Cell Div.* **2**, 7.
- Welcker, M., and Clurman, B.E. (2008). FBW7 ubiquitin ligase: a tumour suppressor at the crossroads of cell division, growth and differentiation. *Nat. Rev. Cancer* **8**, 83–93.
- Welcker, M., Singer, J., Loeb, K.R., Grim, J., Bloecher, A., Gurien-West, M., Clurman, B.E., and Roberts, J.M. (2003). Multisite phosphorylation by Cdk2 and GSK3 controls cyclin E degradation. *Mol. Cell* **12**, 381–392.
- Welcker, M., Orian, A., Grim, J.E., Grim, J.A., Eisenman, R.N., and Clurman, B.E. (2004). A nucleolar isoform of the Fbw7 ubiquitin ligase regulates c-Myc and cell size. *Curr. Biol. CB* **14**, 1852–1857.
- Welcker, M., Larimore, E.A., Frappier, L., and Clurman, B.E. (2011). Nucleolar targeting of the fbw7 ubiquitin ligase by a pseudosubstrate and glycogen synthase kinase 3. *Mol. Cell. Biol.* **31**, 1214–1224.
- Welcker, M., Larimore, E.A., Swanger, J., Bengoechea-Alonso, M.T., Grim, J.E., Ericsson, J., Zheng, N., and Clurman, B.E. (2013). Fbw7 dimerization determines the specificity and robustness of substrate degradation. *Genes Dev.* **27**, 2531–2536.

References

- Werner, A., Disanza, A., Reifenberger, N., Habeck, G., Becker, J., Calabrese, M., Urlaub, H., Lorenz, H., Schulman, B., Scita, G., et al. (2013). SCFFbxw5 mediates transient degradation of actin remodeller Eps8 to allow proper mitotic progression. *Nat. Cell Biol.* *15*, 179–188.
- Wertz, I.E., Kusam, S., Lam, C., Okamoto, T., Sandoval, W., Anderson, D.J., Helgason, E., Ernst, J.A., Eby, M., Liu, J., et al. (2011a). Sensitivity to antitubulin chemotherapeutics is regulated by MCL1 and FBW7. *Nature* *471*, 110–114.
- Wertz, I.E., Kusam, S., Lam, C., Okamoto, T., Sandoval, W., Anderson, D.J., Helgason, E., Ernst, J.A., Eby, M., Liu, J., et al. (2011b). Sensitivity to antitubulin chemotherapeutics is regulated by MCL1 and FBW7. *Nature* *471*, 110–114.
- Won, K.A., and Reed, S.I. (1996). Activation of cyclin E/CDK2 is coupled to site-specific autophosphorylation and ubiquitin-dependent degradation of cyclin E. *EMBO J.* *15*, 4182–4193.
- Wong, R.W., Blobel, G., and Coutavas, E. (2006). Rae1 interaction with NuMA is required for bipolar spindle formation. *Proc. Natl. Acad. Sci. U. S. A.* *103*, 19783–19787.
- Woo, J.-S., Suh, H.-Y., Park, S.-Y., and Oh, B.-H. (2006). Structural basis for protein recognition by B30.2/SPRY domains. *Mol. Cell* *24*, 967–976.
- Wu, C., Daniels, R.W., and DiAntonio, A. (2007a). DFsn collaborates with Highwire to down-regulate the Wallenda/DLK kinase and restrain synaptic terminal growth. *Neural Develop.* *2*, 16.
- Wu, G., Hubbard, E.J., Kitajewski, J.K., and Greenwald, I. (1998). Evidence for functional and physical association between *Caenorhabditis elegans* SEL-10, a Cdc4p-related protein, and SEL-12 presenilin. *Proc. Natl. Acad. Sci. U. S. A.* *95*, 15787–15791.
- Wu, R.-C., Feng, Q., Lonard, D.M., and O'Malley, B.W. (2007b). SRC-3 coactivator functional lifetime is regulated by a phospho-dependent ubiquitin time clock. *Cell* *129*, 1125–1140.
- Wysocka, J., Myers, M.P., Laherty, C.D., Eisenman, R.N., and Herr, W. (2003). Human Sin3 deacetylase and trithorax-related Set1/Ash2 histone H3-K4 methyltransferase are tethered together selectively by the cell-proliferation factor HCF-1. *Genes Dev.* *17*, 896–911.
- Xu, Y., Sengupta, T., Kukreja, L., and Minella, A.C. (2010). MicroRNA-223 regulates cyclin E activity by modulating expression of F-box and WD-40 domain protein 7. *J. Biol. Chem.* *285*, 34439–34446.
- Yada, M., Hatakeyama, S., Kamura, T., Nishiyama, M., Tsunematsu, R., Imaki, H., Ishida, N., Okumura, F., Nakayama, K., and Nakayama, K.I. (2004). Phosphorylation-dependent degradation of c-Myc is mediated by the F-box protein Fbw7. *EMBO J.* *23*, 2116–2125.
- Yang, X., Menon, S., Lykke-Andersen, K., Tsuge, T., Di Xiao, null, Wang, X., Rodriguez-Suarez, R.J., Zhang, H., and Wei, N. (2002). The COP9 signalosome

- inhibits p27(kip1) degradation and impedes G1-S phase progression via deneddylation of SCF Cul1. *Curr. Biol.* **12**, 667–672.
- Yau, R., and Rape, M. (2016). The increasing complexity of the ubiquitin code. *Nat. Cell Biol.* **18**, 579–586.
- Ye, X., Nalepa, G., Welcker, M., Kessler, B.M., Spooner, E., Qin, J., Elledge, S.J., Clurman, B.E., and Harper, J.W. (2004). Recognition of phosphodegron motifs in human cyclin E by the SCF(Fbw7) ubiquitin ligase. *J. Biol. Chem.* **279**, 50110–50119.
- Yin, L., Joshi, S., Wu, N., Tong, X., and Lazar, M.A. (2010). E3 ligases Arf-bp1 and Pam mediate lithium-stimulated degradation of the circadian heme receptor Rev-erb alpha. *Proc. Natl. Acad. Sci. U. S. A.* **107**, 11614–11619.
- Yu, Z.K., Gervais, J.L., and Zhang, H. (1998). Human CUL-1 associates with the SKP1/SKP2 complex and regulates p21(CIP1/WAF1) and cyclin D proteins. *Proc. Natl. Acad. Sci. U. S. A.* **95**, 11324–11329.
- Zhang, W., and Koepp, D.M. (2006). Fbw7 isoform interaction contributes to cyclin E proteolysis. *Mol. Cancer Res. MCR* **4**, 935–943.
- Zhang, P., Chaturvedi, C.-P., Tremblay, V., Cramet, M., Brunzelle, J.S., Skiniotis, G., Brand, M., Shilatfard, A., and Couture, J.-F. (2015). A phosphorylation switch on RbBP5 regulates histone H3 Lys4 methylation. *Genes Dev.* **29**, 123–128.
- Zhao, D., Zheng, H.-Q., Zhou, Z., and Chen, C. (2010). The Fbw7 tumor suppressor targets KLF5 for ubiquitin-mediated degradation and suppresses breast cell proliferation. *Cancer Res.* **70**, 4728–4738.
- Zhao, X., Hirota, T., Han, X., Cho, H., Chong, L.-W., Lamia, K., Liu, S., Atkins, A.R., Banayo, E., Liddle, C., et al. (2016). Circadian Amplitude Regulation via FBXW7-Targeted REV-ERB α Degradation. *Cell* **165**, 1644–1657.
- Zheng, J., Yang, X., Harrell, J.M., Ryzhikov, S., Shim, E.H., Lykke-Andersen, K., Wei, N., Sun, H., Kobayashi, R., and Zhang, H. (2002a). CAND1 binds to unneddylated CUL1 and regulates the formation of SCF ubiquitin E3 ligase complex. *Mol. Cell* **10**, 1519–1526.
- Zheng, N., Schulman, B.A., Song, L., Miller, J.J., Jeffrey, P.D., Wang, P., Chu, C., Koepp, D.M., Elledge, S.J., Pagano, M., et al. (2002b). Structure of the Cul1-Rbx1-Skp1-F boxSkp2 SCF ubiquitin ligase complex. *Nature* **416**, 703–709.
- Zhou, C., Shen, L., Mao, L., Wang, B., Li, Y., and Yu, H. (2015). miR-92a is upregulated in cervical cancer and promotes cell proliferation and invasion by targeting FBXW7. *Biochem. Biophys. Res. Commun.* **458**, 63–69.

6. Annex

6.1. Abbreviations

APS	ammonium peroxodisulfate
APC/C	anaphase-promoting complex/cyclosome
BIR	baculoviral IAP repeat
bp	base pairs
BSA	bovine serum albumin
BTB	bric-a-brac-tramtrack-broad complex
CAND1	Cullin-associated and neddylation-dissociated 1
CPD	CDC4 phosphodegron
CRL	Cullin-RING ubiquitin ligase
ctrl	control
DCAF	DDB1- and CUL4-associated factor
DD	dimerization domain
DDB1	DNA damage-binding protein 1
DMEM	Dulbecco's Modified Eagle's Medium
DMSO	dimethyl sulfoxide
DNA	deoxyribonucleic acid
DTT	dithiothreitol
DUB	de-ubiquitylating enzyme
E1	ubiquitin activating enzyme
E2	ubiquitin conjugating enzyme
E3	ubiquitin ligase
EDTA	ethylenediaminetetraacetic acid
EV	empty vector
FBS	fetal bovine serum
Fig.	Figure
HECT	Homologous to E6-AP carboxyl terminus
HRP	horseradish peroxidase
IBR	in-between-RING
IAP	inhibitor of apoptosis protein
IP	immunoprecipitation
K	lysine

kDa	Kilodalton
M	methionine
MBP	maltose binding protein
min	minute
MYCBP2	MYC binding protein 2
NEM	N-ethylmaleimide
NLS	nuclear localization signal
OD	optical density
PAM	protein associated with MYC
PEI	polyethylenimine
PCR	polymerase chain reaction
PEI	polyethylenimine
RBR	RING-betweenRING-RING
RING	Really Interesting New Gene
RNA	ribonucleic acid
RT	room temperature
SAC	spindle assembly checkpoint
SCF	SKP1-CUL1-F-box protein
SDS-PAGE	sodium dodecyl sulfate polyacrylamide gel electrophoresis
siRNA	small interfering RNA
SKP1	S phase kinase-associated protein 1
SOCS	suppressor of cytokine signaling
T _m	melting temperature
TMD	transmembrane domain
UBD	ubiquitin-binding domain
WCE	whole cell extract
wt	wild-type

6.2. List of figures

Figure 1: The ubiquitin-proteasome pathway	6
Figure 2: Overview of Cullin-RING ubiquitin ligases (CRLs)	10
Figure 3: FBXW7 mediates the SCF-dependent ubiquitylation of important oncoproteins	13
Figure 4: FBXW7 domain organization.....	14

Figure 5: Immunoprecipitation and mass spectrometry identify putative novel FBXW7 α interaction partners	55
Figure 6: WDR5 is a putative novel substrate of FBXW7	57
Figure 7: Analysis of CUL4A, DCAF7, DDB1 and VPRBP as putative FBXW7 α regulators.....	58
Figure 8: Analysis of FBXW2, TRAF2, SHPRH, XIAP and cIAP1 as putative FBXW7 α regulators	60
Figure 9: <i>In vivo</i> interaction between FBXW7 α and XIAP	61
Figure 10: Specific interaction of XIAP with FBXW7 α	62
Figure 11: Interaction between FBXW7 α and XIAP does not depend on F-box and WD40 domains of FBXW7 α	63
Figure 12: Overview of Flag-tagged FBXW7 α mutants.....	65
Figure 13: N-terminal domain of FBXW7 α is required for the interaction with XIAP	67
Figure 14: FBXW7 α does not form a complex with XIAP <i>in vitro</i>	68
Figure 15: Identification of XIAP interaction partners	70
Figure 16: Overview of N- and C-terminal truncated versions of Flag-FBXW7 α for the characterization of the XIAP/RAE1 binding sites within the N-terminal domain.....	71
Figure 17: A short motif within the N-terminal domain of FBXW7 α is required for the interaction with XIAP and RAE1	72
Figure 18: Deletion of amino acid residues 106-126 of FBXW7 α abolishes the interactions with XIAP and RAE1	74
Figure 19: Conservation of amino acid residues 106-126 of FBXW7 α among vertebrates.....	75
Figure 20: Identification of FBXW7 α -XIAP complex components by a sequential immunoprecipitation approach	76
Figure 21: Identification of RAE1 interaction partners.....	77
Figure 22: FBXO45 and MYCBP2 interact with the N-terminal domain of FBXW7 α	79
Figure 23: Overview of Flag-tagged MYCBP2 fragments	80
Figure 24: FBXW7 α , XIAP, RAE1 and FBXO45 interact with the central domain of MYCBP2.....	81
Figure 25: FBXW7 α forms a complex with MYCBP2 and FBXO45	82
Figure 26: FBXO45 directly interacts with the N-terminus of FBXW7 α	83

Figure 27: FBXO45 specifically interacts with the α -isoform of FBXW7.....	84
Figure 28: FBXW7 α protein levels decrease during prolonged mitotic arrest	85
Figure 29: FBXW7 α protein levels are negatively regulated by FBXO45 and MYCBP2 during prolonged mitotic arrest	87
Figure 30: FBXO45 and MYCBP2 promote the ubiquitylation of FBXW7 α	89
Figure 31: FBXW7 α is stabilized upon siRNA-mediated downregulation of FBXO45	90
Figure 32: FBXW7 α interacts with the C-terminus of FBXO45	91
Figure 33: FBXO45 and MYCBP2 promote mitotic slippage.....	93

6.3. List of tables

Table 1: Overview of representative CDC4 phosphodegron (CPD) motifs in Cyclin E, NOTCH1, MYC and JUN.....	15
Table 2: List of primary antibodies.....	31
Table 3: List of siRNAs	32
Table 4: List of primers for the generation of plasmids.....	33
Table 5: List of provided plasmids	36
Table 6: List of plasmids generated by PCR or by PCR-free subcloning	37
Table 7: List of cell lines	39
Table 8: List of antibiotics	39

7. Acknowledgements

I am thankful to Prof. Dr. Ingrid Hoffmann for giving me the opportunity to perform my PhD project in her research group. I am grateful for the interesting research topic, the scientific discussions as well as for the continued support and trust.

I would like to thank Prof. Dr. Frauke Melchior for being the second reviewer of my thesis and for the extremely helpful discussions during my thesis advisory committee meetings. I am very grateful for the invitation to the stimulating lab retreat in Koblenz.

I thank Prof. Dr. Dr. Henri-Jacques Delecluse for attending my thesis advisory committee and for being a member of my examination commission. Moreover, I thank Dr. Thomas Hofmann for joining my examination commission.

My special thanks go to my past and present colleagues in the lab, including Felix Bärenz, Kathrin Brunk, Onur Cizmecioglu, Lena Ehret-Maßholder, Anna Haffner, Petra Hubbe, Anne-Sophie Kratz, Annalena Meyer, Yvonne Schlosser, Miriam Schmitt, Vera Seiler, Shota Suzuki, Barbara Vodicska and Mei Zhu. In addition, I thank the members of the Melchior lab, especially Gregor Habeck, for stimulating discussions, help and advice.

Finally, I am grateful to my family and friends for their support and sympathy.